Università degli studi di Roma "La Sapienza"

DOTTORATO DI RICERCA IN BIOCHIMICA
CICLO XVIII (A.A. 2002-2005)

N-OXIDES SENSING IN *Pseudomonas aeruginosa*: CHARACTERIZATION OF DNR, A TRANSCRIPTIONAL REGULATOR

Dottoranda
SERENA RINALDO

Docente guida
Prof. MAURIZIO BRUNORI

Coordinatore
Prof. PAOLO SARTI

Dicembre 2005

Acknowledgements

The experimental work described in this thesis was carried out in the Department of Biochemical Sciences "A. Rossi Fanelli" at the University of Rome "La Sapienza", under the supervision of Prof. Maurizio Brunori, to whom I am thankful for the great opportunity he gave me and for his continuous support.
I would also like to thank Prof. Francesca Cutruzzolà, who has guided me scientifically during my PhD, and who has been there for me personally.
Additional thanks go to my friends and collegues Dr. Gianna Panetta, Dr. Centola Fabio, Dr. Alessandro Borgia, Dr. Giorgio Giardina and all the "Soppalco".
I especially appreciate the great support given to me by the "ground floor" of the Department, particularly in the last year.
Last but not least, deep thanks to Dr. Alessandro Paiardini for helping me during the homology model construction and for his continuous support during the last 8 years.

CONTENTS

INTRODUCTION

1.1 Metabolism of nitric oxide in bacteria

Reactivity - Understanding the fate of nitric oxide (NO) inside the cell is a major issue in biology, given the large amount of processes controlled by this gas, both physiologically and pathologically.
At low concentration, NO functions as a signaling molecule, whereas at high concentration, NO can be a general poison due to its capability to alter biological macromolecules both directly or indirectly through NO-derived species.
At high levels, the gas reacts mainly with heme centers and labile 4Fe–4S clusters and thus inhibits terminal oxidases and aerobic respiration (Poole and Hughes, 2000; Wink and Mitchell, 1998). NO can also react both with molecular oxygen or superoxide (O_2-·) to produce nitration/nitrosation modifications or peroxynitrite (OONO-, Huie and Padmaja, 1993) respectively. Peroxynitrite acts as a strong oxidant by reacting with other molecules and can decompose to the highly reactive hydroxyl (HO·) and nitrogen dioxide (NO_2·) radicals. It was proposed that most of the damages produced by the presence of NO is mediated by peroxynitrite (Packer, 1996), which causes, if present at 1 mM concentration, cell death in *E.* coli in 5 seconds upon exposure (Brunelli et al., 1995).
In addition, NO-derived species can react with thiols present in small molecules and proteins, thereby disrupting protein activity as well as depleting the reduced glutathione pool to generate nitrosylated glutathione (GSNO), which in turn can modify proteins.

Production - Eukaryotic cells are able to produce NO through enzymatic oxidation of L-arginine by NO synthases. The NO production is tightly regulated being NO a molecule able to control a plethora of important processes such as signaling, neuronal communication, vasodilatation, smooth muscle relaxation, and inhibition of platelet aggregation. However, these functions are achieved by using low amounts of NO and, once the concentration of NO rises above micromolar levels, the molecule becomes harmful and causes serious deleterious effects, namely tissue inflammation, chronic infection, malignant transformations, and degenerative diseases. Nevertheless, high concentrations of NO are used to fight invading prokaryotic pathogens and parasites (Bastian and Hibbs, 1994; Nathan and Hibbs, 1991).
The NO released by macrophages is not the only source of NO that microbes need to deal with, because this compound is also produced abiotically (*e.g.* by decomposition of nitrite) and biotically by denitrifiers (Zumft, 1997) and as a product of side reactions in ammonification and nitrate assimilation/respiration (Corker and Poole, 2003). The NO homeostasis in denitrifiers will be discussed in the next section.
In non-denitrifiers, nitrogen is assimilated by the enzimatic reduction of nitrate

and nitrite to nitrite and ammonia respectively (Figure 1, bold lines). The enzymes involved in this process are the nitrate reductase (encoded by the *nar* and *nap* genes) and the nitrite reductase (encoded by the *nrf* and *nirB* genes). As side reactions these enzymes can produce NO as reported by Corker and Poole, (2003); NO is also produced by a non enzymatic nitrite reduction (Figure 1, gray line).

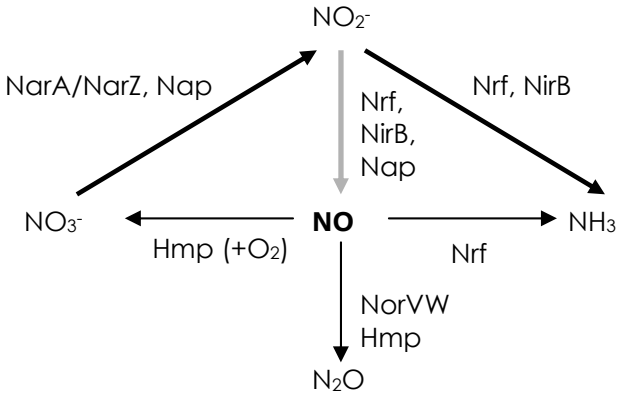

Figure 1. *NO metabolism in E. coli. Nitrate under anaerobic conditions is reduced to ammonia, using nitrite as intermediate (bold lines). Nitrate and nitrite reductases (Nar/Nap and Nrf/Nir respectively) can reduce in a side reaction nitrite to NO (gray line), which can also be formed chemically from nitrite. NO in the presence of oxygen can be oxidised by flavohemoglobin (Hmp) to nitrate. In the absence of oxygen, NO is reduced to nitrous oxide (N_2O) mainly by the flavorubredoxin (NorVW).*

Scavenging in non denitrifers - Nitric oxide is shown to cause a significant alteration of the global *E. coli* gene transcription profile that includes the increase of the transcript level of genes encoding for detoxification enzymes, iron-sulfur cluster assembly systems, DNA-repairing enzymes, and stress response regulators.
The most prominent detoxifying entities that have been identified are the NO dioxygenase, NO denitrosylase, and NO reductase activities associated with the *hmp*-encoded flavohemoglobin and the NO reductase activity associated with the *norVW*-encoded flavorubedoxin and flavorubedoxin reductase (Figure 1). Other detoxifying activities include NO reductase activity (Zumft, 2005) contributed by Nrf nitrite reductase and by different cytochromes and cytochrome oxidases and truncated globins (Poole, 2005).
Flavohemoglobin plays a key role in nitrosative stress among bacteria due to its versatile reaction chemistry and wide distribution. Flavohemoglobin is organized in two distinct domains: a N-terminal, globin-like domain, containing the b-heme, and a C-terminal domain belonging to the ferredoxin-NADP+ reductase family (Ermler *et al.*, 1995). Hmp functions as an

NO oxygenase in the presence of oxygen or as a denitrosylase (Gardner, 2005). Hmp can also act as a NO reductase under anaerobic conditions by reducing NO to N_2O (Wu *et al.*, 2003).
A more efficient NO reductase among bacteria is encoded by the norRVW operon, where norR represents the NO-inducible transcription regulator, norV the flavorubredoxin enzyme and norW an NADH:flavorubredoxin oxidoreductase. Flavorubredoxins belong to the family of A-type flavoproteins which are widespread through the anaerobic or facultatively anaerobic bacteria and archaea (Saraiva *et al.*, 2004). The proteins have a two-domain structure: an N-terminal β-lactamase fold and a C-terminal short-chain flavodoxin-like fold. Flavorubredoxins as such, or the combination of the A-type flavoprotein and rubredoxin, catalyze the reduction of NO under anaerobic conditions (Gomes *et al.*, 2002).

Regulation of tolerance in non denitrifers -A number of transcriptional regulators have been implicated in modulating gene expression in response both to NO and reactive nitrogen species.
As reported in the next section, the *E. coli norR* gene encodes a homologue of the NO-modulated NorR1 and NorR2 regulators of *Ralstonia eutropha*, required for the induction of *norV* promoter. *E. coli* norR protein contains a mononuclear non-heme iron centre which binds reversibly NO; the NO-activated form of norR protein positively regulates the transcription of the *norVW* genes (D'Autreaux *et al.*, 2005).
The NO-mediated induction of the *hmp* gene was reported to be under aerobic conditions dependent on MetR, a LysR family DNA-binding protein involved in the regulation of the methionine biosynthetic pathway, which requires as a coregulator homocysteine (Hcy). The presence of nitrosating agents can deplete MetR of Hcy by S-nitrothiols formation, and the MetR Hcy-free form up-regulates *hmp* transcription (Poole and Hughes, 2000).
Under anaerobic conditions, *hmp* gene transcription is dependent on the iron-sulfur cluster containing FNR (Fumarate and Nitrate Reductase Regulator) regulator, which acts, as will be reported in more detail in the next section, mainly as an oxygen responsive regulator. FNR is under normal conditions an *hmp* repressor as a dimer; the oxygen labile $[4Fe\text{-}4S]^{2+}$ center, which controls protein dimerization and DNA binding activity, in presence of NO is converted into the $[2Fe\text{-}2S]^{2+}$ state inducing monomer formation in the FNR protein. The FNR form modified by NO binds the *hmp* promoter with lower affinity, inducing flavohemoglobin expression (Cruz-Ramos *et al.*, 2002).
Other *E. coli* systems are able to respond to nitrosative stress, such as the SoxRS regulon, which encods a two-component ROS (reactive oxygen species) responsive regulators. NO binds to the binuclear iron-sulfur center of SoxR, forming a dinitrosyl-iron-dithiol active complex that induces *soxS* (Nunoshiba, *et al.*, 1993).
The presence of NO was shown to cause the formation of a non-heme iron-nitrosyl species in the *E. coli* Fur (ferric uptake regulator), leading to the inactivation of its repressor activity and thus resulting in a general

derepression of the iron metabolism (D'Autreaux *et al.*, 2002).
Recent studies focused on the modifications in the transcription pattern in presence of NO and RNOS among bacteria indicate that NO tolerance regulation depends mainly on the oxygen tension.
The *E. coli* response to reactive nitrogen species during aerobic growth in rich media is a composite response in which NorR and Fur have major roles, SoxR and OxyR have minor roles, and additional regulators remain to be identified (Mukhopadhyay *et al.*, 2004).
Anaerobic nitrosative stress caused a strong induction of the transcriptional levels of *norVW* operon and *hmp* genes, suggesting that flavohemoglobin is able to protect *E. coli* against NO under anaerobic conditions.
Only 10% of the genes up-regulated in the presence of NO under anaerobic conditions are also induced in an aerobic environment, indicating that the conditions chosen to study the effects of NO are of crucial importance (Justino *et al.*, 2005).
In summary, NO induces global changes on the metabolism of *E. coli* which are modulated by the environmental conditions (i. e. oxygen tension). Moreover, low oxygen tension is required for the colonization of most of the pathogenic organism like bacteria (Hassett *et al.*, 2002) and protozoan (Sarti *et al.*, 2004), suggesting that anaerobic conditions are crucial in the study of pathogenic NO resistance mechanisms.
Consequently, bacteria have evolved sensitive and specific sensors, usually at the level of transcription, to monitor different redox signals such as the presence or absence of oxygen, NO, cellular redox state or reactive oxygen species.

1.2 Gas and redox sensors

Redox sensing and balancing -Energy metabolism together with the biosynthesis of cell components and related processes, involves redox reactions in which electrons and/or hydrogen atoms are transferred between donor and acceptor molecules.
Redox reactions are central to both anabolic and catabolic metabolism and the ability to maintain redox balance is therefore vital to all organisms; an increase in oxidation reactions (oxidative stress), in fact, can damage essential cellular components.
Oxidative stress occurs as a consequence of an imbalance in favour of pro-oxidants. It can be caused by exposure to increased levels of the reactive oxygen species (ROS) superoxide (O_2^-), hydrogen peroxide (H_2O_2) and the hydroxyl radical (HO•) that are produced by the stepwise one-electron reduction of molecular oxygen. Moreover the presence of N-oxides can favour the enzymatic and chemical formation of nitric oxide (NO) which *per se* or by reacting with ROS can act as a pro-oxidant agent.
Superoxide and hydrogen peroxide are generated endogenously when bacteria grow under aerobic conditions by autooxidation of flavin cofactors of redox enzymes (Imlay, 2002). The highly reactive hydroxyl radical is

generated when hydrogen peroxide reacts with Fe2+ in the Fenton reaction, thereby linking cellular iron status to oxidative stress.
The sensing mechanisms are many and varied, and can involve redox-active cofactors such as heme, non-heme iron, flavins, pyridine nucleotides and iron–sulphur clusters, or redox-sensitive amino-acid side chains such as cysteine thiols (Green and Paget, 2004).

Oxygen and oxidative stress sensors - Bacteria like *Escherichia coli*, i.e. facultative anaerobes, can switch between aerobic and anaerobic metabolism by monitoring environmental oxygen. The FNR protein is an iron-sulfur cluster containing protein which acts as the global regulator of anaerobiosis by sensing oxygen (Green *et al.*, 2001).
The FNR protein belongs to the CRP-FNR (where CRP stands for cAMP Receptor Protein) superfamily of transcription regulators (see below), with an N-terminal sensor domain and a C-terminal DNA binding domain, linked through an α-helix involved in the dimer formation. The N-teminal sequence contains a cysteine-rich motif involved in the iron-sulfur cluster formation, whose organization depends on the oxygen tension.

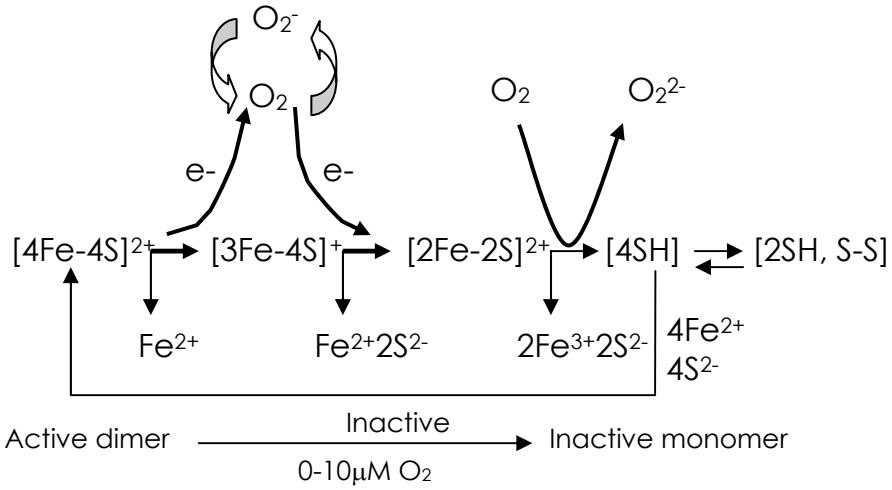

Figure 2. *A mechanism for direct oxygen sensing by FNR protein. The transition from active to inactive protein upon exposure to oxygen is a biphasic process, in which oxygen converts the $[4Fe\text{-}4S]^{2+}$ form into the inactive $[2Fe\text{-}2S]^{2+}$ one, which in turn forms apo-FNR.*

Under low oxygen tension, the protein forms a homodimer containing one $[4Fe\text{-}4S]^{2+}$ cluster; in this form, FNR activates its target promoters by binding to the DNA (Kiley and Beinert, 1999).
Oxygen is sensed by a mechanism which involves the interconversion of the

$[4Fe\text{-}4S]^{2+}$ cluster to the apo form, with the formation of the monomer unable to bind DNA (Figure 2).
Oxygen is also an effector molecule which can regulate chemotaxis as in the case of the *Bacillus subtilis* HemAT protein, a heme-containing signal transducer involved in directing movement of the bacterium within an oxygen gradient (Hou *et al*., 2001). In this case heme is coordinated to a typical globin fold and is used as an oxygen sensor. Oxygen binding activates the linked histidine kinase domain, which modulates the activity of proteins that control flagella rotation.
Another heme-based sensor is FixL, a member of the two component system FixLJ, which regulates nitrogen fixation, a strictly anaerobic process, in diazotrophic bacteria. Under oxygen-limiting conditions, no oxygen is bound to the sensor domain and this permits the reversible autophosphorylation of a histidine residue in the FixL transmitter domain. Phosphotransfer to the receiver domain of FixJ activates the regulator and consequently the genes involved in the nitrogen fixation (Gilles-Gonzalez *et al.*, 1995).
Among the CRP-FNR superfamily of transcription regulators, there are other FNR-like proteins able to form a less reactive iron-sulfur cluster, as in the case of FlpA from *Lactococcus lactis.* This regulator contains a Rieske-like cluster, where the iron atom is coordinated by 2 cysteine and 2 histidine residues, which confers more stability towards oxygen (Green *et al.*, 2001). Upon oxygen exposure the metal centre is disassembled and the protein is able to bind DNA. This evidence has suggested that this transcription factor can act as a global sensor of the oxidative stress rather than of oxygen *per se* (Green *et al.*, 2001).
Bacteria have developed different strategies to respond to the oxidative stress, by discriminating between different ROS.
Elevated levels of hydrogen peroxide induce the activation of several antioxidant defensive genes like hydroperoxidase (*katG*), alkyl hydroperoxide reductase (*ahpCF*), a regulatory RNA (*oxyS*), the ferric uptake regulator (*fur*) and the glutathione reductase (*gorA*) (Zheng and Storz, 2000). In *E. coli* the protein which senses the hydrogen peroxide content is OxyR, a transcriptional regulator which activates the genes reported above. This protein is able to sense peroxides through an active cystein (Cys199), which, if oxidised to sulfenic acid, is forced out of the hydrophobic pocket where is located. The oxidised Cys199 is then located closer to the Cys208, thereby promoting disulphide-bond formation and the conformational remodelling of OxyR. The result is a change in the DNA-binding specificity of OxyR, recruitment of RNA polymerase to OxyR-dependent promoters and transcriptional activation (Choi, H. *et al*., 2001). More recently it was shown that a different derivative of the OxyR protein can be produced by using both ROS and S-nitrosothiols. These modified forms of OxyR are transcriptionally active but different in structure, cooperative properties, DNA binding affinity and promoter activity (Kim *et al.*, 2002). This versatility has suggested a possible role of OxyR in the sensing of nitrosative stress (see below).

The presence of superoxide also induce a specific response through the regulon SoxRS. The *E. coli* SoxR transcription factor activates the expression of the *soxS* gene in response to exposure to superoxide-generating agents. The elevated levels of the SoxS protein cause the increased expression of genes involved in the superoxyde scavenging like superoxide dismutase (*sodA*), glucose-6-phosphate dehydrogenase (*zwf*), aconitase (*acnA*) (Zheng and Storz, 2000).
SoxR forms a homodimer in solution, and each dimer contains two redox-active [2Fe-2S] cluster. The reduced form, inactive, upon exposure to superoxide-generating agents, switchs to the oxidised active form able to activate its target promoter (Ding and Demple, 1997). As reported for OxyR, SoxR is also a sensor of the nitrosative stress, by sensing NO through the iron sulfur cluster centre.

Nitric oxide sensors -Most of the oxygen/ROS sensors described above, due to the chemistry of their redox centre, are able to interact *in vitro* also with the NO molecule. Recent studies indicates that sensors such FNR, OxyR or SoxR may act as NO sensor *in vivo* depending on the oxygen tension (Mukhopadhyay *et al.*, 2004 and Justino *et al.*, 2005). NO can modulate also the activity of the ferric uptake regulator (Fur) *via* nitrosyl formation with the non-heme iron cofactor (D'Autreaux *et al.*, 2002); this evidence confirms the presence of a linker between cellular iron status and nitrosative/oxidative stress.
Recent evidences indicate that redox sensors of nitrosative stress have developed high specificity towards NO by increasing the affinity for this molecule.
As an example, the NO sensor from *Clostridium botulinum* involved in the chemotaxis machinery regulation, has an NO-binding heme domain similar to that of human soluble guanylyl cyclase (sGC) which show a femtomolar sensitivity towards NO (Nioche *et al.*, 2004), due to its heme moiety organization. Moreover, the NO-scavanger cytochrome c' (cyt c') from *Alcaligenes xylosoxidans* can discriminate between NO and other typical heme ligands. The crystallographic data of cyt c', in fact, show that carbon monoxide (CO) and NO can bind to opposite sides of heme, causing different responses of the protein through conformational changes (Andrew *et al.*, 2001).
The regulatory protein in enteric bacteria known to serve exclusively as an NO-responsive transcription factor is NorR (Gardner *et al.*, 2003). In *E. coli*, NorR activates the transcription of the norVW genes encoding a flavorubredoxin (FlRd) and an associated flavoprotein, which together have NADH-dependent NO reductase activity (Gardner *et al.*, 2003).
NorR protein was found also in the *Ralstonia eutropha* bacterium, a truly denitrifying proteobacterium, as a NO-dependent regulator of the NO-reductase enzyme (Pohlmann *et al.*, 2000).
NorR proteins show the typical modular structure of NtrC-like proteins (Morett and Segovia, 1993; North *et al.*, 1993) containing a central nucleotide-

binding domain (AAA^+ domain) and a C-terminal helix-turn-helix motif. Moreover, NorR proteins share a conserved GAF domain (named for cyclic GMP-specific and stimulated phosphodiesterases, *Anabaena* adenylate cyclases and *E. coli* FhlA) in the N-terminal region which is involved in signal reception and transmission. NorR activity depends on the function of the minor sigma factor 54 (RpoN) (Roèmermann *et al.*, 1989).
The function of the GAF domain is to sense the signal and inhibit the ATPase activity of the central AAA^+ domain when NorR is in its inactive state (Gardner *et al.*, 2003); the central catalytic AAA^+ domain of enhancer binding proteins is required to couple nucleotide hydrolysis to the formation of open promoter complexes by σ54-RNA polymerase (Cannon *et al.*, 2000). Binding of NO to the GAF domain stimulates the ATPase activity of NorR, enabling the activation of transcription by RNA polymerase.
Recent studies on the NorR protein from *E. coli* indicate that the N-terminal sensor domain contain a non-heme iron atom involved in the NO sensing by nitrosyl formation (D'Autreaux *et al.*, 2005), which activates the protein.
In denitrifier bacteria other NO and N-oxides sensors have been detected by genetic and computational analysis. To date the biochemical mechanism by which NO interacts with this class of regulators is not understood.
Moreover the global responce of bacterial cell to NO is controlled by a network of NO/redox sensors which can activate different scavenging mechanisms depending on the balance between N-oxide and oxygen in the medium.
An overview of the mechanisms of NO tolerance in denitrifying bacteria will be discussed in the next section.

1.3 Denitrification and nitric oxide homeostasis: DNR-type of regulators

Denitrification - Denitrification represents one of the major processes involved in the nitrogen cycle, which is entirely carried out by bacteria. In this pathway nitrogen oxides like nitrates and nitrites can be used as the only nitrogen source and as terminal electron acceptors under anaerobic growth conditions (Zumft, 1997), through their progressive reduction to molecular nitrogen (Figure 3). Four reductases are involved in this process: nitrate, nitrite, nitric oxide and nitrous oxide reductases encoded by the *nar*, *nir*, *nor* and *nos* genes respectively. The process is carried out, in gram negative bacteria, both in the periplasmic space and in the inner membrane and small protein like azurins and cytochrome c are also involved as electron donors (Figure 3). Denitrification is a facultative process induced by the presence of nitrates/nitrites and low oxygen tension and the activity of the four enzymes is regulated both kinetically and transcriptionally to avoid toxic intermediate accumulation (i. e. nitric oxide).
The expression of the denitrification gene clusters is tightly controlled by redox signaling through a cascade of oxygen-responsive regulators activating the N-oxides-responsive ones.

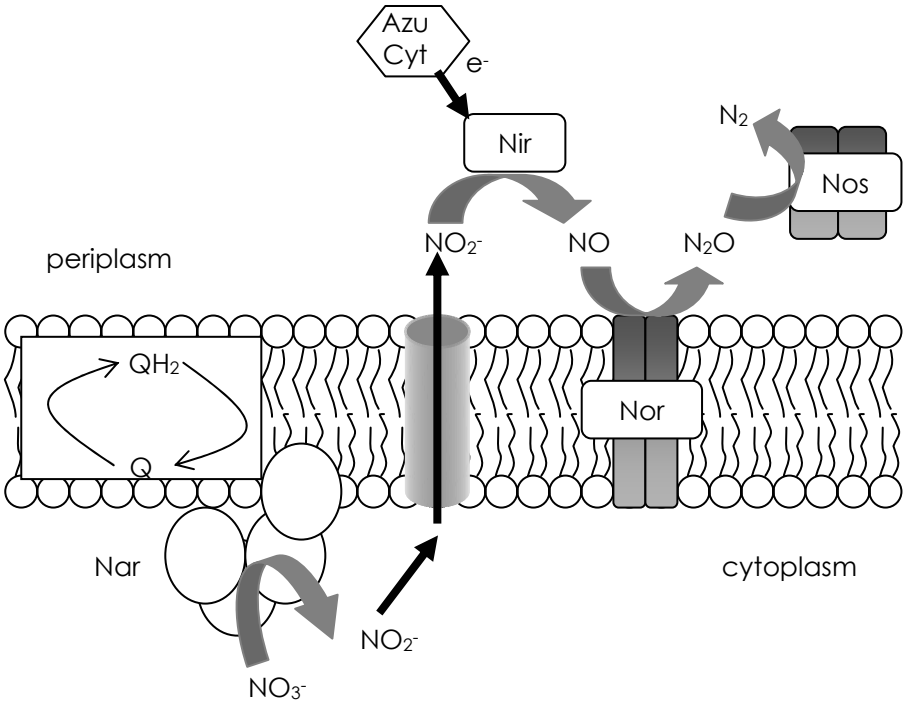

Figure 3. *Schematic representation of the denitrification in Gram negative bacteria. Q/QH_2 indicates the quinol mediated electron transfer; Azu and cyt are azurin and cytochromes respectively.*

These regulators control the nitric oxide (NO) homeostasis maintaining the steady-state concentration of nitrite and NO below cytotoxic levels; as a consequence, free NO concentration is in the nanomolar range. These conserved NO-sensors belong to the CRP-FNR superfamily of bacterial regulators.

NO-responsive elements belonging to the CRP-FNR superfamily of transcription factors -The denitrification pathway is transcriptionally regulated by redox-linked transcription factors mostly belonging to the CRP-FNR superfamily (Korner *et al.*, 2003; figure 4) structurally related to the CRP protein from *Escherichia coli* (McKay and Steitz, 1981). The CRP-FNR proteins are constant in size with approximatly 230-250 amino acid residues, the first 150-170 residues corresponding to the effector domain (Korner *et al.*, 2003). These regulators respond to both extracellular and intracellular signals by binding the allosteric effector either directly (as for cAMP in CRP from *E. coli*, Figure 5) or through a prosthetic group (as for the iron-sulfur cluster of FNR from *E. coli*) (Unden and Schirawski, 1997). All members of this superfamily bind DNA with a C-terminal helix-turn-helix domain which interacts with the

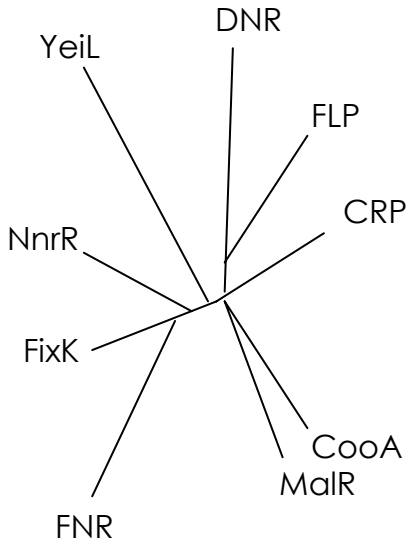

Figure 4. *The main branches of the Crp-Fnr superfamily of transcription factors (modified from Korner et al., 2003).*

major groove of target DNA sequence, the FNR box (TTGATN$_4$ATCAA) (Korner *et al.*, 2003).

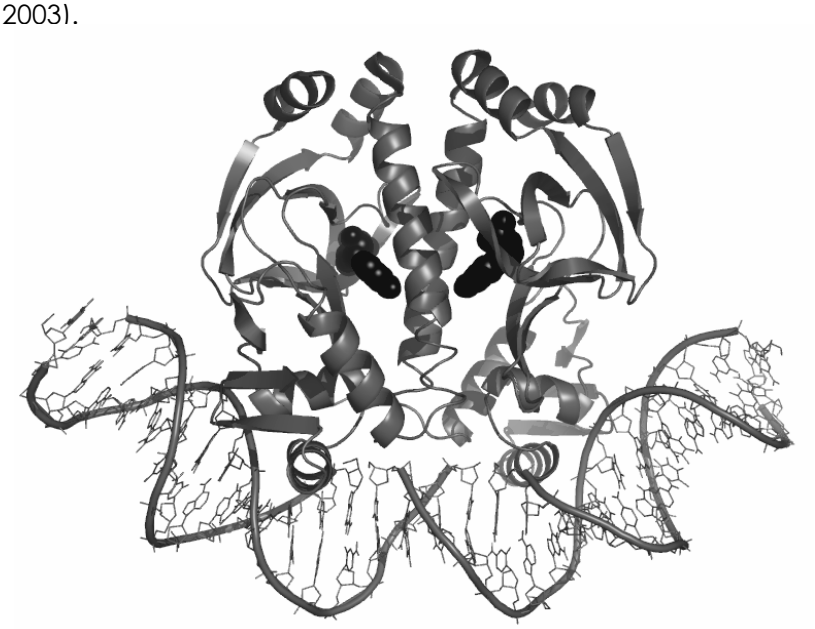

Figure 5. *CRP protein from E. coli. Crystal structure of a CRP-DNA complex (Schultz et al., 1991; pdb code: 1cgp). The cAMP molecules bound to the sensor domain of the protein (in black) trigger DNA binding.*

Multiple members of these regulators, belonging to different subgroups, can either co-exist in the same host or regulate the same metabolic pathway in

different organisms (Korner *et al.*, 2003). This is the case for the regulators of denitrification and in general for NO-responsive components which belong to three different subgroups of the CRP-FNR superfamily (FNR, DNR and NnrR) and can control N-oxide homeostasis both under anaerobic and aerobic conditions (Korner *et al.*, 2003). To date no structural information and limited biochemical data are available on the last two subgroups involved in the regulation of denitrification, while the first one is well characterized and was discussed in the previous section.

The DNR-type of transcription regulators -All members of the DNR subgroup share the same motif (E-SR amino acid residues) involved in recognition of the binding site on DNA, while most members of the NnrR subgroup contain an histidine instead of a glutamate residue. Both groups of regulators (DNR and NnrR) do not contain enough cysteines for iron-sulfur clusters formation contrary to FNR, suggesting a different mechanism of N-oxide(s) sensing.
Members of both NnrR and DNR subgroups are found in facultatively anaerobic bacteria; the transcriptional regulation is exerted in the presence of N-oxide(s) and under low oxygen tension. In *Rhodobacter sphaeroides* and in *Paracoccus denitrificans* for example, it was shown, by genetic approach, that the transcriptional regulators designated respectively NnrR (belonging to the NnrR-type) and Nnr (belonging to the DNR subgroup) can both activate the expression of the nitrite and NO reductase genes in response to NO (Kwiatkowski and Shapleigh, 1996 and Van Spanning *et al.*, 1999).
The members of DNR-type class of regulators found in the *Pseudomonas* sp. (Arai *et al.*, 1997 and Vollack and Zumft, 2001) share an high sequence identity (Figure 6) but may not fulfil an identical physiological role. This is not surprising given that *Pseudomonads* are well known for their metabolic flexibility which reflects the capability of the different species to survive as free living organisms in soil, water and animals, where are often responsible for diseases.
In *Pseudomonas stutzeri* there are at least three regulators (DnrD, DnrS, DnrE) involved in the NO-sensing (DnrD), activation of the nitrate pathway (DnrE) and possibly in redox sensing (DnrS) under anaerobic conditions (Korner *et al.*, 2003).
The DnrD transcription factor induces the expression of *nirSTB*, *norCB*, *nosZ* operons (encoding respectively nitrite, nitric oxide and nitrous oxide reductases) in the presence of NO but not nitrite (the *nos* gene is activated also in presence of high concentration of nitrous oxide). The NO concentration required for the *nir-nor* operons activation is in the range of 5-50 nM (Vollack and Zumft, 2001). DnrD overexpression *per se* is not sufficient for the transcription of the *nir-nor* operons, indicating that additional factors may be required (Vollack and Zumft, 2001).

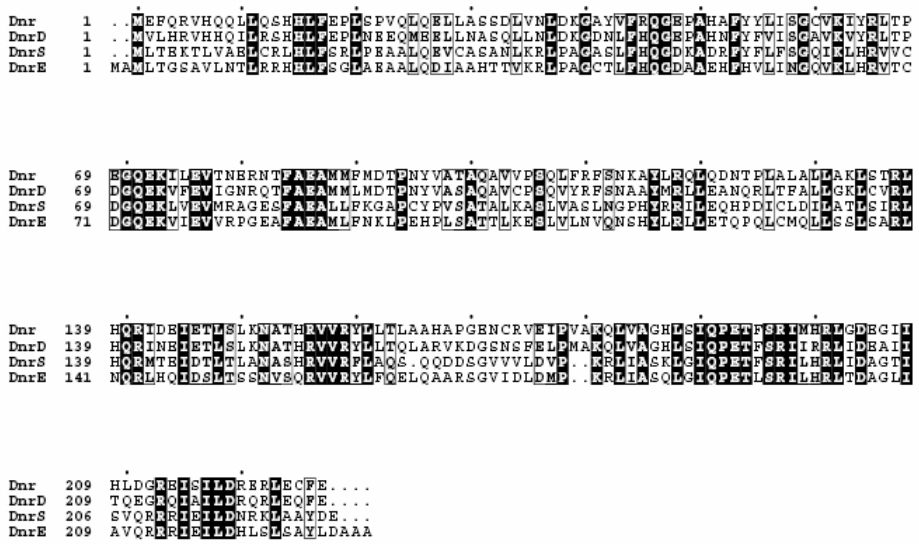

Figure 6. Multiple alignment of DNR protein sequences from Pseudomonas aeruginosa (DNR) and Pseudomonas stutzeri (DnrD, DnrS and DnrE). Amino acid one-letter code is used. Dashes represent insertions and deletions; numbers at the beginning of each sequence indicate absolute sequence numbering. Invariant positions are boxed in black; alignment columns displaying amino acid with the same physico-chemical properties are boxed in white with the conserved residues shown in bold.

NO sensing in Pseudomonas aeruginosa -P. aeruginosa is one of the most important pathogens in lung chronic infections associated for example to cystic fibrosis, where it uses denitrification as the anaerobic energy producing pathway (Hassett *et al.*, 2002).
Low oxygen tension and the presence of N-oxides produced by the host defence mechanism induce high levels of expression of *nir-nor* operons (Hassett *et al.*, 2002). Under anaerobic conditions, the denitrification pathway works both as a source of electrons and as NO scavenger given that the classical flavohemoglobin-mediated detoxification pathway is not active (Arai *et al.*, 2005).
The induction of denitrification by oxygen depletion requires ANR (anaerobic regulation of arginine deaminase and nitrate reduction), a FNR-like global regulator for anaerobic gene expression in *P. aeruginosa* (Galimand *et al.*, 1991).

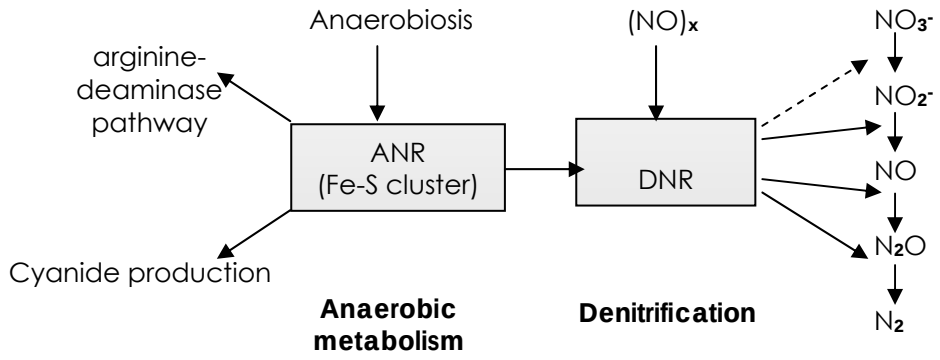

Figure 7. *Signaling and components of the regulation of the denitrification in P. aeruginosa. ANR represents the global regulator of anaerobiosis, which activates the regulators of denitrification, arginine deaminase and cyanide production pathway. The DNR protein in the presence of N-oxides (presumably NO) activates the transcription of the enzymes involved in the denitrification. The substrates and products of each N oxide-reducing system are shown.*

ANR induces the expression of the DNR protein (Dissimilative Nitrate Respiration regulator, belonging to DNR sub-type), which activates, in the presence of N-oxide(s), the *nirS*, *norCB*, *nosR* promoters (Arai *et al.*, 1997, 1995, 2003) (Figure 7).

strains	***dnr***	***nirS***	***norB***
anr-	-	-	-
dnr-		-	-
anr- pDNR		+	+

Table I. *Transcriptional activation analysis of the dnr, nirS and norB promoters carried out by using reporter gene systems (Arai et al., 1995, 1997, 1999). P. aeruginosa mutants lacking the anr (anr-) or dnr (dnr-) genes are not able to activate these promoters. The anr- strain transformed with a plasmid carrying the dnr gene (anr-pDNR) recovers the nirS and norB promoters activation.*

Mutants without the *anr* or *dnr* genes are not able to induce *nirS* and *norCB* promoters under growth conditions where denitrification should be active (Arai *et al.*, 1995). *anr* defective strains are not able to activate the transcription of the *dnr* gene but denitrification can be induced after

transformation with a plasmid carring the *dnr* gene (Arai *et al.*, 1997). DNR-mediated transcriptional activation of denitrification depends on endogenous NO concentration (Arai *et al.*, 1999, 2003); the transcriptional activation analysis is summarized in Table I.
The sequence alignment shown in Figure 6 clearly indicates a higher degree of similarity of DNR from *P. aeruginosa* with DnrD, in agreement with the involvment of DNR in NO-sensing. Given that only one DNR-type regulator is found in the *P. aeruginosa* genome, in this pathogen the role of the DnrE and DnrS might be played by different factors.

AIM OF THE PROJECT

All denitrifiers can keep the steady-state concentration of nitrite and nitric oxide (NO) below cytotoxic levels controlling the expression of denitrification gene clusters by redox signaling through transcriptional regulators belonging to the FNR-CRP superfamily.
NO-responsive regulators belong to three different subgroups of the CRP-FNR superfamily (FNR, DNR and NnrR) and can control N-oxide homeostasis both under anaerobic and aerobic conditions. The FNR-type share a cystein rich motif involved in the formation of an iron-sulfur cluster as a redox centre which is not present in the other two subgroups.
Most of the regulators involved in the regulation of denitrification, belonging either to the DNR and NnnR subgroups, regulate nitrite reductase (*nir*), nitric oxide reductase (*nor*) and nitrous oxide reductase (*nos*) gene expression. The NO dependence of the transcriptional activity of promoters regulated by these transcription factors has suggested that these factors may act as NO sensors *in vivo*.
To date, structural and functional information on this class of gas sensors is not available. Understanding the structure-function relationships of these transcription factors can provide new data about the biochemistry of NO in bacteria and can shed light on the global regulation of denitrification.
Controlling the denitrification pathway in the future could be a powerful tool in the control of the nitrate contents in wastewater and of the greenhouse gas production. In fact, nitrate, irrespective of its role as essential plant nutrient, has become a pollutant of groundwater and surface water, causing a major problem for the supply of drinking water. N_2O is next to CO_2 and CH_4 in its importance as a potent greenhouse gas (its efficiency is much higher than that of CO_2).
Moreover, recent studies indicate that the ability to denitrify (Hassett *et al.*, 2002) and in general, to survive to anaerobiosis (Sarti *et al.*, 2004) are responsible for the NO-resistence of many pathogens. Among denitrifiers, *Pseudomonas aeruginosa* is one of the most studied organism due to its capability to colonize different environments also as an opportunistic pathogen, mainly in cystic fibrosis patients.
The lung epithelium of this patients shows a mucus layer, due to an altered ions transport, which blocks the normal mucociliary clearance; the mucus adheres to the epithelium, forming an oxygen gradient layer. *P. aeruginosa* can penetrate this layer and chronically colonize the epithelium surface by using denitrification as energy source and resistance mechanism towards the NO released by the defence host systems; during the chronic infection, the *nir* and *nor* genes are overexpressed.
A new therapeutical approach in treatment of *P. aeruginosa* infections is attenuation of bacterial virulence, such that the organism fails to colonize, by using antipathogenic drugs instead of antibiotic compounds (Hentzer and Givskov, 2003). One of these new targets could be indeed the inhibition of the denitrification pathway.

To gain insights into the molecular and structural basis of the NO-dependent regulation of denitrification in *Pseudomonas aeruginosa*, we have recently expressed in *Escherichia coli* and partially characterized the DNR protein. Our studies have been focused on the characterization of the purified protein to determine the molecular basis of the NO-sensing.
Among NO-sensors, studies on the DNR subtype of regulators have been carried out by genetic and microbiological approaches.
To date it is known that DNR proteins are required for the N-oxides dependent transcriptional activation of genes involved in the denitrification pathway (Van Spanning *et al.,* 1999; Arai *et al.*, 1999, 2003).
The evidence of a direct interaction between DNR proteins and their target promoters was inferred by sequence analysis of both proteins and target promoters. All DNR proteins, in fact, share a helix-turn-helix motif in the C-terminal domain assumed to be involved, by sequences comparison, in the DNA binding. Moreover, this domain contains an FNR-box binding motif which is a signature of the FNR-like transcriptional regulators and the DNR-dependent promoters share an FNR box (Körner *et al.*, 2003).
To demonstrate the hypothesis that DNR activates the denitrification pathway by binding to the FNR box on its target promoters, we characterized the nitrite reductase (nirS) promoter binding activity of DNR containing cell extracts of *P. aeruginosa* (native DNR).
Moreover we have also proceeded in the functional analysis of the recombinant protein, by assaying *in vitro* the DNA binding activity, to understand which environmental signals can control the DNR-mediated denitrification activation.

MATERIALS AND METHODS

Protocols used for the common molecular biology and biochemistry tecniques, if not indicated, are described in Molecular cloning: a laboratory manual (Sambrook et al., 1989).

3.1 Cloning, expression and purification of DNR from *P. aeruginosa*

Cloning- The following oligos (5'-CATGCCATGGAATTCCAGCGCGTCCAC-3', 5'-CCGCTCGAGTCACTCGAAGCACTCCAGGCGTTCGC-3') were chosen to amplify by PCR the *dnr* gene by introducing extra NcoI-XhoI restriction sites at the 5' and 3' ends, respectively. The genomic DNA obtained from *Pseudomonas aeruginosa* PAO1 strain was used as template and the purified PCR product, verified by sequencing, was ligated into a NcoI-XhoI pET28b vector (Novagen) (Rinaldo *at al.*, 2005).
The pET-DNR vector was transformed into BL21(DE3) *Escherichia coli* strain (strain A) and cotransformed with the pHPEX3 vector (a kind gift of D.C. Goodwin, University of Auburn, USA) into the same strain (strain B). This vector, encoding an *E. coli* outermembrane-bound heme receptor (ChuA), is used for the overexpression of hemoprotein (Varnado CL and Goodwin DC, 2004).
The oligos (5'-GGAATTCCATATGGAATTCCAGCGCGTCCACCAGC-3', 5'-CCGC TCGAGTCACTCGAAGCACTCCAGGCGTTCGC-3') were used to clone the *dnr* gene into the pET28b vector in frame with a 5'-sequence encoding for a hisidine tag (his-tag); extra NdeI-XhoI restriction sites at the 5' and 3' ends, respectively, were also introduced.
The *dnr* gene was linked to the his-tag motif through a sequence encoding a thrombin site, useful to remove the tag from the purifed protein.
The pET-DNRHIS vector was transformed into BL21(DE3) *Escherichia coli* strain (strain A); the expression conditions reported for the strain A were followed for both vectors (see below).

Expression in E. coli - Expression of the protein was obtained at 37°C in Luria Bertani (LB) medium containing 30μg/ml kanamicin or 30μg/ml kanamicin+25μg/ml tetracycline for the double transformed strain. Aerobic cultures (0,75 l in 2 l flasks) were shaken at 250 rpm; anaerobic culture were pooled (1,5 l in 2 l flasks) and shaken at 100 rpm in sealed flasks after induction. Protein expression was induced with 1 mM IPTG (isopropyl β-d-thiogalactoside) when OD_{600} was 0,4 (Rinaldo at al., 2005) and carried out also in presence of 0,3 mM ALA (δ-aminolevulinic acid) for strain A, if indicated; 20μM hemin was added in strain B culture upon induction. Cells were then grown for 15 hours. In the anaerobic culture, 30' after induction, 1/40 of saturated atmosphere of carbon monoxide (CO) gas was added.
Cell growths without heme, inducers and/or plasmids were also carried out

for both strains, as a control, by using the same conditions discussed above.

Purification from strain A (pET-DNR) - Cells were resuspended in 50 mM Tris-HCl buffer (pH 8.0), 50 mM NaCl, 2 mM EDTA, 2 mM 2-ME (β-mercaptoethanol) and 1 mM PMSF (Phenylmethylsulfonyl fluoride) and sonicated. The cell extract was centrifuged 30' at 12000 rpm to remove any insoluble material. The soluble fraction was dialyzed against 20 mM Tris-HCl pH 7.2, 2 mM EDTA, 2 mM 2-ME (buffer A) and then applied on a Q-Sepharose Fast Flow (Amersham) column; the protein was eluted with a 35-500 mM NaCl gradient in the same buffer. The fractions containing the protein were pooled together and applied on a Heparin Sepharose 6 Fast Flow (Amersham) column after dialysis against buffer A. The protein was eluted with 100 mM NaCl, concentrated and applied on a Superdex 75 gel filtration column (Amersham) equilibrated in 20 mM Tris-HCl pH 7.2, 2 mM EDTA and 150 mM NaCl (Rinaldo at al., 2005). After the first purification, 2-ME was removed from all the purification steps, due to the fact that no changes in protein yield and solubility were observed.
Fractions containing DNR were pooled, frozen in liquid nitrogen and stored at -70 °C. In all the purification steps DNR protein was detected through SDS-PAGE and western blot analysis. Polyclonal antibodies were obtained in rabbit from the recombinant protein purified from *E. coli* (Davids Biotechnologie, Germany).
The extinction coefficient at 280 nm was determined by the Bradford assay (Sigma) to be 10.5 mM^{-1} cm^{-1} (per monomer).

Purification from strain B - The soluble fraction was obtained as reported for the DNR purification from strain A; the sample was fractionated using ammonium sulfate precipitations at different percentages (20%, 40% and 50%) to remove the excess of free heme; fraction containing DNR protein was recovered in the 50% pellet. The precipitated proteins were resuspended and dialyzed against 20 mM Tris-HCl pH 7.2, 50 mM NaCl (Buffer B) and then applied on a Q-Sepharose Fast Flow (Amersham) column; upon elution through a 50-600 mM NaCl gradient in the same buffer, the protein was recovered in two different peaks. Each peak was pooled and applied on a Superdex 75 gel filtration column (Amersham) equilibrated in 20 mM Tris-HCl pH 7.2, and 300 mM NaCl.
The same protocol, without the ammonium sulfate precipitation step, was used for strain A grown in anaerobiosis in presence of ALA. Anaerobic cell extracts were purified preequilibrating all the buffers with a nitrogen atmosphere; nitrogen was also bubbled in all the buffers during the chromatographic steps. Fractions containing DNR were stored under nitrogen at the end of each chromatographic step.

Purification from strain A (pET-DNRHIS) - The soluble fraction was obtained as reported for the DNR purifiication from strain A (pET-DNR) without 2-ME; the sample was applied on a HiTrap™ Chelating HP column (Amersham)

containing nickel sulfate salt and equilibrated with 20 mM Tris-HCl pH 7.2, 300 mM NaCl; the protein eluted either with 100mM and 300mM imidazole, in the same buffer. To remove the his-tag from the purified protein, the sample was dialyzed against 20 mM Tris-HCl pH 7.2, 300 mM NaCl and proteolytic digestion with 20 units of thrombin (Amersham), at RT for 15 hours, was carried out. The sample was then applied on a second nickel column equilibrated with 20 mM Tris-HCl pH 7.2, 300 mM NaCl. Under these experimental conditions, the thrombin enzyme was recovered in the flowthrough, while the his-tag free protein and the his-tag tails eluited in presence of 100 and 300 mM imidazole, respectively.
The DNR protein was dialyzed against 20mM Tris-HCl, 300 mM NaCl, to remove imidazole, frozen with liquid nitrogen and stored at -70°C.
Detection of DNR protein in all the purification steps was obtained through SDS-PAGE and western blot analysis, using anti his-tag polyclonal antibodies from rabbit (Santa Cruz Biotechnology, Inc.).

3.2 Biochemical characterization of DNR

Aggregation state - The aggregation state was determined on a FPLC column (Superdex 75 16/30) and further confirmed by HPLC (G3000SWxl Tosoh Biosep), at different NaCl concentration, in 20 mM tris-HCl pH 7.2 buffer (Rinaldo at al., 2005). The molecular weight calibration curve was obtained using protein standards (BSA 67 kDa, ovalbumin 43 kDa, chymotrypsinogen 25 kDa and RNase A 13.7 kDa - Amersham).

ANS binding - ANS (8-anilino-1-naphthalenesulfonic acid, SIGMA) binding was carried out by titrating a DNR solution either 2, 4 or 7 μM (monomer) in 50 mM Tris-HCl pH 7.2, 150 mM NaCl with a 1 mM ANS solution in water. The dissociation constant of ANS-DNR complex was calculated using the following relation (when $ANS_{tot}>DNR_{tot}$):

$$1/I = 1/n\psi\,[DNR]_{tot} + (K/n[DNR]_{tot}\psi)(1/[ANS]_{free})$$

where I is the observed fluorescence intensity, K is the dissociation constant for a dye-site complex, n are the total number of sites on protein, and ψ is the proportionality constant connecting the fluorescence intensity to the concentration of the probe-site complex.
If $ANS_{tot}>DNR_{tot}$, the plot of 1/I vs. $1/[ANS]_{tot}$ will be linear for fixed protein concentration with a common abscissa intercept, for different protein concentration, of –1/K, as described in Horowitz and Criscimagna (1985).
The number of binding sites on protein was assaied by titrating an ANS solution (either 1, 2 or 4 μM) with excesses of DNR and was calculated using the following relation:

$$1/I = 1/\psi\,[ANS]_0 + (K/\psi n[ANS]_0)(1/[DNR]_0).$$

In this case, the plots of 1/I vs 1/[DNR], for different ANS concentrations should have a common abscissa intercept of -n/K, as described in Horowitz and Criscimagna (1985).
In all cases, the signal was corrected for the fluorescence emission signal of free ANS in the same buffer.
For the experiments in which ANS bound to DNR was displaced by heme, 1 µl aliquots of a 0.2 mM solution of hemin were added to 2 ml solutions of 35 µM ANS and either 2 µM or 5 µM DNR protein.
All fluorescence emission spectra were recorded in a quartz cuvette (1 cm light path, Helma) between 400 and 600 nm on Fluoromax single photon counting spectrofluorometer (Jobin Yvon). The excitation wavelength was 350 nm.

Heme titration and reconstitution - Heme binding *in vitro* was assayed by titrating a 11,2 µM DNR monomer solution with increasing amounts of a freshly prepared solution of 0.5 mM ferric hemin (Sigma) in 10 mM NaOH. Titrations were carried out in 20 mM Tris-HCl pH 7.2 and 100 mM NaCl.
The cAMP binding protein (CRP) from *E. coli* was also titrated (17.1 µM monomer solution) with heme as a negative control. CRP was expressed from an overproducing *E. coli* strain transformed with CRP gene cloned into pET30-a plasmid (a kind gift of James C. Lee, University of Texas Medical Branch at Galveston); the protein was purified as described in Heyduk and Lee (1989).
For each heme/protein mixture a spectrum was recorded between 260 and 700 nm on a Hewlett Packard spectrophotometer. The difference between absorbance at 412 and 380 nm was plotted as a function of the mole fraction of heme.
The DNR apoprotein was reconstituted with a 1.5 stoichiometric excess of hemin in 20 mM Tris-HCl pH 7.2 and 300 mM NaCl at 16°C. Excess of free hemin was removed by gel filtration on a Sephadex G-25 column (Amersham).
Spectra of the heme-reconstituted DNR were recorded on a Hewlett Packard spectrophotometer, using a 1 cm quartz cuvette (Helma). The reduced derivative - obtained by adding an excess of sodium dithionite - was incubated in anaerobiosis under a saturated atmosphere of CO gas or with 10 µl of a 2 mM nitric oxide (NO) solution (20 °C and pH 7,2) to obtain the corresponding derivative.

Cysteines titration -The determination of free thiols in the protein was assayed using the Ellman's reagent (DTNB, 5,5'-Dithio-bis(2-nitrobenzoic acid), Riddles *et al.*, 1983) in 100mM Tris-HCl pH 7.5, 2mM EDTA solution and 6 M guanidine hydrochloride, if indicated; the absorbance at 412 nm was recorded using a Hewlett Packard spectrophotometer, in a 1 cm cuvette. The extinction coefficient used was 0.183 per 10 µM of free thiol.

Circular dicroism (CD) spectra- CD spectra were collected, using a JASCO

CD spectrophotometer with a 0.1 cm quartz cuvette (Hellma), at 20°C between 200 and 250 nm; a 8μM monomer solution in 20 mM Tris-HCl pH 7.2, 300 mM NaCl buffer was used for all experiments. To obtain the metal-bound derivative, 0.02-1 mM of a metal solution ($CuCl_2$, $ZnCl_2$, $CaCl_2$, $MgCl_2$, $MnCl_2$, $CuSO_4$) was added, if indicated.
Equilibrium thermal denaturations were followed at 222 nm, between 20°C and 80°C, using the experimental conditions reported above. The data were analyzed according to standard two-state equation (Fersht, 1999) for thermal unfolding:

$$\Delta G_{D\text{-}N(T2)} = \Delta H_{D\text{-}N(T1)} + \Delta C_p(T2\text{-}T1) - T2\,(\Delta S_{D\text{-}N(T1)} + \Delta C_p(T2/T1))$$

where ΔC_p was estimated from the size of the protein and from literature data (Myers *et al.*, 1995 and Privalov *et al.*, 1971). Variation of the value of ΔC_p does not affect the calculation of the free energy of unfolding. Three measurements were averaged to determine the T_m.

Model construction and evaluation -Protein dimeric model of DNR was constructed with the MODELLER-7 package (Šali *et al.*, 1995), using the hypothetical Transcription Regulator from *Bacteriodes Thetaiotaomicron* Vpi-5482 (pdb code: 1zyb) as template. Ten different models were built and evaluated using several criteria: the model displaying the lowest objective function (Šali *et al.*, 1995) was taken as the representative one, and analysed with PROSAII (Sippl, 1993) to monitor its stereochemical quality. The initial alignment was then subjected to minor changes in the attempt to increase the poorly modelled loop regions. The final overall PROSAII plot showed a structure of good quality.
Protein monomeric models of DNR in its putative inactive and active forms were constructed using as templates the hypothetical Transcription Regulator from *Bacteriodes Thetaiotaomicron* Vpi-5482 (pdb code: 1zyb) and the CRP protein from *E. coli* (pdb code: 2cgp, Passner and Steitz, 1997), respectively, following the same procedure described above.
Computation of the electrostatic potential at protein surface was performed with the facility provided by PyMol (Delano, 2002).

3.3 Mutagenesis

Site-directed mutants (H7A and N152STOP) were obtained on the pET-DNRHIS template, using a QuikChange site-directed mutagenesis kit (Stratagene). The mutations were verified by sequencing. Expression and purification were carried out as reported for the wildtype his-tag containing protein.

3.4 Purification of native DNR from *Pseudomonas aeruginosa* cell extract

The cell extract from *Pseudomonas aeruginosa*, grown under low oxygen tension and in presence of nitrate, was purchased from University of East Anglia (Wolfson Fermentation Laboratory, Norwich, UK) as an ammonium sulfate fractionated sample. The fraction containing DNR (95% ammonium sulfate pellet) was resuspended and dialyzed against 20 mM phosphate buffer pH 7.0. The sample was separated in batch with a DE-52 (Wathman) resin, equilibrated with the same buffer, and eluted with increasing amount of NaCl in the same buffer; the protein was recovered mainly with in the 300 mM NaCl elution step. The obtained pool was enriched in the DNR protein using a nickel column (HiTrap™ Chelating HP Columns - Amersham) equilibrated with 20 mM Tris-HCl pH 7.2, 300 mM NaCl; a partially purified DNR protein was eluted with a 100mM imidazole step. Other chromatocgraphic steps (Q-sepharose, Heparin, Superdex 75 gel filtration) were performed to increase the yield of the DNR protein, using the same conditions reported for the recombinant protein.
DNR was detected in all the purification steps by western blot analysis (see above) and by DNA binding assay (see below).

3.5 DNA binding assay of DNR

Electrophoretic mobility shift assays (EMSA). DNA fragment containing the nitrite reductase gene (*nirS*) promoter was amplified by PCR from the PAO1 genomic DNA (nirS prom) and end-labelled using polynucleotide kinase (Biolabs) and [γ^{33}P]-ATP. Double stranded oligonucleotides containing the FNR-box target sequence from the *nirS* and NO-reductase (*norBC)* genes promoters were also used instead of the *nir* promoter fragment.
Binding reaction was carried out at room temperature (RT) either in 20 or 30 μl volume containing binding buffer (50 mM Tris-HCl, pH 8.0, 7,5 % glycerol, 100 mM KCl, poly dI-dC 50 μg ml^{-1}, 1 mM EDTA), 70 fmol of labelled DNA and cell extract (~20 μg of proteins) or purified protein (~15 μg). The samples were separated on a 7.5 % polyacrylamide gel containing 1x TBE buffer (also used as running buffer), and run either at 4°C or RT, at 80 V for 2-3 hours.
Anaerobic EMSA were carried out using a glove-box (Belle T, UK) or an Atmosbag (Aldrich) box under nitrogen flux.
For the EMSA in presence of competitors, increasing amounts (10-50 folds excess) of unlabelled nirS prom or 500bp DNA fragments were added (10-50 folds excess); different dilutions (2000-50000 folds dilutions) of anti-DNR antibodies solution were also used as competitors.
Binding reaction was also carried out at room temperature (RT) in 20 μl volume containing binding buffer (50 mM Tris-HCl, pH 8.0, 7,5 % glycerol, 100 mM KCl, 1 mM EDTA), 200 ng of unlabelled DNA and partially purified protein (~80 μg). The samples were separated on a 0.8 % agarose gel containing 1x

TBE buffer (also used as running buffer), and run at RT, at 80 V for 2-3 hours.
The DNA-protein(s) complex was extracted from the gel by cutting the agarose band. The band was then eluted by freeze and thaw, and the protein contents was detected by SDS-PAGE, western blot and mass spectrometry (see above).

Reporter gene assay - The *dnr* gene was cloned into the pACy184 (Biolabs) vector by PCR under the constitutive *tet* promoter; extra EcoRV restriction sites and ribosome binding sequences were added. The gene was then excised by HindIII-BamHI endonucleases digestion and cloned into pUC19 (Biolabs) vector, under the *lac* promoter; the pUC-DNR vector was then transformed into the MC1000 (*fnr*$^+$) and JRC1728 (*fnr*$^-$) *E. coli* strains.
As a reporter system, the pRW50 vector was used (a kind gift of S. Busby, UK), in which the *E. coli lacZ* gene, encoding the β-galactosidase (β-gal) enzyme, is under the control of the *E. coli melR* promoter; the pRW50 vector was transformed into the pUC-DNR containing strain. Single transformants were used as control.
Expression of DNR and β-gal was carried out in LB+0.4% glucose medium containing 25μg/ml tetracycline or 100μg/ml ampicillin+25μg/ml tetracycline for the double transformed strains. Aerobic cultures (10 ml in 150-ml flasks) were shaken at 220 rpm at 37°C. For the anaerobic cultures, ten-milliliter cultures were grown aerobically to log phase and then transferred to 15-ml bottles sealed with Suba seals; the bottles were shaken for 30 min at 37°C to remove the residual oxygen. Additions of 50 mM nitrate, 2 mM nitrite, or 100 mM sodium nitroprusside, as indicated, were then made, and the bottles were incubated without shaking for a further 2.5 h before β-gal was assayed.
The expression of DNR protein was detected by western blot analysis; no inducer was required for the DNR protein expression.
β-gal was assayed in duplicate according to the method of Miller (1992) on at least three independently grown log-phase cultures. Absorption spectra were collected from culture supernatants, obtained as reported in (Sambrook et al., 1989), using a Hewlett Packard spectrophotometer.

RESULTS

4.1 Protein expression and purification.

We have isolated the *dnr* gene from *P. aeruginosa* genomic DNA by PCR and inserted it in the expression vector PET28b (Novagen). The pET-DNR vector was transformed in BL21 (DE3) *E. coli* strain (hereinafter strain A). High level of protein expression was obtained at 37°C after overnight induction with 1 mM IPTG (Figure 8A); the protein was found to be mainly in the soluble fraction of the total cell extract (Figure 8B, lane 1 and 2). High yields (15 mg/lt) of a protein pure to the homogeneity were obtained (Figure 8B, lane 3), using the purification procedure reported in Materials and Methods (Rinaldo et al., 2005).

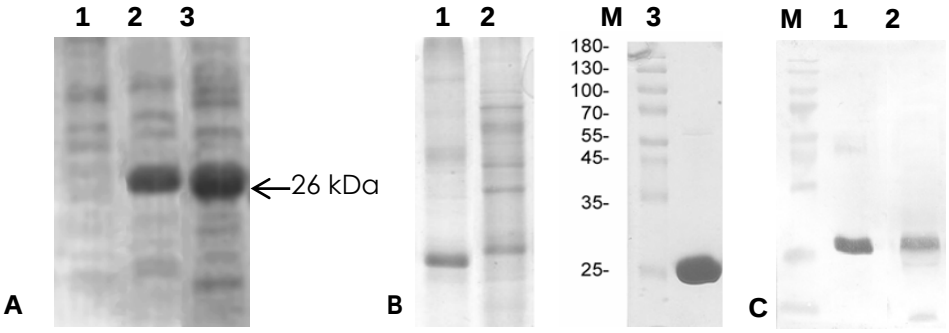

Figure 8. *Expression and purification of the DNR protein, SDS/PAGE. (A) Lane 1: total cell extract from strain A without IPTG. Lane 2: total cell extract from strain A at 2 hours after induction with 1 mM IPTG. Lane 3: total cell extract from strain A at 18 hours after induction. (B) Lane 1: soluble fraction of the extract from strain A at 18 hours after induction. Lane 2: insoluble fraction. Lane M: molecular mass markers 10–180 kDa (MBI Fermentas, Munich,Germany). Lane 3: purified DNR protein. (C) DNR detection by western blot analysis using a 1:10000 dilution of a polyclonal antibody against DNR (Davids Biotechnologie). Lane M: molecular mass markers 10–180 kDa (MBI Fermentas, Munich,Germany). Lane 1. Purified DNR protein. Lane 2. E. coli (pET-DNR) cell extract at 18 hours after induction.*

One mg of purified protein was used to produce polyclonal antibodies from rabbit (Davids Biotechnologie). Western blot analysis indicates that the produced antibodies were able to identify the DNR with high specificity (figure 8C).

4.2 Biochemical characterization

The molecular weight of the purified protein was 26054,16 (as determined by mass spectrometry, Prof. Schininà E., University of Rome La Sapienza, I). Determination of the N-terminal sequence has confirmed that the recombinant protein is correctly maturated in *E.coli*. The CD spectrum of the protein showed that DNR has a secondary structure content which suggest that the purified protein is folded in solution (see below).
DNR is mainly a dimer in solution, as shown by gel filtration (Figure 9) of the purified protein in 20 mM Tris-HCl and 150 mM NaCl. Higher aggregation states are populated at lower salt concentration (not shown), and thus all experiments have been carried out at salt concentrations ≥ of 150 mM NaCl.

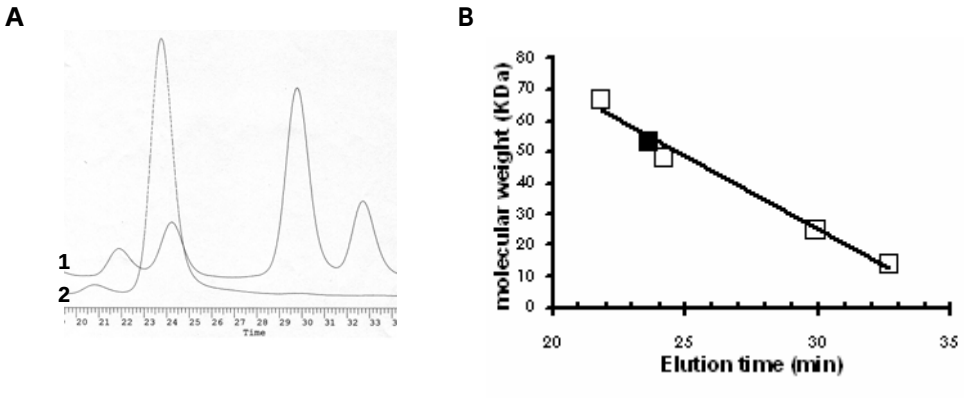

Figure 9. *Aggregation state of the purified protein. (A) DNR was run on a gel filtration column in comparison with molecular mass markers. The elution profile of the DNR sample (trace 2) is superimposed on that of the markers (trace 1, from left to right: BSA 67 kDa, ovalbumin 43 kDa, chymotrypsinogen 25 kDa and RNase A 13.7 kDa). (B) Linear dependence of the elution times of the markers on their molecular weight (open squares). The calculated molecular weight for the DNR protein in solution was ~53 KDa, corresponding to the dimer (closed square).*

No difference in the aggregation state was observed in presence of reducing agents such as β-mercaptoethanol (2-ME), neither by gel filtration nor by SDS-PAGE (not shown).

Cysteines titration -The free thiols content of the purified protein was determined using the Ellman's reagent (Riddles *et al.*, 1983) both in the absence and in the presence of denaturing agent as guanidine hydrochloride (6 M). In both experiments, a value of 0.8 free thiol per monomer was obtained.

Binding of ANS -As reported for the *E. coli* CRP protein (Heyduk and Lee, 1989), titration with ANS (8-anilino-1-naphthalenesulfonic acid) was performed to get some insights on the DNR structural organization.
The fluorescence signal of ANS, if bound in a nonpolar environment, is significantly increased and the maximum of emission is shifted from about 530 nm to below 500 nm. The DNR sample (2 μM) in presence of increasing ANS amounts (2-35 μM) showed a maximum fluorescence emission at 460 nm (Figure 10), which indicates complex formation between the protein and the ANS ligand.

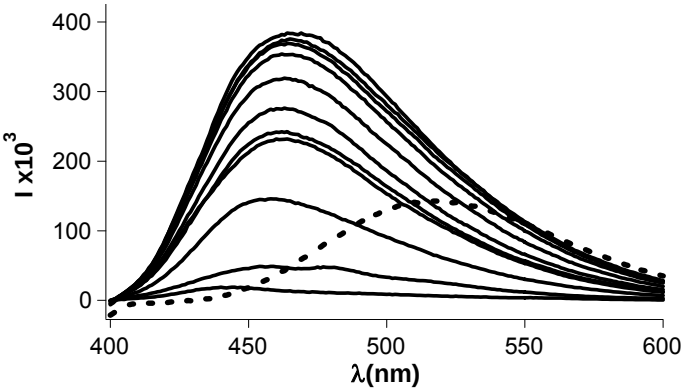

Figure 10. *Fluorescence emission spectra of DNR-ANS complex at different ANS concentration (2-35 μM range). As a control the intrinsic fluorescence emission spectra of 35 μM ANS is also shown (dashed line).*

To determine the dissociation constant (K_D) for the ANS ligand, different concentrations of the purified DNR (2, 4 and 7μM monomer) were titrated with increasing amounts of ANS (2-35 μM) and the experimental data are shown in Figure 11A. The stoichiometry of the DNR-ANS complex was determined by titrating different ANS concentrations (1,2 and 4 μM) with increasing amounts of DNR (1-28 μM) under the same experimental conditions (Figure 11B).
The data, analyzed as described in Horowitz and Criscimagna (1985), showed that DNR binds the ANS molecule with a K_D of 6.2±0.6 μM and a stoichiometry of 0.40±0.05 mol of ANS per monomer of protein.

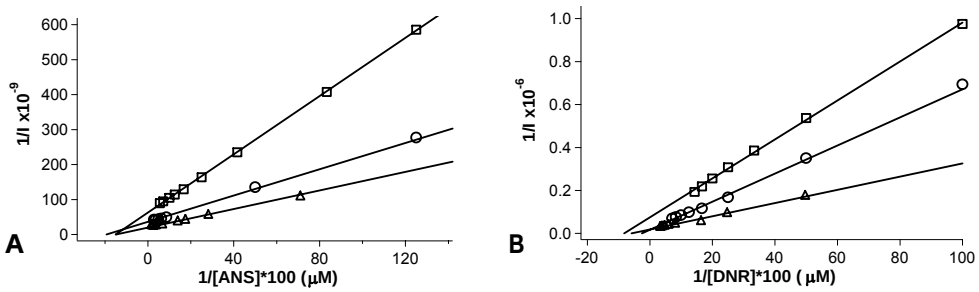

Figure 11. *Characterization of the binding of ANS to DNR. (A) The dissociation constant for the ANS–DNR complex was obtained from the abscissa intercept as described in the Materials and Methods section. Protein concentrations used: 2 μM (□), 4 μM (○) and 7 μM (△). (B) The number of binding site(s) for the ANS to the DNR protein were calculated from the abscissa intercept as described in the Materials and Methods section. ANS concentrations used: 1 μM (□), 2 μM (○) and 4 μM (△).*

Heme titration -To further investigate the features of the hydrophobic pocket of DNR, a titration was also carried out with heme on both DNR (Figure 12A) and CRP (Figure 12B), as negative control, by adding aliquots of a hemin (Fe^{3+}-protoporphirin IX) solution.

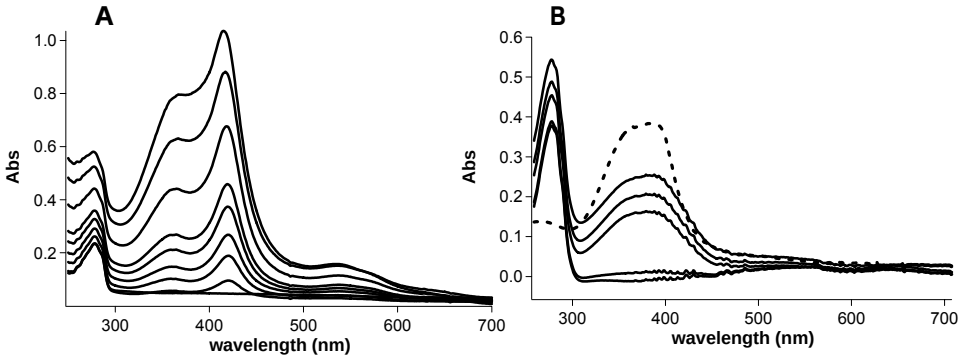

Figure 12. *(A) Absorption spectra of DNR protein in the presence of increasing amounts of heme. (B) Absorption spectra of CRP protein in the precence of increasing amounts of heme. As a control the spectrum of a heme solution (8 μM) at pH 7.0 is also shown (dashed line).*

For each heme/protein mixture a spectrum was recorded in the 260-700 nm range. In these spectra, the absorbance at 412 nm reports on the

concentration of the heme bound to the protein, while the absorbance at 380 nm measures the concentration of the free heme. Absolute spectra show that a spectral shift consistent with heme iron coordination is observed for DNR, but not for CRP, where only aspecific binding could be observed (Figure 12).
The difference between the absorbance at 412 nm and at 380 nm (A_{412}-A_{380}) was plotted as a function of the mole fraction of hemin added; formation of the complex is maximized when DNR monomer and heme are present in a 1 to 0.6 ratio, respectively (Figure 13). The stoichiometry of binding is assumed to be one heme per dimer.

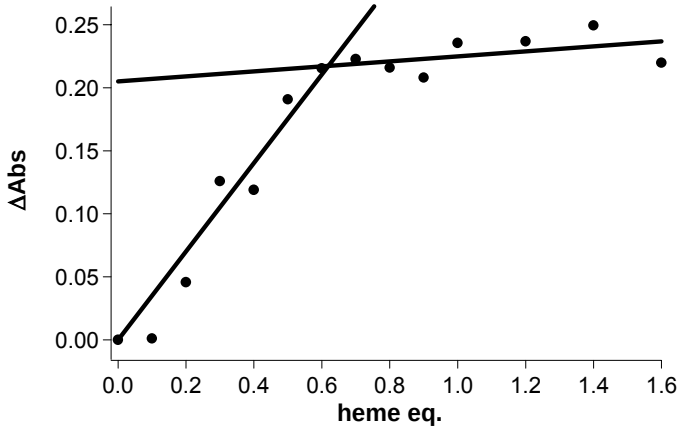

Figure 13. *Binding of heme. Plot of delta absorbance value (A412-A80) of DNR/heme solution as a function of heme equivalents*

Heme reconstitution and spectroscopic properties -The absorbance peaks for the heme-reconstituted protein at 412 nm and 530 nm suggest a ferric state of the coordinated iron (Figure 14A, black line). In anaerobiosis and in presence of an excess of dithionite, the ferrous derivative formation was confirmed by spectroscopical changes in the Soret band, shifted from 412 nm to 426 nm (Figure 14A, gray line). The reduced protein was also incubated with carbon monoxide (CO) and nitric oxide (NO) and the corresponding derivatives are shown in the Figure 14B. The spectroscopical transition of the reduced form to the NO-bound derivative is characterized by an isosbestic point at 408 nm; the NO-bound derivative showed a peak at 398 nm, which resembles a five-coordinated state of the iron (Figure 14B, inset). NO binding was observed also in absence of reducing agents, under nitrogen atmosphere (not shown).

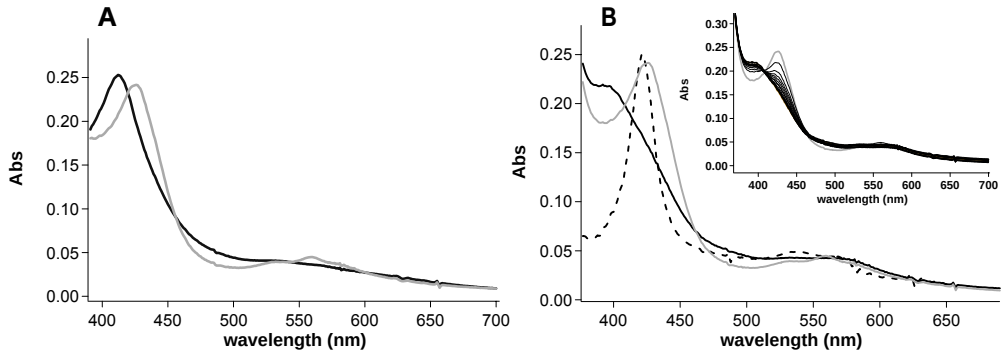

Figure 14. *DNR-heme complex. (A) Absorbance spectra of the oxidized (black line) and reduced (gray line) forms. (B) Absorbance spectra of reduced DNR-heme complex (gray line) bound to NO (black line) or CO (dashed line). NO-bound complex formation is also shown (inset).*

Displacement of ANS.

In order to determine whether heme is able to displace the bound ANS, a competition experiment was carried out by titrating the ANS-saturated protein with increasing amounts of heme, following the changes in fluorescence emission of ANS (Figure 15).

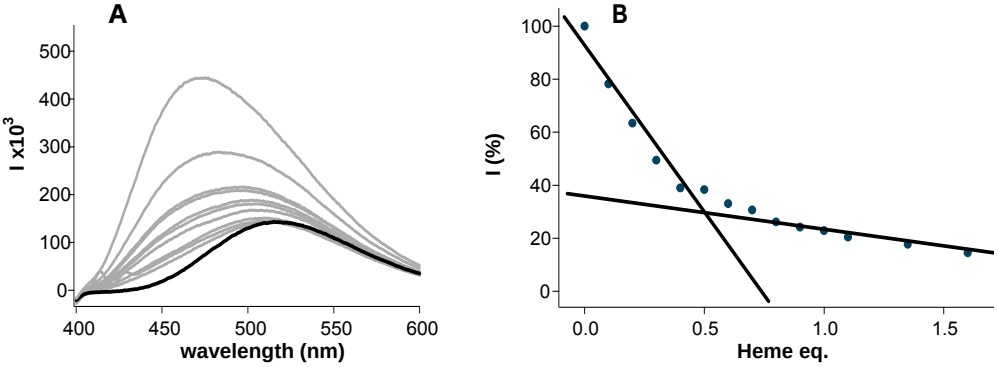

Figure 15. *Displacement of ANS from its complex with DNR by the addition of hemin. (A) Fluorescence spectra showing the reduction in fluorescence intensity of ANS bound to DNR (gray line) upon the addition of 1 μl aliquots of 0.2 mM hemin solution. The black line shows the spectrum of ANS alone. The samples contained 35 μM ANS and 5 μM protein. (B) Fraction of fluorescence enhancement in the spectra shown in A (enhancement in the absence of hemin is taken to be 100) is plotted as a function of the equivalents of hemin added to the sample of ANS-DNR complex.*

In the sample of DNR-ANS, we have observed, upon the addition of hemin, a stepwise reduction in the fluorescence enhancement to a value indicative of the absence of specific binding of ANS (Figure 15A).
Full ligand substitution is obtained at 0.5:1 stoichiometric ratio (heme:DNR monomer), thus suggesting that the two molecules compete for the same binding site (Figure 15B).

CD spectra and thermal melting experiments -Circular dicroism spectra were collected to determine the secondary structure content of the protein in solution; the experiment was carried out either with the purified protein or with the heme reconstituted protein. No significant variations in the CD spectra were observed (Figure 16A). To determine the stability of both proteins, equilibrium thermal denaturations, followed at 222 nm, were performed; the calculated temperature of melting was 55 °C for both proteins (Figure 16B).

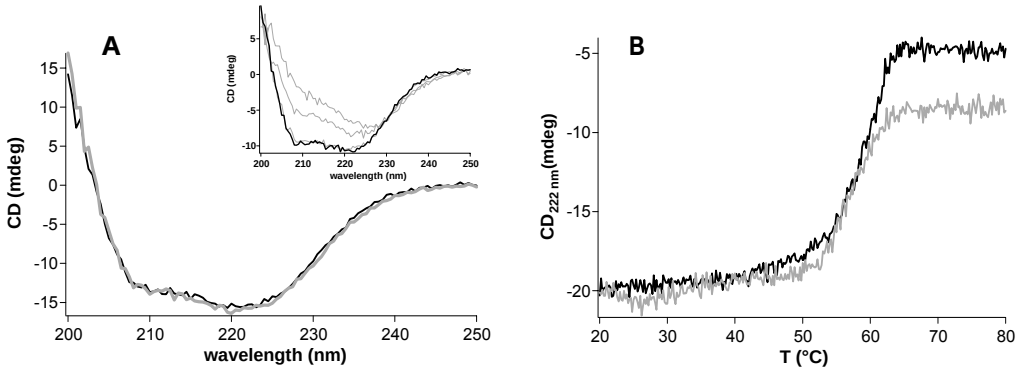

Figure 16. *Circular dicroism (CD) analysis of 8 μM purified DNR (black line) and heme reconsitud (gray line) protein. (A) CD spectra carried out at 20°C. The CD spectrum of the purified protein was also collected in presence of either 0.02, 0.2 or 1 mM $CuCl_2$ (inset, gray lines). (B) Equilibrium thermal denaturation experiments as a function of temperature in the range 20-80°C in 20 mM Tris-HCl pH 7.2, 300 mM NaCl; the graph shows the CD data at 222 nm recorded at 1 degree intervals. The T_m was calculated as described in Materials and Methods.*

In order to assign a role to metals in the DNR activity, the same experiments were also carried out in presence of different metals ($CuCl_2$, $ZnCl_2$, $CaCl_2$, $MgCl_2$, $MnCl_2$, $CuSO_4$). Increasing amounts of Cu (Figure 16A, inset) or Zn (not shown) ions caused a loss of the α-helix content, in favour of the β-sheet content, destabilizing the protein (data not shown). The presence of the other metals tested didn't change the CD properties of the protein.

Construction of the three-dimensional homology model of DNR- A dimeric structure of DNR, using as template the crystal structure of 1zyb, was obtained by a homology modelling approach; the reliability of the obtained structure was assured by a sufficient high percentage of sequence identity between the two proteins (22 %) and a good energy profile of the model, showing no misfolded or incorrectly modeled regions.
The obtained structure shows a remarkable similarity with the quaternary structural organization of this superfamily of proteins: the long a-helix linking the N-terminal with the C-terminal domain interacts with the helix contributed by the other monomer to form a hinge between the two subunits (Figure 17).

Figure 17. *Model of the structure of dimeric DNR from P. aeruginosa. The structure is represented as ribbons, and the two monomers are in black and gray, respectively.*

To investigate the putative conformational changes the protein undergoes upon NO-mediated activation, a second model of the DNR protein, based on the active form of CRP from *E. coli* (pdb code: 2cgp) was built and a superposition of the two DNR models is shown in the figure 18.

Figure 18. *Superposition of the two DNR models obtained using as templates CRP protein from E. coli (pdb code: 2cgp, in gray) and the crystal structure of 1zyb (in black).*

4.3 His-tagged DNR protein: expression, purification and characterization.

The DNR protein was engineered to facilitate the purification by introducing a tag. The dnr gene was amplified by PCR and cloned into the pET28b vector in frame with a 6xHistidine tail at the N-terminal of the protein. The plasmid (pET-DNR-HIS) was then transformed into BL21(DE3) *E. coli* strain and the protein was expressed both in presence of 1 mM IPTG or in the absence of inducers (Figure 19A). The DNR-HIS protein was detected by western blot, using commercial anti-histag antibodies (Figure 19A, lane 3). High yields of purified protein (50 mg/l of cell culture) were obtained after a single step of purification, using a nickel HiTrap™ Chelating HP column (Amersham - affinity chromatography). The his-tag tail was then removed by thrombin proteolysis (Figure 19B).

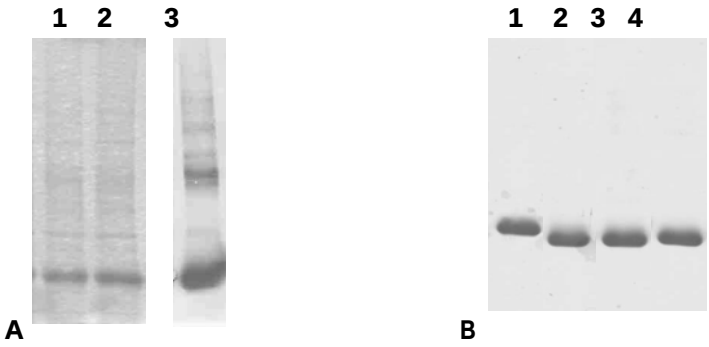

Figure 19. *Expression and purification of the DNR-HIS protein, SDS/PAGE. (A) Lane 1: overnight cell extract without IPTG. Lane 2: overnight cell extract after induction with 1 mM IPTG. Lane 3: western blot analysis of overnight cell extract after induction with 1 mM IPTG using anti his-tag antibodies (Santa Cruz Biotechnology, Inc.). (B) Lane 1: purified DNR-HIS protein. Lane 2-4: room temperature incubation of DNR-HIS with 20 units of thrombin at different times (2h, 4h and 15 h, respectively).*

DNR-HIS protein, as assayed by gel filtration, populates mainly aggregation states higher then the dimer also in presence of 150-300 mM NaCl.
Furthermore, the protein precipitates upon addition of heme, during the titration experiments; so a preliminary characterization was attempted by using only the thrombin-digested protein, which is mainly in the dimeric state in presence of 300 mM NaCl (not shown). This protein, however, also populates high molecular weight aggregates, more then the native protein, as also assayed by native poly-acrylamide gel (Figure 20, lane 1 and 3).

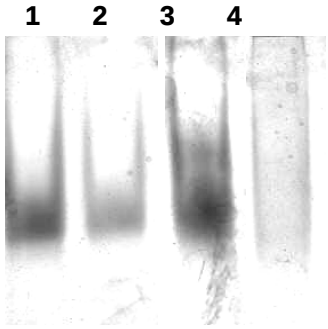

Figure 20. *Poly-acrylamide native gel. Lane 1, purified DNR protein. Lane 2, heme-reconstituted DNR. Lane 3, DNR-HIS protein after proteolysis with thrombin. Lane 4, the same protein , after heme-*

The digested DNR-HIS protein was able to bind *in vitro* the heme, but only

aggregates were detectable in the heme-reconsituted form (Figure 20, lane lane 4).
Due to the difficulty to purify the dimer, the native protein was chosen for the biochemical characterization and activity assays; however, the pET-DNR-HIS vector was used as template for the mutagenesis.

4.4 Mutagenesis: preliminary characterization of the H7A and N152STOP mutants.

The histidine 7 to alanine (H7A) mutation was carried out to determine whether this residue is involved in the heme binding. The H7A mutant was purified as described for the DNR-HIS protein and the thrombin-digested form was characterized.
As reported for the wild-type protein, a heme titration was performed; the mutant was able to bind the cofactor *in vitro* (Figure 21A) and the formation of the complex is maximized when H7A monomer and heme are present in a 1 to 0.54 ratio, respectively (Figure 21B). The calculated stoichiometry of binding is assumed to be one heme per dimer.

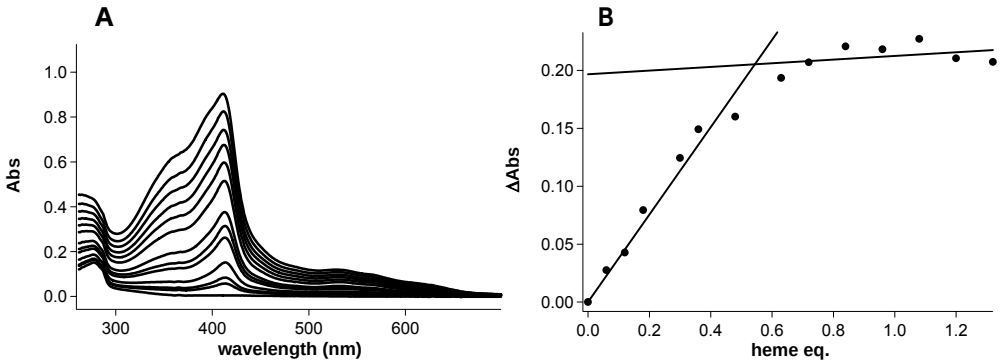

Figure 21. *Binding of heme. (A) Absorbance spectra of the H7A mutant in presence of increasing amount of heme. (B) Plot of delta absorbance (A_{412}-A_{380}) of a H7A/heme solution as a function of heme equivalents.*

The asparagine residue 152, located at the end of the dimerization α-helix in the sequence, was also mutated (in collaboration with G. Giardina, University of Rome) into a stop codon to assign a role to the N-terminal domain in the *in vitro* heme binding. The purified and his-tag free protein was stable as a dimer (as assayed by gel filtration, data not shown) and upon heme titration, was able to bind the cofactor *in vitro*(Figure 22A).
The formation of the complex is maximized when N152STOP monomer and heme are present in a 1 to 0.40 ratio, respectively (Figure 22B).

The calculated stoichiometry of binding is assumed to be one heme per dimer.

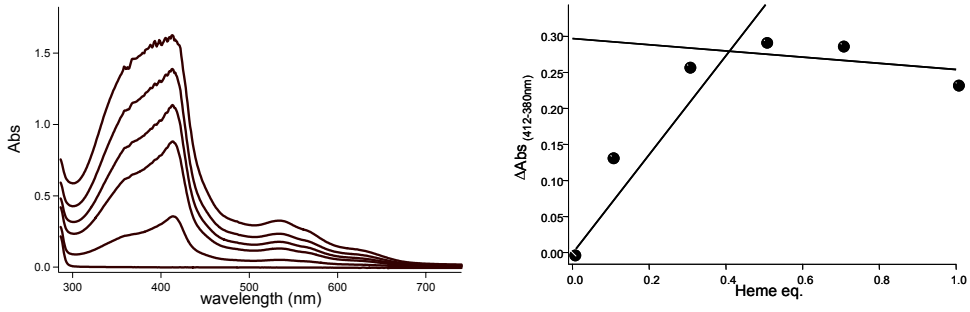

Figure 22. *Binding of heme. (A) Absorbance spectra of the N152STOP mutant in presence of increasing amount of heme. (B) Plot of delta absorbance (A_{412}-A_{380}) of a N152STOP/heme solution as a function of heme equivalents.*

4.5 *in vitro* DNA binding activity of native DNR

Purification -To characterize the DNA binding activity, the DNR protein was partially purified from the homologous background (PAO1 *Pseudomonas aeruginosa* strain). Due to the pathogenity of *P. aeruginosa,* cell growth under low oxygen tension and in presence of nitrate was carried out at the University of East Anglia (Wolfson Fermentation Laboratory, Norwich, UK).
The cell extract was then separated by ammonium sulfate precipitations and the protein was recovered mainly in the 95% precipitate, as confirmed by western blotting (not shown). The sample was then separated on an anion exchange resin (DE-52, Wathman) as shown in Figure 23A , lane 2.
To enrich the sample with the DNR protein, different chromatographic steps were performed (see Materials and Methods section) and the eluate after a nickel column, as an example, is shown in Figure 23A, lane 3; fractions containing DNR, belonging to each separation, have shown a DNA binding activity (see below).

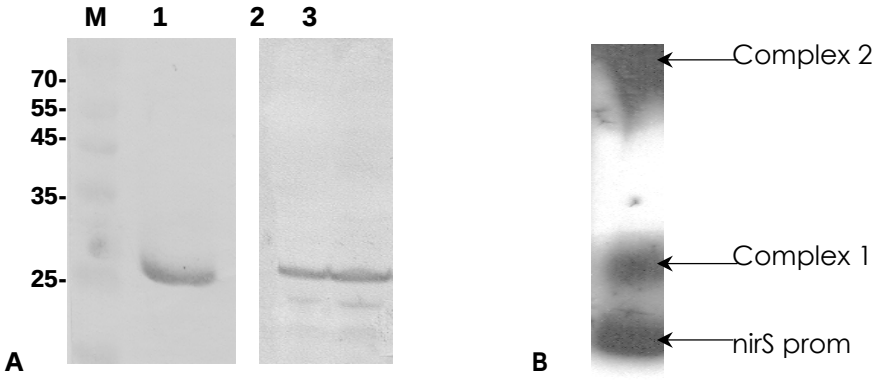

Figure 23. *DNR from P. aeruginosa. (A) SDS/PAGE and western blot detection. Lane M: molecular mass markers 10–180 kDa (MBI Fermentas, Munich,Germany). Lane 1: purified DNR protein. Lane 2: DE-52 eluate. Lane 3: nickel column eluate. (B) DNA binding activity of DNR detected by EMSA. The retardation of the DNA migration indicates that two different complexes were formed (complex 1 and complex 2). Unbound DNA (nirS prom), is also shown.*

DNA binding activity (EMSA) -As assessed by reporter gene experiments in *P. aeruginosa* (Arai *et al.,* 1997), DNR activates *in vivo*, as a transcriptional regulator, the denitrification pathway in response to NO. To demonstrate the direct involvement of the protein in the promoter activation, DNA binding assay (by electrophoretic mobility shift assays - EMSA) were performed.
As a target the nitrite reductase promoter (hereinafter nirS prom) was used, amplified by PCR as a 200 bp fragment with the DNA binding sequence (FNR-box) located in the middle.
The radiolabelled nirS prom was incubated either with PAO1 cell extract or with fractions containing DNR belonging to different chromatographic steps (see above). A retardation in the DNA migration were detected in the EMSA assay, in presence of the DNR protein; the DNA binding activity was obtained in air and two different complexes were populated (Figure 23B).
Competition assays were carried out to demonstrate the specificity towards the nirS prom in the complex formation. Incubation of the reaction mixture with increasing amounts of unlabelled nirS prom mainly affects complex 1 (Figure 24A). As a control, the reaction mixture was incubated with increasing amounts of a 500 bp DNA fragment, as a non specific competitor; the complex 2 content decreased while an increase in the complex 1 band was observed (Figure 24B).

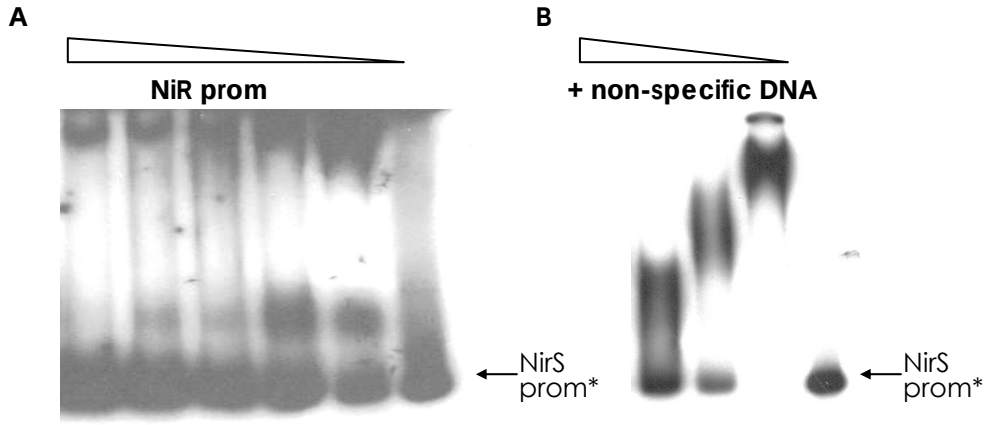

Figure 24. *Dissociation of DNR-nirS prom complexes with competitors detected by EMSA. 10-50 folds excess of competitors were used. (A) The unlabelled nirS prom competes with the ^{33}P radiolabelled one (*)for the complex 1 formation. (B) In the presence of a nonspecific competitor, complex 2 dissociates to form complex 1.*

To demonstrate a direct involvement of the DNR protein in the complex 1 formation, anti-DNR antibodies were used to test their ability to capture the DNR protein eventually present in the complex. The presence of anti-DNR antibodies caused the dissociation of the complex 1, thus suggesting that DNR is involved in complex formation (Figure 25).

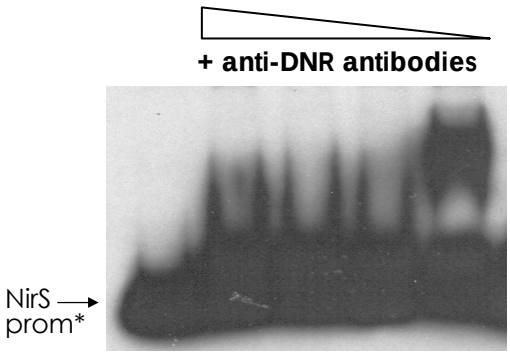

Figure 25. *Dissociation of DNR-nirS prom complex 1 with increasing amounts of antibodies anti-DNR (*2000-50000 fold dilutions) *as competitors. The competition was detected by EMSA and the (*) indicates the migration of free radiolabelled nirS prom.*

4.6 *in vitro* DNA binding activity of recombinant DNR

The DNA binding assay shown above demonstrates for the first time that DNR activates the *nirS* gene by a direct interaction with its promoter. To better characterize the DNR-DNA complex, we performed the same experiments reported in the previous section using the recombinant protein obtained in *E. coli*.
The EMSA assay indicated that the purified protein was not able to bind DNA *in vitro* either in air or, under low oxygen tension, in presence of nitrite or NO (not shown). The same experiments were carried out also using the heme-reconstituted protein and the corresponding NO-bound derivative; we decided to carry out the experiments under low oxygen tension to reproduce more closely the conditions required for the activity of the protein *in vivo* (Arai *et al.*, 1999, 2003). Using these experimental conditions, it was not possible to produce *in vitro* an active form of the DNR protein; therefore different expression systems and/or growth conditions were attempted to obtain upon expression *in vivo* a protein able to bind DNA.

Expression and purification in the presence of heme - In order to assign to the heme cofactor a role in the DNR activity, a different expression system was set to obtain an hemoprotein *in vivo* (Figure 26A) using the expression protocol reported by Varnado C.L. and Goodwin D.C. (2004). The pET-DNR vector was co-transformed with the pHPEX3 vector, overexpressing an outermembrane-bound receptor for heme incorporation, into the BL21-DE(3) *E. coli* cells (hereinafter strain B); the BL21(DE3) *E. coli* strain carrying the pHPEX3 vector alone was used as control.
Protein expression was induced as reported for strain A and the protein was recovered mainly in the soluble fraction of the cell extract (not shown); absorbance spectra of this sample showed a peak at 412 nm which is indicative of a ferric state of the coordinated iron in the heme cofactor. Moreover, the absorbance spectra collected using the control strain showed only a peak at 395 nm, which is due to the contribution of free heme in the sample (Figure 26B).
The protein was then purified by changing the protocol discussed above. Due to the hydrophobic nature of the heme cofactor, protein aggregation and nonspecific interactions with the chromatographic resins were avoided by removing excess of free heme with ammonium sulfate precipitations. The protein sample was recovered in the 50% ammonium sulfate pellet and then applied on a Q-sepharose column (in 20 mM Tris-HCl, 50 mM NaCl).
DNR protein eluted at two different salt concentrations, 120 mM (pool 1) and 200 mM (pool 2) NaCl respectively, and each pool was purified separately using a gel filtration column.

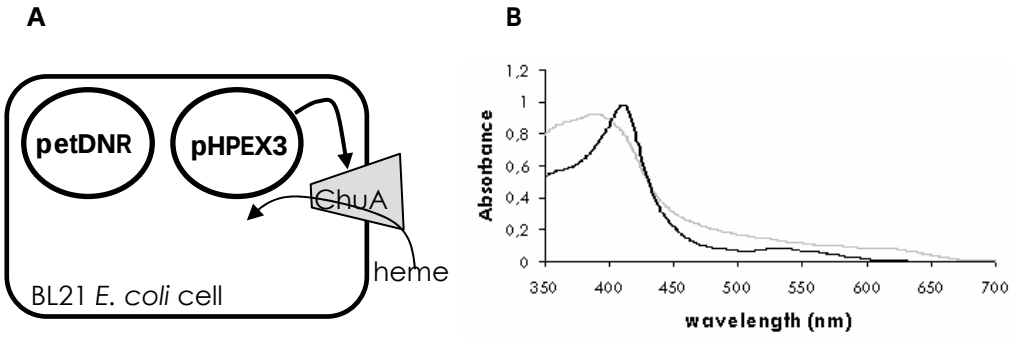

Figure 26. *DNR expression from strain B. (A) Schematic representation of the expression system used. Upon induction of DNR expression with 1 mM IPTG, 20 μM hemin (SIGMA) was added in the growth medium. (B) Absorbance spectra of soluble fractions of strain B (black line) and BL21-PHEX3 (gray line) cell extracts. The presence of a peak at 412 nm indicates that the heme iron is mainly in the ferric in the strain B.*

Purified protein belonging to the different pools showed a different absorbance spectrum (Figure 27) and the DNA binding activity was assayed separately.

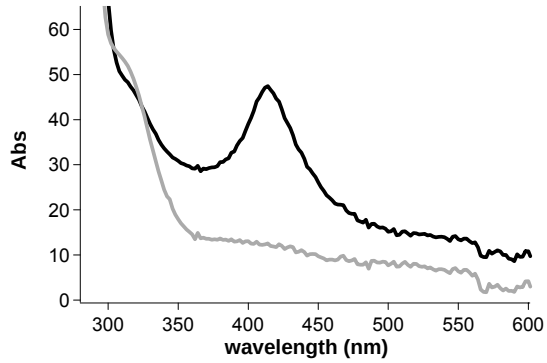

Figure 27. *Absorbance spectra of DNR purified protein. The peak at 412 nm observed in the pool 2 (black line) is absent in the pool 1 fractions (gray line).*

DNA binding assay (EMSA) -Fractions containing the purified DNR protein, belonging to each pool, were incubated with radiolabelled nirS prom and EMSA assays were carried out (Figure 28). A retardation in the DNA migration was observed only in samples containing DNR protein belonging to pool 2 (Figure 28B). The same experiment was carried out under low oxygen tension

and in presence of N-oxides (see Materials and Methods), but changes in the yield of the complex (DNR+DNA) formation were not observed (not shown). Moreover, the DNA binding activity was lost after 2-3 days of storage of the protein at 4°C.

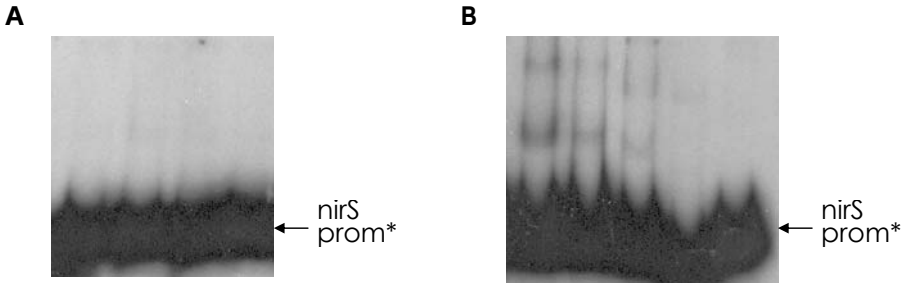

Figure 28. *DNA binding activity of DNR protein analyzed by EMSA. Each sample contained fraction of purified DNR belonging to pool 1 (A) and pool 2 (B), respectively. The (*) indicates the migration of free radiolabelled nirS prom.*

Expression under low oxygen tension - To increase the amount of DNR+DNA complex formation, different growth conditions were assayed. *E. coli* cultures were grown under low oxygen tension and in presence of carbon monoxide (CO) gas, to stabilize the heme-protein complex.
To avoid the protein aggregation problems encountered during the purification of DNR from strain B, strain A was used and the expression was carried out in the presence of an heme precursor (δ-aminolevulinic acid, ALA). As a control the expression was also assaied in air in the presence of the heme precursor. All the conditions were tested also for *E. coli* BL21(DE3) strain without the *dnr* gene.

DNA binding assay (EMSA) -The soluble fraction of the cell exctracts was incubated with the radiolabelled nirS prom DNA and an EMSA assay was performed (Figure 29). Both the strain A and the control strain grown under low oxygen tension in presence of CO gas were able to retard the DNA migration; however the two complexes migrate differently in the gel (Figure 29A, lanes 3 and 6). Competition assays, in presence of increasing amount of unlabelled nirS prom, indicated that the DNR containing samples (strain A) show higher specificity towards the nirS prom then the control sample (Figure 29B).

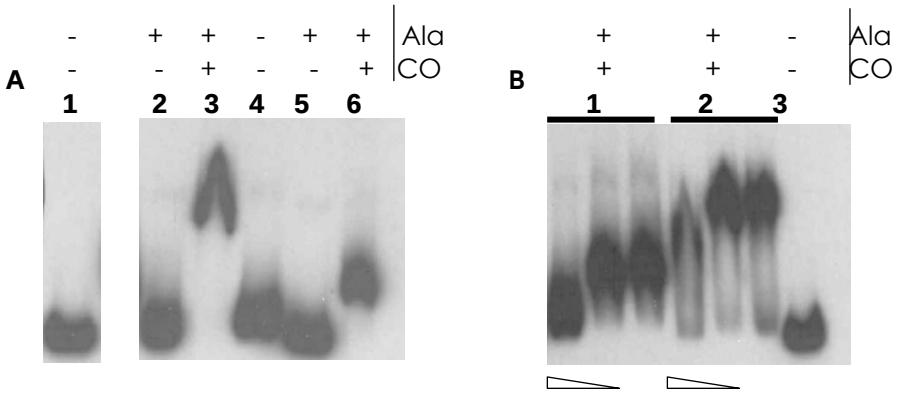

Figure 29. *EMSA of DNA binding activity using cell extracts. (A) lane 1: radiolabelled nirS prom. Lane 2 and 3: BL21(DE3). Lane 4, 5 and 6: BL21(DE3)+pET-DNR. (B) Competition assay in presence of 10-50 folds excess of unlabelled probe as competitor by using BL21(DE3)+pET-DNR (sample 1) and BL21(DE3) (sample 2). Sample 3: radiolabelled nirS prom. Ala: δ-aminolevulinic acid; CO: carbon monoxide.*

The soluble fraction of both cell exctracts were then separated on a Q-sepharose column; all the purification steps and the storage of the protein samples were carried out under nitrogen. Each fraction was then tested for the DNA binding activity (Figure 30). High yields of specific complex were formed in some of the DNR containing fractions (Figure 30A).

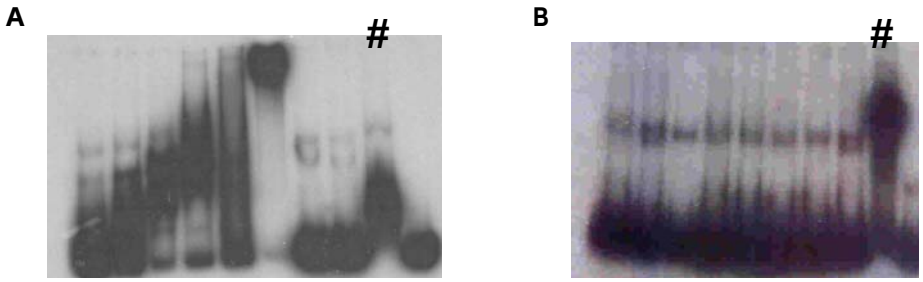

Figure 30. *Complex formation in EMSA using protein samples after the Q-sepharose column. (A)Fractions containing DNR were incubated with radiolabelled nirS prom. (B) Fractions belonging to the control strain were incubated with radiolabelled nirS prom. As a control the corresponding total cell extract was also run (#).*

Fractions able to bind DNA were pooled and incubated with unlabelled nirS prom; the sample was then separated using an agarose gel (see Materials and Methods) and the complex was detected by ethidium bromide staining (Figure 31A). The complex was then extracted from the gel by cutting the

band and the proteins were eluted and analyzed by SDS/PAGE (not shown) and western blot (Figure 31B). The DNR protein was detected in the complex by using the specific anti-DNR antibody and the other proteins were analyzed by mass spectrometry. No other DNA binding protein was detected in the proteins sample (not shown).

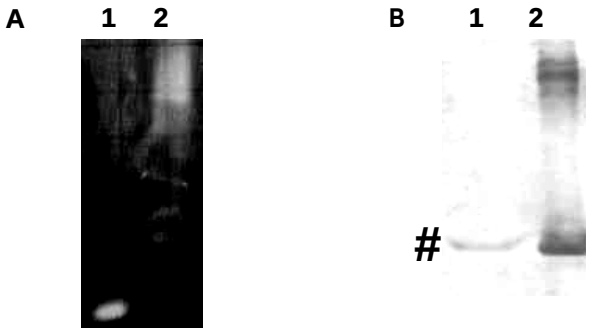

Figure 31. *DNA-DNR complex formation. (A) EMSA on agarose gel; lane 1: unlabelled nirS prom; lane 2: partially purified DNR protein incubated with unlabelled nirS prom. (B) DNR detection by western blot analysis. Lane 1: DNA-DNR complex sample; lane 2: purified DNR protein (#).*

4.7 *in vivo* DNA binding activity of recombinant DNR

Reporter gene - As reported in the previous section, we demonstrated that DNR, also in the recombinant form, is able to bind *in vitro* the nirS prom DNA fragment. To get some insights in the N-oxides mediated activity of DNR as transcriptional regulator, we decided to characterize it also *in vivo* by the reporter gene assay.
The reporter gene (*lacZ*) was cloned downstream to the *melR* promoter from *E.coli* to obtain the pRW50 vector (a gift from S. Busby, UK); this target promoter contains a FNR-box similar to that present in the nirS promoter from *P. aeruginosa*, used in the DNA binding assays *in vitro*.
The *dnr* gene was cloned under the control of the *lac* promoter,weaker then the T7 promoter, in the pUC19 (Biolabs) vector, to lower the expression level of the DNR protein.
Due to the high conservation of the FNR-box target sequence among bacteria, the vectors were co-transformed into a *fnr- E. coli* strain (JRC1728), to minimize the background signal. As a control the double transformed wild type strain *fnr*$^{+}$ (MC1000) was also tested (not shown).
Different conditions were performed to test the capability of DNR to activate the *melR* promoter and the data are reported in the figure 32. The results

indicate that the recombinant form of the DNR protein is not very efficient in this reporter system in the induction of the transcription of the reporter gene either in air or under low oxygen tension in presence of N-oxides.

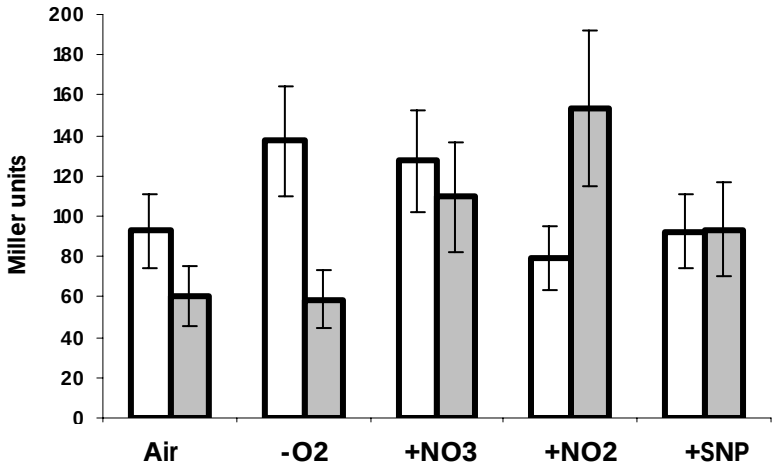

Figure 32. *lacZ reporter gene assay. The β-galactosidase activity were reported as Miller units; the white bars refer to the control fnr⁻ (JRC1728) E. coli strain while the gray ones refer to the same strain carring the pUC-DNR plasmid. All the samples were grown under low oxygen tension (-O_2) except the sample grown in air as control.*

DISCUSSION

Denitrifiers can use nitrate instead of oxygen as the final electron acceptor in the respiratory chain by reducing it to dinitrogen (Zumft, 1997). The step wise reduction of nitrate, catalyzed by four reductases (nitrate, nitrite, NO and nitrous oxide reductases), produces as an obligatory intermediate NO, which may be toxic for cells. Denitrifiers can keep the steady-state concentration of NO below cytotoxic levels by controlling both the expression and the catalytic efficiency of the four reductases involved.
The expression of genes of the denitrification pathway and the N-oxide(s) homeostasis are controlled by NO-responsive regulators belonging to the DNR and NnrR subgroups of the CRP-FNR superfamily. The NO dependence of the transcriptional activity of promoters regulated by these transcription factors has suggested that they may act as NO sensors *in vivo* (Zumft, 2002).
To date, structural and functional information on this class of gas sensors is not available.
In order to understand the biochemical basis of the NO-dependent regulation of the DNR proteins, we have characterized the DNR protein from *P. aeruginosa* and its DNA binding activity.

5.1 DNA binding activity of native DNR

Direct interaction of DNR-like proteins with the putative target promoters was not previously shown. Thus to assign a role to the DNR protein in the promoter's activation we first had to demonstrate that this interaction can indeed occur. A DNR-enriched sample was thus obtained from the total cell extract of *P. aeruginosa* grown under conditions where denitrification should be active (Arai *et al.*, 1995) (i.e. in presence of nitrates and under low oxygen tension).
The protein sample containing DNR was able to form two different complexes with the promoter of the *nirS* gene, one of the putative target promoters (Figure 33). Only one of these complexes proved to be specific: increasing amounts of unlabelled *nirS* promoter or anti-DNR antibody decrease formation of this complex.
These results showed for the first time the direct involvement of a DNR protein in DNA binding *in vitro*, supporting the hypothesis that this class of proteins regulates denitrification *via* direct activation of the target promoters. Moreover these experiments provide a suitable functional assay for the characterization of the NO-dependent DNA binding activity of DNR *in vitro*.

TAGGGATTAGGACCGCACGCTATTCACAGTTGGAAGGTGCCACAAG
CGCAAAGCAACGCAATCTTGATTCCGGTCAAGCAAGGGTAAAGACC
CTGCTTTCTATGATCCTTTCGCGCCATGAATTCCCGGGAGTTCCCGACG
CAGCCACCCCCAAAACACTGCTAAGGGAGC**G**CCTCGCAGGGCTC
CTGAGGAGATAGACC

Figure 33. *nirS promoter sequence from P. aeruginosa. The black sequence represents the FNR box which is located 100 bp upstream the putative transcription start site (bold G).*

5.2 Biochemical and functional characterization of the recombinant DNR (rDNR).

Protein production and general characterization - We have cloned the *dnr* gene from *P. aeruginosa* and purified to homogeneity the protein expressed in *E. coli* using the pET system. The recombinant protein (hereinafter rDNR), produced in high yield (15 mg/lt), is soluble and stable as a dimer (Rinaldo *et al.*, 2005). The dimeric aggregation state is not modified by using reducing agents such β-mercaptoethanol. Only 1 free thiol/monomer was titrated on the protein both in the absence and in the presence of denaturing agents, whereas the total cysteines content deduced from the aminoacid sequence is three/monomer.
Far UV circular dichroism spectra indicate that the protein is folded; the calculated thermal stability (55°C) is in agreement with that reported for the homologous protein CRP from *E. coli* (Blaszczyk and Wasylewski 2003).
To simplify the purification procedure, a fusion rDNR protein with a his-tag sequence was also obtained. The purified protein however was not suitable for the biochemical and functional characterization because of the formation of high molecular weight aggregates. Therefore the native wt DNR protein was used for all the experiments discussed in this section.
In order to characterize the DNA binding activity of DNR, EMSA assays were attempted also with the purified rDNR from *E. coli*. We carried out these experiments also in anaerobiosis by using a nitrogen saturated glove box, in the presence of nitrite or NO. No DNA binding activity was detected by using the purified protein expressed in *E. coli*, suggesting that some cofactor(s) or partner component may be required for the DNA binding activity and the NO sensing.

Cofactor and binding site(s): the hydrophobic cleft - To obtain some insight on the DNR structural organization, ANS (8-anilino-1-naphthalenesulfonic acid) titrations were performed (Rinaldo *et al.*, 2005); due to the high similarity with CRP from *E. coli*, parallel experiments were carried out using CRP.

In the presence of DNR, the fluorescence intensity of ANS increases dramatically with a concomitant blue shift of the wavelength for maximum emission from about 530 nm to 460 nm. Such changes are taken as characteristic of the formation of a protein-ANS complex (Stryer, 1965). ANS titrations on CRP indicates that the protein binds 1 molecule of ANS per monomer with a K_D= 600 μM and a maximum emission wavelength for the CRP-ANS complex at 480 nm. In the presence of 200 μM cAMP, the dissociation constant of CRP-ANS is roughly unchanged (about 500 μM) but the number of binding sites is reduced from 2 to about 1.2/dimer, suggesting that at least one ANS binding site is involved in the cAMP binding (Heyduk and Lee, 1989).
ANS experiments on DNR indicate that the protein binds 1 molecule of ANS per dimer with a K_D= 6.2 μM, suggesting that DNR has a different hydrophobic pocket as compared to CRP. This conclusion is consistent with the maximum emission wavelength of the ANS-DNR and ANS-CRP complexes, which is 460 nm for the ANS bound to DNR, while the CRP-ANS complex peaks at 480 nm. This difference suggests a decrease of solvent accessibility to the hydrophobic cleft of DNR where ANS is bound.
This consideration is consistent with kinetic studies on apomyoglobin, where the formation of intermediates during the folding process (with lower solvent accessibility to the hydrophobic pocket then the unfolded state) results in ANS fluorescence enhancement and a shift towards lower wavelengths of the maximum fluorescence peak (Sirangelo *et al.*, 1998).
The higher affinity for ANS of DNR compared to CRP and the different stoichiometry suggest that DNR may present a different structural organization of the effector domain, indicating that the hydrophobic cleft is a likely candidate for the binding of the cofactor(s) required for NO-mediated activation.
An hydrophobic cleft is clearly observable at the junction between the N-terminal domain and the dimerization helix of the structures obtained by homology modelling using as templates CRP protein from *E. coli* (hereinafter 1cgp) and 1zyb (Figure 34).
The CRP structure used as template for modelling DNR protein is the cAMP bound form, which is the active state able to bind DNA. In this state, the helix-turn-helix domain is rotated towards the β-sheet rich region of the sensor domain.
On the other hand, the 1zyb structure used as a second template displays a different organization of the helix-turn-helix domain, which doesn't involve the interaction with the sensor domain in the region where the hydrophobic cleft is located.

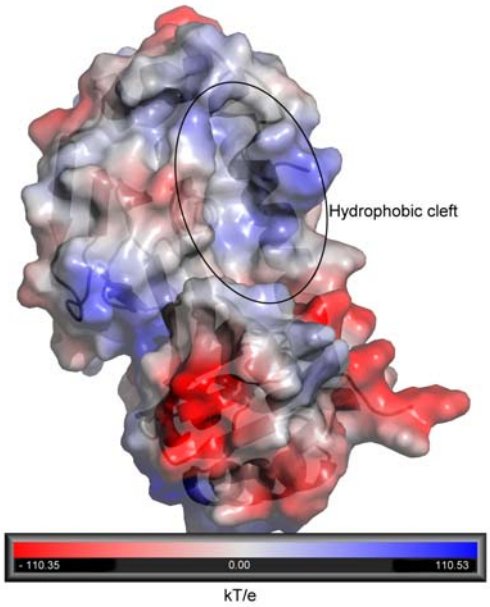

Figure 34. *Model of the distribution of the electrostatic potential, provided by PyMol (Delano, 2002), mapped onto the Connolly surface of one monomer of DNR from Pseudomonas aeruginosa, expressed as kT/e units (1kT/e = 26 mV. at room temperature). Red and blue spots indicate regions negatively and positively charged, respectively. A hypothetical hydrophobic cleft, in which the heme moiety could be accommodated, is highlighted.*

Due to the good energy profile of the two models, both the conformations were assumed to be possible for the DNR protein and a superiposition of the two models was performed. A major contribution to the conformational differences observed between the two model structures comes from the bending of the helix connecting the two domains, and a structural rearrangement of the N-terminal helix of the sensor domain; interestingly, most of this conformational differences involve secondary structure regions surrounding the hydrophobic cleft (Figure 18). Comparison of the two model structures suggests that the conformational change involving the helix-turn-helix domain may be a model of the switch between the active and inactive state of the protein, as reported for the CRP protein (Schultz *et al.*, 1991).
To further investigate the features of the hydrophobic pocket of DNR, titrations with different ligands were attempted; due to the fact that DNR proteins may act as N-oxides sensors, a heme titration was obviously carried out.
Heme titration experiments *in vitro* indicate that the protein binds 1 heme per

dimer and the heme-reconstituted protein is stable as a dimer. The fact that the CRP protein, which shares the same domain organization, is not able to bind the heme *in vitro* suggests that the observed binding site may be a characteristic feature of the DNR protein. The H7A mutant of DNR was still able to bind the heme *in vitro* indicating that this histidine residue is not directly involved in the heme binding. Moreover the N152STOP mutant, which lacks the C-terminal helix-turn-helix domain, is also able to bind the heme *in vitro*. This finding shows that the sensor N-terminal domain is involved in heme binding, suggesting a possible role of the heme in the sensing activity of DNR.
The displacement of ANS bound to DNR by addition of heme indicates that the hydrophobic cleft which is likely to be ANS binding site, is involved in the heme binding, and that the affinity for heme is higher then that for ANS.
To assign a role in NO sensing to the heme-DNR complex a NO-bound derivative was obtained after reduction of the heme with dithionite. Interestingly, the NO-bound derivative shows a peak at 398 nm which is indicative of a five-coordinated form of the heme iron and thus absence of the "proximal" bond with the protein. Reduced hemoprotein saturated with NO can be either six-coordinate or five-coordinate (with breakage of the bond with the proximal histidine)(Table II); the five-coordinated form of the heme-NO complex is reported to be typical of the heme-based sensor domain of the soluble guanylyl cyclase enzyme. Upon NO binding, conformational changes occur and the guanylyl cyclase activity is enhanced (Koesling, 1999).
This evidence has suggested that DNR can sense NO by binding to the heme iron and forming a five-coordinated derivative of the iron of the heme with the proximal histidine-iron bond broken; this ligands rearrangement can modify the C-terminal organization and trigger the DNA binding.

Fe(II)-NO	Coordination	Soret (nm)	Visible (nm)
Six-coordinated	His	420	548, 579
Five-coordinated	-	398	537, 572

Table II. *Absorbance peaks of NO-bound derivative of hemoproteins. The absorbtion maximum of the six-coordinated (Antonini and Brunori, 1971) and five-coordinated (Koesling, 1999) forms are shown.*

Experimental evidence indicates that the native DNR protein from *P. aeruginosa* is able to bind the Hi-Trap chelating resin loaded with nickel or zinc ions. This interaction presumably involves the histidine rich N-terminal

arm, which DNR share with the DNR proteins from *P. stutzeri* (Figure 6). To better evaluate the specificity of the interaction between native DNR from *P. aeruginosa* and metals, titrations and reconstitutions with different metal ions were also attempted.
Circular dichroism experiments indicate that metals (like copper or zinc) can reduce the α-helical content and favour the β one. This effect is reported to be typical of the non-specific interaction of metals with proteins (Golynskiy *et al.*, 2005), suggesting that, at least under the experimental conditions used, specific metal-binding sites are not present and, possibly, are not crucial for promoter activation. This interpretation is also supported by the fact that the native DNR can form a complex with DNA also in presence of EDTA, a well-known chelating agent (see above).

DNA binding activity - DNA binding was initially assayed using the heme-reconstituted protein and its NO-bound derivative; however, no DNA-DNR complex was formed under these experimental conditions. This result may be a consequence of the experimental setting. The heme containing protein has a higher tendency to aggregate thyus impairing the DNA-protein interaction. Moreover, the NO bound derivative was obtained by adding an excess of dithionite and NO-saturated solution, which *per se* can alter the DNA migration and produce DNA damage.
To assign a role to the heme in the DNA binding activity, we thus attempted to express and purify DNR directly as the heme-containing protein.
The DNR protein was coexpressed with an outermembrane pore which favours heme internalization, and hemin was added to the growth medium after induction of protein expression (Varnado and Goodwin, 2004). Two pools of purified DNR protein which showed different spectroscopic properties were obtained. Only the pool characterized by an absorbance peak at 412 nm was able to form a complex with DNA, indicating that expression in the presence of heme leads to biosynthesis of an active pool of heme-DNR protein complex. The ability of the purified protein to form a complex with DNA was observed for 2-3 days after purification. However, complex formation was not improved upon incubation under nitrogen with NO and/or nitrite.
To increase and stabilize the active form of DNR, protein expression under low oxygen tension was also attempted. To favour heme biosynthesis, a heme precursor (δ-aminolevulinic acid, ALA) was used instead of free heme and the overexpression of the outermembrane pore was omitted. The free heme, in fact, due to its capability to interact with hydrophobic molecules can favour aggregates formation and different steps in the purification protocol had to be introduced to remove it.
Moreover, to stabilize the heme-protein complex, 1/40 of saturated atmosphere of carbon monoxide (CO) was also added, to the growth medium.
Both the *E. coli* control strain and that carrying the *dnr* gene were able to bind the *nirS* promoter *in vitro,* but only the latter showed specificity towards

the DNA probe. A semi-purified DNR sample, obtained under nitrogen flux, formed a complex with the *nirS* prom; a western blot analysis of this complex, using anti-DNR antibody, demonstrates the involvment of DNR in the DNA binding.

Our results indicate that the DNR protein from *P. aeruginosa* may sense NO by forming a complex with the protein-bound heme group. The active form of the protein was obtained under low oxygen tension during growth and purification, suggesting that oxygen is damaging. However other cofactor(s) or partner, induced in the cell grown at low oxygen tension, may be required. Interestingly, this proposal is supported by the results obtained by Vollack and Zumft (2001) in which the homologous DnrD protein from *P. stutzeri* was expressed in *E. coli* as a hemoprotein (Vollack and Zumft, 2001). However, overexpression of the DnrD protein in a *dnrD* mutant of *P. stutzeri* uncoupled from the NO mediated activation is unable to induce the denitrification pathway.

It is known that among the CRP-FNR superfamily of transcription factors, heme is used as a redox cofactor to sense gases different from oxygen. The heme-containing transcriptional factor CooA (CO-oxidation activator protein) regulates the expression of genes involved in the oxidation of carbon monoxide (CO) in the bacterium *Rhodospirillum rubrum* (Aono *et al.*, 1996). CooA is a homodimeric protein that senses the presence of CO in a highly reducing environment in the cytoplasm and responds by binding a specific DNA sequence. DNA binding allows a precise interaction with RNA polymerase, leading to the transcription of operons that encode proteins involved in the oxidation of CO to CO_2 and reduction of protons to H_2 (Roberts *et al*., 2005).

This evidence outlines the importance of the redox state of the cell in modulating the effectiveness of the inducer molecule, suggesting that growth conditions are crucial for the production of the active state of these regulators. This may presumably be the case also for DNR protein.

To further test the growth conditions which may enrich the active form of DNR, DNA binding assay *in vivo* were performed by using a reporter gene. As a target, an *E. coli fnr*-like promoter was chosen instead of the *nirS* promoter because while both promoters share an FNR box, only the former is optimized for the *E. coli* transcription machinery. To avoid a background signal due to the *E. coli* FNR protein, an *fnr* mutant strain was used. Significant promoter activation was not detected, even when the cells were exposed to N-oxides under low oxygen tension. As indicated in the literature, the nature of the NO donor or the conditions used to decrease oxygen tension can alter or modulate the activity of this class of gas sensors (Justino *et al.*, 2005; D' Autreaux *et al.*, 2002). Among the DNR type of regulators, the choice of the NO donor or the N-oxide species seems to be crucial.

As an example, in *P. stutzeri* the SNP compound concentration able to trigger the dnrD-mediated response of the *nirSTB* and *norCB* operons is around 1 mM, while the concentration of the NO gas required is around 5-50 nM (Vollack and Zumft, 2001). On the other hand, heterologous expression of

Nnr from *P. denitrificans* in *E. coli* can activate the *melR* promoter in presence of a concentration of SNP as low as 100 μM (Hutchings *et al.*, 2000).

5.3 Conclusions and future perspectives

Our results demonstrate for the first time that the DNR protein regulates the denitrification pathway by binding to the target promoters. The active state of DNR is formed in *P. aeruginosa* under low oxygen tension and in the presence of nitrates. The partially purified native DNR can bind DNA in air, suggesting that the N-oxide(s) induced active protein is possibly modified and thus is stable in the presence of oxygen, after biosynthesis in anaerobiosis.
Considering several other NO sensors, it is not surprising that a derivative of DNR bound to NO can be stable in air; as an example, the heme-containing NO sensor from *Clostridium botulinum* shows a particular geometry of the heme moiety which confers a femtomolar affinity towards NO and consequently a very large stability of the NO bound derivative in air ($t_{1/2}$= 70 h) (Nioche *et al.*, 2004).
The recombinant apo-form of DNR expressed in *E. coli* is unable to bind DNA. We demonstrated that rDNR is able to bind the *nirS* promoter only when heme is present in the growth medium. Moreover, low oxygen tension during both the growth and the purification procedure favours and stabilizes the active state of the protein.
Protein expression in *E. coli* in the presence of N-oxides by using weaker promoters is currently in progress. β-gal reporter gene experiments run in parallel will help us to find the proper growth conditions.
Among NO sensors, the DNR subtype is not well characterized due to the difficulty to obtain the active recombinant form in *E. coli*. Probably, these proteins require some other cofactor(s) and/or partner which are synthesized in *E. coli* less than in the homologous background. For these reasons, we are setting an expression and reporter gene system in *P. putida*, which is a host closer to *P. aeruginosa* then *E. coli.* Cloning and complementation assays are also in progress in *Paracoccus denitrificans*, in collaboration with Dr. van Spanning (Free University, Amsterdam, NL).
The growth conditions and the N-oxide species that will produce the DNR-dependent promoter activation, assayed *in vivo*, will then be applied to set up a purification protocol and to characterize the DNA binding activity *in vitro*.

The biochemical characterization carried out during the thesis work provided very useful information on the DNR protein. As discussed above, we have detected a hydrophobic cleft (through ANS titrations and homology modelling analysis) structurally different from that of CRP. This hydrophobic cleft, located in the sensor domain, is involved in the heme binding *in vitro*; the heme reconstituted protein can form a NO bound derivative.

To further investigate the nature of the axial ligand and the NO binding properties of the heme, MCD and EPR experiments are now in progress in collaboration with A. Thomson and M. Cheesman (Norwich, UK).
Understanding the mechanism of NO sensing in pathogens is a hot topic in NO research. However, too little structural information is available to draw a molecular picture of this process. The biochemical characterization described in this project will hopefully lead to the determination of the 3D structure of DNR by crystallography, presently in progress in our lab (Dr. G. Giardina).

REFERENCES

1. Andrew, C.R., Green, E.L., Lawson, D.M. and Eady, R.R. (2001) Resonance Raman studies of cytochrome *c'* support the binding of NO and CO opposite sides of the heme: implication for ligand discrimination in heme-based sensors. *Biochemistry* **10**, 4115-4122.
2. Antonini, E. and Brunori, M. (1971) Hemoglobin and Myoglobin in their Reactions with Ligands, North-Holland Publishing.
3. Aono, S., Nakajima, H., Saito, K. and Okada, M. (1996) A Novel Heme Protein That Acts as a Carbon Monoxide-Dependent Transcriptional Activator in *Rhodospirillum rubrum*, *Biochem. Biophys. Res. Commun.* **228**, 752-756.
4. Arai, H., Igarashi, Y. and Kodama, T. (1995) Expression of the nir and nor genes for denitrification of Pseudomonas aeruginosa requires a novel CRP/FNR-related transcriptional regulator, DNR, in addition to ANR, *FEBS Lett.* **371**, 73-76.
5. Arai, H., Kodama, T. and Igarashi, Y. (1997) Cascade regulation of the two CRP/FNR-related transcriptional regulators (ANR and DNR) and the denitrification enzymes in Pseudomonas aeruginosa, *Mol. Microbiol.* **25**, 1141-1148.
6. Arai H., Kodama, T. and Igarashi, Y. (1999) Effect of nitrogen oxides on expression of the nir and nor genes for denitrification in Pseudomonas aeruginosa, *FEMS Microbiol. Lett.* **170**,19-24.
7. Arai, H., Mizutani, M. and Igarashi, Y. (2003) Transcriptional regulation of the nos genes for nitrous oxide reductase in Pseudomonas aeruginosa, *Microbiology* **149**, 29-36.
8. Arai, H., Hayashi, M., Kuroi, A., Ishii, M. and Igarashi, Y. (2005) Transcriptional regulation of the flavohemoglobin gene for aerobic nitric oxide detoxification by the second nitric oxide-responsive regulator of Pseudomonas aeruginosa, *J. Bacteriol.* **187**, 3960-3968.
9. Bastian, N.R. and Hibbs, J.B. (1994) Assembly and regulation of NADPH oxidase and nitric oxide synthase, *Curr. Opin. Immunol*. **6**, 131-139.
10. Blaszczyk, U., Wasylewski, Z. (2003) Interaction of cAMP receptor protein from Escherichia coli with cAMP and DNA studied by differential scanning calorimetry, *J Protein Chem.* **22**, 285-93.
11. Brunelli, L., Crow, J.P., and Beckman, J.S. (1995) The comparative toxicity of nitric oxide and peroxynitrite to *Escherichia coli*, *Arch. Biochem. Biophys.* **316**, 327-334.
12. Cannon, W.V., Gallegos, M.T. and Buck, M. (2000) Isomerization of a binary sigmapromoter DNA complex by transcription activators, *Nature Struct. Biol.* **7**, 594-601.
13. Choi, H., Kim, S., Mukhopadhyay, P., Cho, S., Woo, J., Storz, G. and Ryu, (2001) S. Structural basis of the redox switch in the OxyR transcription factor, *Cell* **105**, 103–113.

14. Corker, H. and Poole, R., (2003) Nitric oxide formation by Escherichia coli. Dependence on nitrite reductase, the NO-sensing regulator Fnr, and flavohemoglobin Hmp, *J Biol Chem.* **278** 31584-92.
15. Cruz-Ramos, H., Crack, J., Wu, G., Hughes, M.N., Scott, C., Thomson, A.J., Green, J. and Poole, R.K. (2002) NO sensing by FNR: regulation of the Escherichia coli NO-detoxifying flavohaemoglobin, Hmp, *EMBO J.* **21**, 3235-3244.
16. D'Autreaux, B., Touati, D., Bersch, B., Latour, J.M., and Michaud-Soret, I. (2002) Direct inhibition by nitric oxide of the transcriptional ferric uptake regulation protein via nitrosylation of the iron, *Proc. Natl. Acad. Sci. U. S. A.* **99,** 16619–16624.
17. D'Autreaux, B., Tucker, N.P., Dixon, R. and Spiro, S. (2005) A non-haem iron centre in the transcription factor NorR senses nitric oxide, *Nature* **437**, 769-772.
18. DeLano, W.L. (2002) The PyMOL Molecular Graphics System, DeLano Scientific, San Carlos, CA, USA.
19. Ding, H. and Demple, B. (1997) *In vivo* kinetics of a redox-regulated transcriptional switch, *Proc Natl Acad Sci USA* **94**, 8445–8449.
20. Ermler, U., Siddiqui, R.A., Cramm, R. and Friedrich, B. (1995) Crystal structure of the flavohemoglobin from Alcaligenes eutrophus at 1.75 A resolution, *EMBO J.* **14**, 6067–6077.
21. Fersht, A. (1999) Structure & Mechanism in Protein Science: A Guide to Enzyme Catalysis & Protein Folding, W. H. Freeman & Company.
22. Gardner, A.M., Gessner, C.R. and Gardner, P.R. (2003) Regulation of the nitric oxide reduction operon (norRVW) in *Escherichia coli*. Role of NorR and j 54 in the nitric oxide stress response, *J. Biol. Chem.* **278**, 10081-10086.
23. Gardner P.R., (2005) Nitric oxide dioxygenase function and mechanism of flavohemoglobin, hemoglobin, myoglobin and their associated reductases, *J. Inorg. Biochem.* **99**, 247–266.
24. Galimand, M., Gamper, M., Zimmermenn, A. and Haas, D. (1991) Positive FNR-like control of anaerobic arginine degradation and nitrate respiration in Pseudomonas aeruginosa, *J. Bacteriol.* **173**, 1598-1606.
25. Gilles-Gonzalez, M.A., Gonzalez, G. and Perutz, M.F. (1995) Kinase activity of oxygen sensor FixL depends on the spin state of its heme iron, *Biochemistry* **34**, 232–236.
26. Golynskiy, M.V., Davis, T.C., Helmann, J.D., Cohen, S.M. (2005) Metal-induced structural organization and stabilization of the metalloregulatory protein MntR, *Biochemistry* **44**, 3380-3389.
27. Gomes, C.M., Giuffre`, A., Forte, E., Vicente, J.B., Saraiva, L.M., Brunori, M. and Teixeira, M. (2002) A novel type of nitric-oxide reductase. Escherichia coli flavorubredoxin, *J. Biol. Chem.* **277**, 25273–25276.
28. Green, J., Scott, C. and Guest, J.R. (2001) Functional versatility in the CRP-FNR superfamily of transcription factor: FNR and FLP, *Adv. Microbiol. Rev.* **44**, 1-34.

29. Green J. and Paget M. S., (2004) Bacterial redox sensors, *Nat. Rev. Microbiol.* **2**, 954-66.
30. Hassett, D.J., Cuppoletti, J., Trapnell, B., Lymar, S.V., Rowe, J.J., Yoon, S.S., Hilliard, G.M., Parvatiyar, K., Kamani, M.C., Wozniak, D.J., Hwang, S.H., McDermott, T.R. and Ochsner, U.A. (2002) Anaerobic metabolism and quorum sensing by Pseudomonas aeruginosa biofilms in chronically infected cystic fibrosis airways: rethinking antibiotic treatment strategies and drug targets, *Adv. Drug. Deliv. Rev.* **54**, 1425-1443.
31. Hentzer, M. and Givskov, M. (2003) Pharmacological inhibition of quorum sensing for the tratment of chronic bacterial infections. *J. Clin. Invest.* **112**, 1300-1307.
32. Heyduk, T. and Lee, J.C. (1989) Escherichia coli cAMP receptor protein: evidence for three protein conformational states with different promoter binding affinities, *Biochemistry* **28**, 6914-24.
33. Horowitz, P.M. and Criscimagna, N.L. (1985) Differential binding of the fluorescent probe 8-anilinonaphthalene-2-sulfonic acid to rhodanese catalytic intermediates, *Biochemistry* **24**, 2587-93.
34. Hou, S., Freitas, T., Larsen, R.W., Piatibratov, M., Sivozhelezov, V., Yamamoto, A., Meleshkevitch, E.A., Zimmer, M., Ordal, G.W. and Alam, M. (2001) Globin-coupled sensors: a class of heme-containing sensors in Archaea and Bacteria, *Proc. Natl. Acad. Sci. USA* **98**, 9353–9358.
35. Huie, R.E. and Padmaja, S. (1993) The reaction of NO with superoxide, *Free Radic. Res. Commun*. **18**, 195-199.
36. Hutchings, M.I., Shearer, N., Wastell, S., van Spanning, R.J. and Spiro, S. (2000) Heterologous NNR-Mediated Nitric Oxide Signaling in *Escherichia coli*, *J. Bacteriol.* **182**, 6434-6439.
37. Imlay, J. A. (2002) How oxygen damages microbes: oxygen tolerance and obligate anaerobiosis, *Adv. Microbial Phys.* **46**, 111–153.
38. Justino, M.C., Vicente, J.B., Teixeira, M. and Saraiva, L.M. (2005) New Genes Implicated in the Protection of Anaerobically Grown *Escherichia coli* against Nitric Oxide, *Biol. Chem.* **280**, 2636-2643.
39. Kiley, P.J. and Beinert, H. (1999) Oxygen sensing by the global regulator, FNR: the role of the iron-sulfur cluster, *FEMS Microbiol. Rev.* **22**, 341-352.
40. Kim, S.O., Merchant, K., Nudelman, R., Beyer, W.F. Jr., Keng, T., DeAngelo, J., Hausladen, A., Stamler, J.S., (2002) OxyR: a molecular code for redox-related signalling, *Cell* **109**, 383-396.
41. Koesling, D. (1999) Studing the structure and the regulation of soluble guanylyl cyclase, *Methods* **19**, 485-493.
42. Korner, H., Sofia H.J. and Zumft, W.G. (2003) Phylogeny of the bacterial superfamily of Crp-Fnr transcription regulators: exploiting the metabolic spectrum by controlling alternative gene programs, *FEMS Microbiol. Rev.* **27**, 559-592.

43. Kwiatkowski, A.V. and Shapleigh, J.P. (1996) Requirement of nitric oxide for induction of genes whose products are involved in nitric oxide metabolism in Rhodobacter sphaeroides 2.4.3., *J. Biol. Chem.* **271**, 24382-8.
44. McKay, D.B. and Steitz, T.A. (1981) Structure of catabolite gene activator protein at 2.9 A resolution suggests binding to left-handed B-DNA, *Nature (London)* **290**, 744-749.
45. Miller, J. H. (1992) A short course in bacterial genetics, Cold Spring Harbor Laboratory Press, Cold Spring Harbor, N.Y.
46. Morett, E. and Segovia, L. (1993) The s54 bacterial enhancer-binding protein family: mechanism of action and phylogenetic relationship of their functional domains, *J Bacteriol* **175**, 6067-6074.
47. Mukhopadhyay, P., Zheng , M., Bedzyk , L.A., LaRossa, R.A. and Storz, G. (2004) Prominent roles of the NorR and Fur regulators in the *Escherichia coli* transcriptional response to reactive nitrogen species, *Proc. Natl. Acad. Sci. USA* **101**, 745-750.
48. Myers, J.K., Pace, C.N. and Scholtz, J.M. (1995) Denaturant m values and heat capacity changes: Relation to changes in accessible surface areas of protein unfolding, *Protein Sci* **4**, 2138-2148.
49. Nathan, C.F. and Hibbs, J.B. (1991) Role of nitric oxide synthesis in macrophage antimicrobial activity, *Curr. Opin. Immunol*. **3**, 65-70.
50. Nioche, P., Berka, V., Vipond, J., Minton, N., Tsai, A. and Raman, C. S. (2004) Femtomolar sensitivity of a NO sensor from *Clostridium botulinum, Science* **306**, 1550-1553.
51. North, A.K., Klose, K.E., Stedman, K.M., and Kustu, S. (1993) Prokaryotic enhancer-binding proteins reflect eukaryotic-like modularity: the puzzle of nitrogen regulatory protein C, *J. Bacteriol.* **175**, 4267-4273.
52. Nunoshiba, T., DeRojas-Walker, T., Wishnok, J. S., Tannenbaum, S. R. and Demple, B. (1993) Activation by nitric oxide of an oxidative-stress response that defends Escherichia coli against activated macrophages, *Proc. Natl. Acad. Sci. USA* **90,** 9993–9997.
53. Packer, L. (1996) Nitric oxide, part B: Physiological and pathological process, *Method Enzymol* **269**.
54. Passner, J. M. and Steitz, T. A. (1997) The Structure of a CAP-DNA Complex Having Two Camp Molecules Bound to Each Monomer, *Proc.Nat.Acad.Sci.USA* **94**, 2843-7.
55. Pohlmann, A., Cramm, R., Schmelz, K. and Friedrich, B. (2000) A novel NO-responding regulator controls the reduction of nitric oxide in Ralstonia eutropha, *Mol. Microbiol.* **38**, 626-638.
56. Poole, R. K. (2005) Nitric oxide and nitrosative stress tolerance in bacteria, *Biochem. Soc. Trans.* **33**, 176-180.
57. Poole, R. K. and Hughes, M. N., (2000) New functions for the ancient globin family: bacterial responses to nitric oxide and nitrosative stress, *Mol. Microbiol.* **36**, 775-783.
58. Privalov, P.L., Kechinashvili, N.N. and Atanossov, B.A. (1971) Thermodynamic analysis of thermal transitions in globular proteins. I.

Calorimetric study of ribotrypsinogen, ribonuclease and myoglobin, *Biopolymers* **10**,1865-1890.
59. Riddles, P.W., Blakeley, R.L. and Zerner, B. (1983) Reassessment of Ellman's reagent, *Method Enzymol.* **91**, 49-60,
60. Rinaldo, S., Giardina, G., Brunori, M., Cutruzzola, F. (2005) N-oxide sensing in Pseudomonas aeruginosa: expression and preliminary characterization of DNR, an FNR-CRP type transcriptional regulator, *Biochem. Soc. Trans.* **33**, 184-6.
61. Roberts., G.P., Kerby R.L., Youn, H. and Conrad M. (2005) CooA, a paradigm for gas sensing regulatory proteins, *J Inorg. Biochem.* **99**, 280-92.
62. RoÈmermann, D., Warrelmann, J., Bender, R.A., and Friedrich, B. (1989) An rpoN-like gene of *Alcaligenes eutrophus* and *Pseudomonas facilis* controls expression of diverse metabolic pathways, including hydrogen oxidation, *J. Bacteriol.* **171**, 1093-1099.
63. Šali, A., Potterton, L., Yuan, F., Van Vlijmen, H. and Karplus, M. (1995) Evaluation of comparative protein modeling by MODELLER, *Proteins* **23**, 318-326.
64. Sambrook, J., Fritsch, E. F., and Maniatis, T. (1989) Molecular cloning: a laboratory manual, 2nd ed., Cold Spring Harbor Laboratory, Cold Spring Harbor, NY.
65. Saraiva, L.M., Vicente, J.B. and Teixeira, M. (2004) The role of the flavodiiron proteins in microbial nitric oxide detoxification, *Adv. Microb. Physiol.* **49**, 77-129.
66. Sarti, P., Fiori, P.L., Forte, E., Rappeli, P., Teixeira, M., Mastronicola, D., Sanciu, G., Giuffre`, A. and Brunori, M. (2004) *Trichomonas vaginalis* degrades nitric oxide and expresses a flavorubredoxin-like protein: a new pathogenic mechanism?, *Cell. Mol. Life Sci.* **61**, 618–623.
67. Schultz, S. C., Shields, G. C. and Steitz, T. A. (1991) Crystal structure of a CAP-DNA complex: the DNA is bent by 90 degrees, *Science* **253**, 1001-7.
68. Sippl, M.J. (1993) Recognition of errors in three-dimensional structures of proteins, *Proteins* **17**, 355-362.
69. Sirangelo, I., Bismuto, E., Tavassi, S. and Irace, G. (1998) Apomyoglobin folding intermediates characterized by the hydrophobic fluorescent probe 8-anilino-1-naphthalene sulfonate, *Biochim. Biophys. Acta.* **1385**, 69-77.
70. Unden, G. and Schirawski, J. (1997) The oxygen-responsive transcriptional regulator FNR of Escherichia coli: the search for signals and reactions, *Mol. Microbiol.* **25**, 205-10.
71. Van Spanning, R.J., Houben, E., Reijnders, W.N., Spiro, S., Westerhoff, H.V. and Saunders, N. (1999) Nitric oxide is a signal for NNR-mediated transcription activation in Paracoccus denitrificans, J. Bacteriol. **181**, 4129-4132.

72. Varnado, C.L. and Goodwin, D.C. (2004) System for the expression of recombinant hemoproteins in *Escherichia coli*, *Protein Expr. Purif.* **35**, 76-83.
73. Vollack, K.U. and Zumft, W.G. (2001) Nitric oxide signaling and transcriptional control of denitrification genes in *Pseudomonas stutzeri*, *J. Bacteriol.* **183**, 2516-26.
74. Wink, D. A. and Mitchell, J. B. (1998) Chemical biology of nitric oxide: Insights into regulatory, cytotoxic, and cytoprotective mechanisms of nitric oxide, *Free Radic. Biol. Med*. **25**, 434-456.
75. Wu G., Wainwright, L.M., Poole, R.K. (2003) Microbial globins, *Adv. Microb. Physiol.* **47**, 255–310.
76. Zeng, M. and Storz, G. (2000) Redox sensing by prokariotic transcription factors, *Biochem. Pharmacol.* **59**, 1-6.
77. Zumft, W.G. (1997) Cell biology and molecilar basis of denitrification, *Microbiol. Mol. Biol. Rev*. **61**, 533-616.
78. Zumft, W.G. (2002) Nitric oxide signaling and NO dependent transcriptional control in bacterial denitrification by members of the FNR-CRP regulator family, *J. Mol. Microbiol. Biotechnol.* **4**, 277-86.
79. Zumft, W.G. (2005) Nitric oxide reductases of prokaryotes with emphasis on the respiratory, heme–copper oxidase type, *J. Inorg. Biochem.* **99**, 194–215.

ATTACHMENTS

Cutruzzolà F., Rinaldo S., Centola F., Brunori M. (2003) NO production by Pseudomonas aeruginosa cd1 nitrite reductase, *IUBMB Life* **55**, 617-21. Review.

Rinaldo S., Giardina G., Brunori M., Cutruzzolà F. (2005) N-oxide sensing in *Pseudomonas aeruginosa*: expression and preliminary characterization of DNR, an FNR-CRP type transcriptional regulator, *Biochem Soc Trans.* **33**,188-190.

Rinaldo S., Giardina G., Brunori M., Cutruzzolà F. (2005) N-oxides sensing and denitrification: the DNR transcription factors, *Biochem Soc Trans, in press*

Rinaldo S. and Cutruzzolà F. (2005) Nitrite reductases in denitrification. The nitrogen cycle , Elsevier *in press.*

Centola F., Rinaldo S. Brunori M., Cutruzzolà F. (2005) Histidine 369 controls the reactivity of *Pseudomonas aeruginosa* cd1 nitrite reductase with oxygen, *submitted*.

IUBMB *Life*, 55(10–11): 617–621, October–November 2003

Taylor&Francis healthsciences

Review Article

NO Production by *Pseudomonas aeruginosa* cd_1 Nitrite Reductase

Francesca Cutruzzolà*, Serena Rinaldo, Fabio Centola and Maurizio Brunori
Dipartimento di Scienze Biochimiche, Universita' di Roma "La Sapienza", 00185 Rome, Italy

Summary

The structural and catalytic properties of *Pseudomonas aeruginosa* cd_1 nitrite reductase, a key enzyme in bacterial denitrification, are reviewed in this paper. The mechanism of reduction of nitrite to NO is discussed in detail with special attention to the structural interpretation of function. The ability to stabilize negatively charged molecules, such as the substrate (nitrite) and other ligands (hydroxide and cyanide), is a key feature of catalysis in cd_1NIRs. The positive potential in the active site is largely due to the presence of the two conserved distal histidines, which are involved in both substrate binding and product release.

IUBMB *Life*, 55: 617–621, 2003

Keywords Denitrification; nitrite reductase; cytochrome cd_1; anionic ligands.

INTRODUCTION

In eukaryotes nitric oxide (NO) is a key player in a wide variety of physiological and pathological processes, mostly involving cell to cell signalling and cell–host response. In microrganisms, on the other hand, NO has a well defined biological role as an intermediate in the part of the nitrogen cycle named dissimilatory denitrification, where nitrate is used instead of oxygen as an electron acceptor for energy production and reduced to gaseous nitrogen oxides and nitrogen (NO, N_2O, N_2) (*1*). Denitrification usually prevails at low oxygen tensions or when nitrogen oxides are available as electron acceptors. This metabolic pathway is utilized by human opportunistic pathogens, such as *Pseudomonas aeruginosa*, in microaerofilic environments and high nitrate load conditions (*2*).

The genetic and molecular basis of denitrification have been reviewed (*3–5*). Several redox proteins are involved in this pathway, namely the reductases for nitrate, nitrite, NO and nitrous oxide, and multiple electron donors specific for these enzymes.

Nitrite reductase (NIR) is one of the enzymes in the dissimilative denitrification chain, catalyzing the reduction of nitrite (the toxic product of nitrate reductase activity) to NO. Isolation of NIR from several bacterial sources has shown that there are two distinct classes of nitrite reductases which yield NO as the main reaction product, containing either copper (CuNIR) or heme (cd_1NIR) as cofactor, the heme containing enzyme being more frequent (*6*). This review mainly focuses on the structure–function relationships in the cd_1 nitrite reductase from *Pseudomonas aeruginosa*, with special attention to the NO producing activity of the enzyme.

General Properties

P. aeruginosa cd_1NIR (E.C. 1.9.3.2) (hereinafter Pa-cd_1NIR) was discovered by Horio and coworkers (*7*) and initially studied for its oxygen reductase activity. Later, the work of Yamanaka et al. (*8*) showed that the enzyme is also capable of reducing nitrite, an activity which is the only physiological role of this enzyme. This assignement is based both on kinetic and equilibrium results with the two substrates and on genetic evidence with strains of *P. stutzeri* and *P. aeruginosa* selectively disrupted in the cd_1NIR gene (*9, 10*). The nitrite reductase activity is inhibited by CN^- but insensitive to CO and its reaction product is NO.

The spectroscopic and redox properties of the cd_1NIR from different sources, including that from *P. aeruginosa*, have been reviewed (*11*). Either c-type cytochromes or copper proteins (*11*) can donate electrons to Pa-cd_1NiR *in vitro*, whereas *in vivo* the physiological electron donor could be identified as cytochrome c_{551} (*12*). The interaction is mainly electrostatic in nature and involves the c heme domain on the cd_1NIR.

Structure

Pa-cd_1NIR is a soluble homodimer of 120 KDa and each subunit contains one c heme and one d_1 heme; thus the native dimeric protein carries four metal centres.

Received 12 September 2003; accepted 20 September 2003

Address correspondence to Francesca Cutruzzolà, Dipartimento di Scienze Biochimiche, Universita' di Roma "La Sapienza", P. le A. Moro, 5–00185 Rome, Italy. Tel: +39 6 49910713. Fax: +39 6 4440062. E-mail: francesca.cutruzzola@uniroma1.it

ISSN 1521-6543 print/ISSN 1521-6551 online © 2003 IUBMB
DOI: 10.1080/15216540310001628672

The degree of similarity between different cd_1NIRs is much higher for the C-terminal domain, which interacts with the d_1 heme, than for the N-terminal domain, which contacts the c heme and is particularly low at the N-terminus (*5*).

The high-resolution structure of Pa-cd_1NIR (*13*) shows that each monomer is organized into two distinct domains, one carrying the c heme and the other the d_1 heme (Figure 1A). The former is the electron acceptor pole of the molecule whereas the latter is the site where substrate binds and catalysis occurs. The distances between the hemes within a subunit are about 11 Å edge-to-edge and 20 Å iron-to-iron;

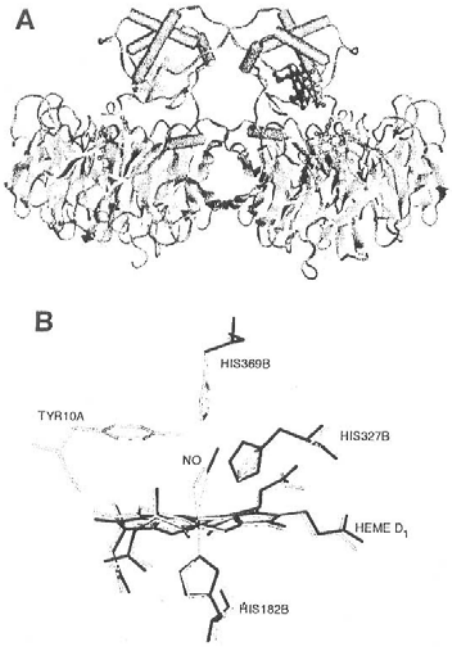

Figure 1. (A) 3D structure of oxidized *P. aeruginosa* cd_1NIR (PDB file 1NIR). The α-helical c heme domain and the β-propeller structure of the d_1 heme domain are shown. The N-terminal arm exchanges between neighbouring monomers. (B) Superposition of the active site of the reduced NO-bound *P. aeruginosa* cd_1NIR wild type (grey) (PDB file 1NNO) and of the same derivative of the H369A mutant (black) (PDB file 1HZV). The residues labels refer to the wild type numbering. The position and orientation of NO is significantly different in the two structures.

those between subunits are much larger (> 35 Å). A semiapoprotein containing only the c heme can be obtained either chemically (*14*) or by recombinant DNA techniques (*15*). The apoprotein can be reconstituted with purified or chemically synthetized d_1 heme (*15, 16*), with good recovery of the spectroscopic properties and of the enzymatic activities.

In Pa-cd_1NIR the c heme domain is mainly α-helical (Figure 1A); the N-terminal segment from the c heme domain extends towards the d_1 heme domain and is inserted in the active site pocket. Unexpectedly a 'domain swapping' has been observed in Pa-cd_1NIR, whereby the N-terminal tail of one monomer contacts the d_1 heme site of the neighbouring monomer (Figure 1A).

The c heme is hexacoordinated and low spin in both reduction states (*17,18*); the iron is His-Met coordinated both in the crystal and in solution, as suggested by spectroscopic studies (*18,19*). The c heme in Pa-cd_1NIR may form a complex with several ligands (NO, CN^-) under conditions in which eukaryotic cytochome c does not.

The d_1 heme (3,8-dioxo-17-acrylate-porphyrindione) is unique to denitrifiers containing the cd_1NIR, where it is synthesized starting from δ-aminolevulinic acid *via* uroporphyrinogen III (*5*). Since it is so unique, it was suggested that it could be responsible for some catalytic features of the enzyme. The presence of the electronegative oxo groups confers to the macrocycle distinct redox properties, rendering it harder to oxidise than the corresponding isobacteriochlorines (*20*), and thus shifting the redox potential of the iron to more positive values. The chemical nature of heme d_1 has been confirmed by inspection of the crystal structures of cd_1NIRs, were is mostly found in a distorted, saddle-like conformation (*13,21–23*).

The d_1 heme binds the physiological oxidants (O_2, nitrite) as well as other heme ligands. The d_1 heme in Pa-cd_1NIR is a low spin, hexacoordinated species in the ferric state, and high spin pentacoordinated in the ferrous state (*17,19*). One axial ligand is always provided by a histidine and the sixth ligand in the low spin ferric form is an hydroxide ion (*13*). In the oxidized cd_1NIR from *Paracoccus pantotrophus* (Pp-cd_1NIR) the sixth ligand was initially assigned to a tyrosine located in the N-terminal segment and thus belonging to the c heme domain (see above) (*21*). This tyrosine residue is poorly conserved among the cd_1NIRs from different species (*5*), and has a marginal role in nitrite reduction as shown by mutagenesis of Tyr10 to Phe in Pa-cd_1NIR (*24*) and of Tyr25 in Pp-cd_1NIR (*25*). The tyrosine-coordinated oxidized state is catalytically inactive and thus represents a resting state of the Pp-cd_1NIR, not found in the other known cd_1NIRs.

Among the other residues found in close proximity of the d_1 heme, an important role in catalysis is played by two conserved histidine residues (His327 and His369) which are hydrogen bonded directly to the ligand hydroxide in the Pa-cd_1NIR oxidized structure (*13*) or to a water molecule in the Pp-cd_1NIR oxidized structure (*21*). These residues were predicted to be good candidates to be involved in the

protonation and dehydration of nitrite; their role is discussed below.

Catalytic Mechanism of Nitrite Reduction

The monoelectronic reduction of nitrite to yield NO is the main activity of cd_1NIR *in vivo*. The mechanism of nitrite reduction involves chemically complex steps such as the transfer of a reducing equivalent into an electron-rich species, e.g. the nitrite anion bound to the d_1 heme iron, followed by protonation and dehydration. Product inhibition may occur, since the NO produced at the catalytic site forms stable complexes with the ferrous d_1 heme and, at acidic pH, also with the c heme (*26*). A possible reaction scheme for cd_1NIR, shown in Figure 2, assumes that functional interactions between the two monomers can be neglected, which may not necessarily be the case.

Catalysis occurs at the d_1 heme with the substrate (nitrite) and product (NO) bound to the iron *via* the nitrogen atom, as seen in the crystal structure of the nitrite bound transient species (*23*) of Pp-cd_1NIR and NO bound reduced derivative of both Pa-cd_1NIR and Pp-cd_1NIR (*22,23*).

A nitrosyl intermediate (d_1-$Fe^{2+}NO^+$) is formed during catalysis, as shown in $^{18}O/^{15}N$ exchange experiments (*27*). Spectroscopic evidence of this species, which is EPR silent, has been obtained by FTIR on the oxidized, NO reacted, *P. stutzeri* enzyme (*28*). The nitrosyl intermediate, which is formally equivalent to (d_1-$Fe^{3+}NO$), is chemically unstable and rapidly decays to d_1-Fe^{3+} plus NO (Figure 2). Formation of a ferrous π-cation radical is facilitated by the oxo groups of the macrocycle which increase the positive charge on the iron; under these conditions, a weakening of the Fe-NO bond is expected and NO dissociation occurs readily in the presence of a nucleophile. Reduction of either transient species leads to the formation of a paramagnetic (d_1-$Fe^{2+}NO$) stable adduct *in vitro* with slow NO dissociation rates, which has been observed by EPR (*29*) (Figure 2).

As detailed above, for cd_1NIR to accomplish a productive turnover, a balance between product release and re-reduction

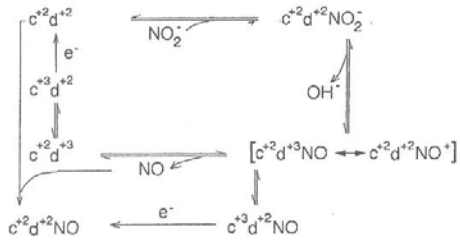

Figure 2. Proposed reaction mechanism for nitrite reduction by *P. aeruginosa* cd_1NIR.

of the d_1 heme is critical to avoid product inhibitory effects. In Pa-cd_1NIR the internal electron transfer between c and d_1 heme is slow ($1-3\ s^{-1}$) (*29,30*) thus allowing enough time for NO dissociation. On the other hand pulse radiolysis studies on the Pp-cd_1NIR and on *Pseudomonas stutzeri* cd_1NIR have shown that the electron transfer rate is much larger in these proteins (*30, 31*). The reason for this difference is still unclear.

It is worthwhile mentioning that the steady state oxidation of macromolecular substrates by Pa-cd_1NIR with nitrite as electron acceptor is much slower at pH above 6.5 (*26*). Thus, under pre-steady state conditions at pH 6.2, the enzyme is locked in the NO inhibited form after one catalytic cycle in the presence of excess reducing equivalents (*29*).

Insight into the molecular mechanism of catalysis comes from the results on the mutants of the two conserved histidines (His327 and His369 in Pa-cd_1NIR) located near the active centre. Substitution of either of the two His with Ala has a dramatic effect on nitrite reduction, but only a marginal effect on the oxygen reductase activity (*32*).

A common feature of the two His mutants in the reaction with nitrite is that they are both trapped in the reduced-NO bound species faster than the wt Pa-cd_1NIR. Given that the intramolecular electron transfer rate was found to be unchanged in these mutants, the increased probability of trapping may originate in a decreased rate of NO dissociation from the ferric d_1 heme. Reduction of the positive potential in the d_1 heme pocket by substitution of either one of the two invariant active site His with Ala may lead to the loss of the hydroxyl coordinated to the ferric d_1 heme iron in the wt enzyme (*13*) which should assist NO dissociation.

On the other hand, the two His are not equally important in controlling the affinity for the anionic substrate nitrite: His369 was shown to be essential. This inequivalence was shown by stopped-flow experiments (*32*) in which no significant amount of the Michaelis complex can be detected for the H369A mutant; the reaction with nitrite proceeds from the reduced state to the reduced NO-bound derivative without detectable intermediates (see Figure 2).

The affinity of ferrous heme proteins for anions is usually very low; a well known example is ferrous hemoglobin which binds cyanide with a $K_d \cong 1$ M. On the contrary, in the case of NIR, the ferrous d_1 heme displays high affinity for both nitrite and cyanide ($K_d = 10^{-6}$ M). The importance of the active site His369 in the stabilization of anionic ligands was confirmed by investigation of cyanide binding to Pa-cd_1NIR mutants (*33*). Since cyanide cannot be reduced, it is a useful probe of the affinity of the ferrous d_1 heme for anions and the role of the immediate structure of the protein in controlling binding. The results show that the mutant H369A exhibits a much lower affinity also for cyanide, with a ten-fold increase in the equilibrium dissociation constant as compared for the wt protein (*33*).

The structure of the reduced and nitrite-reacted forms of Pa-cd$_1$NIR wt and of the H369A mutant were also determined (*22,34*). In the wt the reduced form is pentacoordinated, consistently with spectroscopic evidence, and the product NO, bound to the d_1 heme, has a bent geometry, with a Fe-N distance of 1.8 Å. Besides the absence of the hydroxide ion, which is the sixth coordination ligand of the heme in the oxidized structure, a major difference seen upon reduction of the wt enzyme is the rotation of Tyr10 away from the position adopted in the oxidized form.

In the oxidized form of the H369A mutant a large topological change is seen in the whole c-heme domain, which is displaced 20 Å from the position occupied in the wt enzyme. Moreover, the distal side of the d_1 heme pocket appears to have undergone structural rearrangement and Tyr10 has moved completely out of the active site, together with the N-terminal arm. In the H369A-NO complex, the position and orientation of NO is significantly different from that of the NO bound to the reduced wt structure (Figure 1B) (*34*). Thus in the His mutants, the greater accessibility of the active site resulting from the conformational change of the N-terminus, in combination with the substitution of His with Ala, likely results in a significant change of the electrostatic potential at the active site. This change might result in the destabilisation of the hydroxide ion hydrogen bonded to the iron and explain the different position of NO in the mutant H369A with respect to NO-bound wt complex.

In summary the stabilization of negatively charged molecules, either substrates (nitrite) or ligands (hydroxide and cyanide) is a key feature of catalysis in cd$_1$NIRs. The positive potential in the active site is enhanced by the presence of the two conserved histidines which are involved in both substrate (nitrite) binding and product (NO) release. There are still open questions such as the role of the d_1 heme in the displacement of NO and the role of the redox state of the c heme during catalysis. The latter may be involved in triggering the conformational changes seen upon reduction and related to the low rate of c-to-d_1 electron transfer measured for the Pa-cd$_1$NIR, which we believe to be critical to avoid product inhibition.

ACKNOWLEDGEMENTS

This work was supported from grants from MIUR of Italy (PRIN 2001) and from the University of Rome La Sapienza (Facoltà 2001, 2002).

REFERENCES

1. Stouthamer, A. H. (1989) Bioenergetics and yields with electron acceptors other than oxygen. *In: Handbook on anaerobic fermentations* (Erickson, L.E. and Yee-Chak Fung D., eds.) pp. 345–437, Marcel Dekker, N.Y.
2. Hassett, D. J., Cuppoletti, J., Trapnell, B., Lymar, S. V., Rowe, J. J., Yoon, S. S., Hilliard, G. M., Parvatiyar, K., Kamani, M. C., Wozniak, D. J. *et al.* (2002) Anaerobic metabolism and quorum sensing by Pseudomonas aeruginosa biofilms in chronically infected cystic fibrosis airways: rethinking antibiotic treatment strategies and drug targets, *Adv. Drug. Del. Rev.* **54**, 1425–1443.
3. Berks, B. C., Ferguson, S. J., Moir, J. W. B. and Richardson, D. J. (1995) Enzymes and associated electron transport systems that catalyse the respiratory reduction of nitrogen oxides and oxyanions. *Biochim. Biophys. Acta* **1232**, 97–173.
4. Hollocher, T. C. and Hibbs, J. B. Jr. (1996) Enzymes of bacteria, plants and fungi that process free nitrogen oxides. *In: Methods in nitric oxide research*. (Feelish, M. and Stamler, J.S. eds.) John Wiley & Sons, Ltd, Chichester, United Kingdom.
5. Zumft, W. G. (1997) Cell biology and molecular basis of denitrification, *Microbiol. Mol. Biol. Rev.* **61**, 533–616.
6. Coyne, M. S., Arunakumari, A., Averill, B. A. and Tiedje, J. M. (1989) Immunological identification and distribution of dissimilatory heme cd$_1$ and non heme copper nitrite reductases in denitrifying bacteria, *Appl. Environ. Microbiol.* **55**, 2924–2931.
7. Horio, T., Higashi, T., Sasugawa, M., Kusai, K., Nakai, M. and Okunuki, K. (1960) Purification and properties of cytochrome oxidase from *Pseudomonas aeruginosa*. *Biochem. J.* **77**, 194–201.
8. Yamanaka, T., Otn, A. and Okunuki, K. (1961) A nitrite reducing system reconstructed with purified cytochrome components of *Pseudomonas aeruginosa*. *Biochim. Biophys. Acta* **53**, 294–308.
9. van Spanning, R. J. M., deBoer, A. P. N., Reijnders, W. N. M., Westerhoff, H. V., Stouthamer, A. H. and van der Oost, J. (1997) FnrP and NNR of *Paracoccus denitrificans* are both members of the FNR family of transcriptional activators but have distinct roles in respiratory adaptation in response to oxygen limitation. *Mol. Microbiol.* **23**, 893–907.
10. Zumft, W. G., Dohler, K., Körner, H., Löchelt, S., Viebrock, A. and Frunzke, K. (1988) Defects in cytochrome cd$_1$-dependent nitrite respiration of transposon Tn5-induced mutants from *Pseudomonas stutzeri*. *Arch. Microbiol.* **149**, 492–498.
11. Cutruzzolà, F. (1999) Bacterial nitric oxide synthesis, *Biochim. Biophys. Acta* **1411**, 231–249.
12. Vijgenboom, E., Bush, J. E. and Canters, G. W. (1997) *In vivo* studies disprove an obligatory role of azurin in denitrification in *Pseudomonas aeruginosa* and show that *azu* expression in under control of RpoS and ANR, *Microbiology* **143**, 2853–2863.
13. Nurizzo, D., Silvestrini, M. C., Mathieu, M., Cutruzzolà, F., Bourgeois, D., Fülop, V., Hajdu, J., Brunori, M., Tegoni, M. and Cambillau, C. (1997) N-terminal arm exchange is observed in the 2.15 Å crystal structure of oxidized nitrite reductase from *Pseudomonas aeruginosa*. *Structure* **5**, 1157–1171.
14. Hill, K. E. and Wharton, D. C. (1978) Reconstitution of the apoenzyme of cytochrome oxidase from *Pseudomonas aeruginosa* with heme d_1 and other heme groups. *J. Biol. Chem.* **253**, 489–495.
15. Silvestrini, M. C., Cutruzzolà, F., D'Alessandro, R., Brunori, M., Fochesato, N. and Zennaro, E. (1992) Expression of *Pseudomonas aeruginosa* nitrite reductase in *Pseudomonas putida* and characterization of the recombinant protein. *Biochem. J.* **285**, 661–666.
16. Weeg-Aerssens, E., Wu, W., Ye, R. W., Tiedje, J. M. and Chang, C. K. (1991) Purification of cytochrome cd$_1$ nitrite reductase from *Pseudomonas stutzeri* JM300 and reconstitution with native and synthetic heme d_1, *J. Biol. Chem.* **266**, 7496–7502.
17. Muhoberac, B. B. and Wharton, D. C. (1983) Electron paramagnetic resonance study of the interaction of some anionic ligands with oxidised *Pseudomonas* cytochrome c oxidase, *J. Biol. Chem.* **258**, 3019–3027.

18. Timkovich, R. and Cork, M. S. (1983) Magnetic susceptibility measurements on *Pseudomonas* cytochrome cd_1. *Biochim. Biophys. Acta* **742**, 162–168.
19. Sutherland, J., Greenwood, C., Peterson, J., and Thomson A. J. (1986) An investigation of the ligand binding properties of *Pseudomonas aeruginosa* nitrite reductase, *Biochem. J.* **233**, 893–898.
20. Barkigia, K. M., Chang, C. K., Fajer, J. and Renner, M. W. (1992) Models of heme d_1. Molecular structure and NMR characterization of an iron(III) dioxoisobacteriochlorin (porphyrindione). *J. Am. Chem. Soc.* **114**, 1701–1707.
21. Fülöp, V., Moir, J. W. B., Ferguson, S. J. and Hajdu, J. (1995) The anatomy of a bifunctional enzyme: structural basis for reduction of oxygen to water and synthesis of nitric oxide by cytochrome cd_1. *Cell* **81**, 369–377.
22. Nurizzo, D., Cutruzzolà, F., Arese, M., Bourgeois, D., Brunori, M., Tegoni, M. and Cambillau, C. (1998) Conformational changes occurring upon reduction and NO binding in nitrite reductase from *Pseudomonas aeruginosa*, *Biochemistry* **37**, 13987–13996.
23. Williams, P. A., Fülöp, V., Garman, E. F., Saunders, N. F. W., Ferguson, S. J. and Hajdu, J. (1997) Haem-ligand switching during catalysis in crystals of a nitrogen-cycle enzyme, *Nature* **389**, 406–412.
24. Cutruzzolà, F., Arese, M., Grasso, S., Bellelli, A. and Brunori M. (1997) Mutagenesis of nitrite reductase from *Pseudomonas aeruginosa*: tyrosine 10 is not involved in catalysis, *FEBS Lett.* **412**, 365–369.
25. Gordon, E. H., Sjogren, T., Lofqvist, M., Richter, C. D., Allen, J. W., Higham, C. W., Hajdu, J., Fulop, V. and Ferguson, S. J. (2003) Structure and kinetic properties of *Paracoccus pantotrophus* cytochrome cd_1 nitrite reductase with the d_1 heme active site ligand tyrosine 25 replaced by serine. *J. Biol. Chem.* **278**, 11773–11781.
26. Silvestrini, M. C., Colosimo, A., Brunori, M., Walsh, T. A., Barber, D. and Greenwood, C. (1979) A reevaluation of some basic structural and functional properties of *Pseudomonas* cytochrome oxidase. *Biochem. J.* **183**, 701–709.
27. Kim, C. H. and Hollocher, T. C. (1983) ^{15}N tracer studies on the reduction of nitrite by the purified dissimilatory nitrite reductase of *Pseudomonas aeruginosa*. *J. Biol. Chem.* **258**, 4861–4863.
28. Wang, Y. and Averill, B. A. (1996) Direct observation by FTIR spectroscopy of the ferrous heme-NO^+ intermediate in the reduction of nitrite by a dissimilatory heme cd_1 nitrite reductase, *J. Am. Chem. Soc.* **118**, 3972–3973.
29. Silvestrini, M. C., Tordi, M. G., Musci, G. and Brunori, M. (1990) The reaction of *Pseudomonas* nitrite reductase and nitrite, *J. Biol. Chem.* **265**, 11783–11787.
30. Kobayashi, K., Koppenhofer, A., Ferguson, S. J., Watmough, N. J. and Tagawa, S. (2001) Intramolecular electron transfer from c heme to d_1 heme in bacterial cytochrome cd_1 nitrite reductase occurs over the same distances at very different rates depending on the source of the enzyme, *Biochemistry* **40**, 8542–8547.
31. Farver, O., Kroneck, P. M., Zumft, W. G. and Pecht, I. (2003) Allosteric control of internal electron transfer in cytochrome cd_1 nitrite reductase, *Proc. Natl. Acad. Sci. U S A.* **100**, 7622–7625.
32. Cutruzzolà, F., Brown, K., Wilson, E. K., Bellelli, A., Arese, M., Tegoni, M., Cambillau, C. and Brunori, M. (2001) The nitrite reductase from *Pseudomonas aeruginosa*: essential role of two active site histidines in the catalytic and structural properties, *Proc. Natl. Acad. Sci. USA* **98**, 2232–2237.
33. Sun, W., Arese, M., Brunori, M., Nurizzo, D., Brown, K., Cambillau, C., Tegoni, M. and Cutruzzolà, F. (2002) Cyanide binding to cd(1) nitrite reductase from Pseudomonas aeruginosa: role of the active-site His369 in ligand stabilization, *Biochem. Biophys. Res. Commun.* **291**, 1–7.
34. Brown, K., Roig-Zamboni, V., Cutruzzolà, F., Arese, M., Sun, W., Brunori, M., Cambillau, C. and Tegoni M. (2001) Domain swing upon His to Ala mutation in nitrite reductase of *Pseudomonas aeruginosa*, *J. Mol. Biol.* **312**, 541–554.

188 Biochemical Society Transactions (2005) Volume 33, part 1

N-oxides sensing in *Pseudomonas aeruginosa*: expression and preliminary characterization of DNR, an FNR–CRP type transcriptional regulator

S. Rinaldo, G. Giardina, M. Brunori and F. Cutruzzolà[1]
Department of Biochemical Sciences 'A. Rossi Fanelli', University of Rome La Sapienza, P.le A. Moro 5, 00185 Rome, Italy

Abstract

In denitrifying bacteria, the concentration of NO is maintained low by a tight control of the expression and activity of nitrite and NO reductases. Regulation involves redox-linked transcription factors, such as those belonging to the CRP-FNR superfamily, which act as oxygen and N-oxide sensors. Given that few members of this superfamily have been characterized in detail, we have cloned, expressed and purified the dissimilative nitrate respiration regulator from *Pseudomonas aeruginosa*. To gain insights on the structural properties of the dissimilative nitrate respiration regulator, we have also determined the aggregation state of the purified protein and its ability to bind hydrophobic compounds such as 8-anilino-1-naphthalenesulphonic acid.

Introduction

In denitrifying bacteria, the concentration of extracellular NO is maintained low (nanomolar) by a tight control of the expression and activity of nitrite and NO reductases. Regulation involves redox-linked transcription factors, such as those belonging to the CRP-FNR (where CRP stands for cAMP receptor protein and FNR stands for fumarate and nitrate reductase regulator) superfamily [1], structurally related to the CRP from *Escherichia coli* [2]. FNR belongs to this superfamily, which contains an Fe-S cluster bound to a set of conserved cysteines and the fnr-like proteins (ANR, FnrA, FnrP), active under low-oxygen tension [1]. Other modulatory proteins, such as those of the dnr subtype [3–5], lack the conserved cysteine cluster and regulate both the nitrite reductase (*nirS*) and nitric oxide reductase (*norCB*) gene expressions. The NO dependence of the transcriptional activity of promoters regulated by these proteins has suggested, by genetic approach, that these factors may act as NO sensors *in vivo* [6,7].

Given that no structural information and little biochemical data are available on the dnr-type class of regulators, we have cloned, expressed and purified the DNR (dissimilative nitrate respiration regulator) protein from *Pseudomonas aeruginosa*. In this species, the *dnr* gene is located upstream of the *nir* and *nor* gene clusters, and it was shown to be able to transactivate *in vivo* the *nirS*, *norCB* and *nos* (nitrous oxide reductase) promoters in response to nitrite [8,9]. DNR is 227 amino acids long; primary structural analysis and molecular modelling suggest the presence of three domains. The signal sensing domain is located at the N-terminus, followed by a long dimerization helix, and at the C-terminus a helix–turn–helix domain was found which was involved in the recognition of the DNA target sequence, the FNR box ($TTGATN_4ATCAA$), conserved both in the FNR target promoter and in the *nir–nor* promoters [10].

To gain insights on the structural properties of DNR, we have also determined the aggregation state of the purified protein and its ability to bind hydrophobic compounds such as ANS (8-anilinonaphthalene-1-sulphonic acid).

Key words: anaerobiosis, denitrification, nitric oxide, *Pseudomonas aeruginosa*, sensor, transcriptional regulation.

Abbreviations used: ANS, 8-anilinonaphthalene-1-sulphonic acid; CRP, cAMP receptor protein; DNR, dissimilative nitrate respiration regulator; FNR, fumarate and nitrate reductase regulator; IPTG, isopropyl β-D-thiogalactoside; 2-ME, 2-mercaptoethanol.

[1]To whom correspondence should be addressed (email francesca.cutruzzola@uniroma1.it).

Materials and methods

Cloning

The *dnr* gene was amplified from *P. aeruginosa* PAO1 strain genomic DNA. The purified PCR product, verified by sequencing, was ligated into a pET28b vector (Novagen) to yield the pET-DNR plasmid and transformed into BL21-(DE3) *E. coli* strain for expression.

Expression and purification

Expression of the protein was obtained at 25 and 37°C in Luria–Bertani medium containing 30 μg/ml kanamycin. Expression was induced with 1 mM IPTG (isopropyl β-D-thiogalactoside) and cells were grown for 15 h after induction. Cells were resuspended in 50 mM Tris buffer (pH 8.0), 50 mM NaCl, 2 mM EDTA, 2 mM 2-ME (2-mercaptoethanol) and 1 mM PMSF and sonicated. The cell extract, after centrifugation, was dialysed against 20 mM Tris (pH 7.2), 2 mM EDTA and 2 mM 2-ME (buffer A) and applied on a Q-Sepharose Fast Flow (Amersham Biosciences, Cologno, Monzese, Italy) column; the protein was eluted with a 35–500 mM NaCl gradient in buffer A. The purification was then carried out on a Heparin Sepharose 6 Fast Flow (Amersham Biosciences) column in buffer A (eluted with 100 mM NaCl)

and on a Superdex 75 gel filtration column (Amersham Biosciences) in buffer A with 150 mM NaCl. The molar absorption coefficient at 280 nm was determined by the Bradford assay to be 10.5 $mM^{-1} \cdot cm^{-1}$ (per monomer).

The aggregation state was determined by gel filtration on a Superdex 75 column (Amersham Biosciences) and further confirmed by HPLC (G3000SWxl, Tosoh Biosep) at different NaCl concentrations.

CRP was expressed and purified from an overproducing *E. coli* strain transformed with a cloned CRP gene (a gift from J.C. Lee, University of Texas, U.S.A.) [11].

ANS binding

ANS binding was carried out by titrating a DNR solution either 2 or 5 μM (monomer) in 50 mM Tris (pH 7.5), 150 mM NaCl and 0.5 mM 2-ME with a 1 mM ANS solution in water. The dissociation constant of the ANS–DNR complex was calculated using the following relation (when $ANS_{tot} > DNR_{tot}$):

$$1/I = 1/n\psi\,[DNR]_{tot} + (K/n[DNR]_{tot}\psi)(1/[ANS]_{free})$$

where I is the observed fluorescence intensity, K is the dissociation constant for a dye–site complex, n are the total number of sites on protein and ψ is the proportionality constant connecting the fluorescence intensity to the concentration of the probe–site complex.

If $ANS_{tot} > DNR_{tot}$, the plot of $1/I$ versus $1/[ANS]_{tot}$ will be linear for a fixed protein concentration with a common abscissa intercept of $-1/K$, for different protein concentrations [12].

All fluorescence emission spectra were recorded in a cuvette (1 cm light path) between 400 and 600 nm on a Fluoromax single photon counting spectrofluorimeter (Jobin Yvon). The excitation wavelength was 350 nm.

Results and discussion

Protein expression and purification

The *dnr* gene was isolated from *P. aeruginosa* genomic DNA by PCR and inserted in the expression vector pET28b. High levels of protein expression were obtained at 37°C in BL21 (DE3) *E. coli* strain; after induction with 1 mM IPTG, the protein was found to be mainly in the soluble fraction of the total cell extract (Figure 1A). A slight increase in the solubility was observed when the growth temperature was lowered to 25°C. A purification procedure was devised, which yielded a protein, pure to the homogeneity, in high yields (15 mg/l; Figure 1A).

General characterization

The molecular mass of the recombinant protein was 26054.16 Da (by MS). Determination of the N-terminal sequence has confirmed that the recombinant protein is correctly maturated in *E. coli*. The far-UV CD spectrum suggests that the purified protein is folded in solution (results are not shown).

Figure 1 | (A) Expression and purification of the DNR protein and (B) aggregation state of the purified protein

(**A**) Lane 1: SDS/PAGE of the soluble fraction of the cell extract from *E. coli* BL21(DE3) cells containing the pET-DNR plasmid after induction with 1 mM IPTG. Lane 2: SDS/PAGE of the purified DNR protein. Lane M: molecular mass markers 10–180 kDa (MBI Fermentas, Munich, Germany). (**B**) DNR in 20 mM Tris buffer (pH 7.2) and 150 mM NaCl was run on a gel filtration Superdex 75 column in comparison with molecular mass markers. The elution profile of the DNR sample (trace b) is superimposed on that of the markers (trace a, from left to right: BSA 67 kDa, ovalbumin 43 kDa, chymotrypsinogen 25 kDa and RNase A 13.7 kDa).

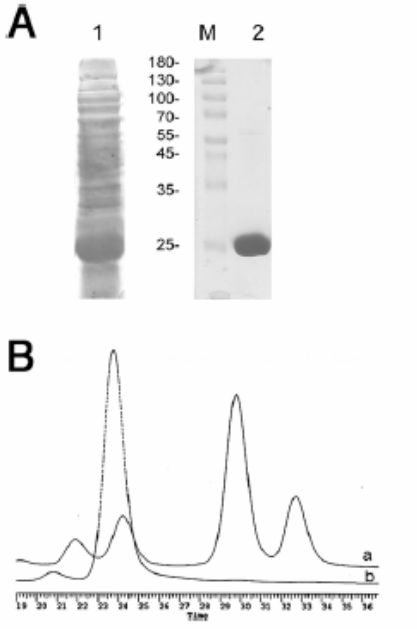

DNR is mainly a dimer in solution, as determined by gel filtration of the purified protein in 20 mM Tris buffer of pH 7.2 and 150 mM NaCl (Figure 1B). Higher aggregation states are populated at low salt concentration and thus all binding experiments have been carried out in the presence of 150 mM NaCl.

Binding of ANS

As reported for the *E. coli* CRP [11], titrations with ANS were performed to get some insights of the DNR structural organization. The emission of ANS increases when the molecule is bound in a non-polar environment with a shift in the wavelength for a maximum emission of approx. 530 to 500 nm.

Figure 2 | Binding of ANS

Protein concentrations: ●, 5 μM and ▼, 2 μM. The dissociation constant for the ANS–DNR complex was obtained from the abscissa intercept as described in the Materials and methods section. Inset: fluorescence emission spectra of the DNR–ANS complex at different ANS concentrations (2–50 μM range).

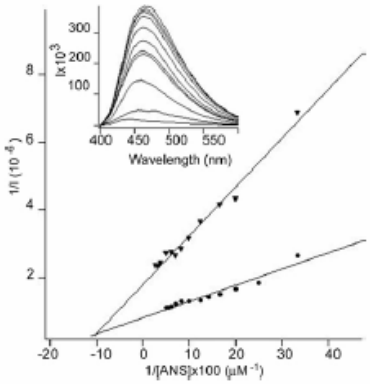

DNR (2–5 μM) was titrated with increasing amounts of ANS (2–50 μM) (Figure 2). The maximum fluorescence emission for the ANS bound to DNR was 460 nm, whereas it was 480 nm with CRP [11]. This difference in the position of the emission peak of ANS suggests that in DNR the hydrophobic cleft where ANS is bound is less solvent accessible, as reported for other proteins [13]. The data were analysed as in [12], and a dissociation constant for ANS of 7 μM (±0.8) was calculated. These results show that DNR binds ANS with higher affinity than CRP ($K_d = 600\ \mu$M) [11].

Experiments on the *in vitro* DNA binding activity and the *in vivo* activation of gene expression by the recombinant DNR are being carried out. A major task will be the determination of the structure of DNR by crystallography; crystallization experiments are in progress.

Funds from the Ministero Istruzione, Università e Ricerca of Italy (COFIN 2003) and from the European Union COST Action 856 are gratefully acknowledged.

References

1 Korner, H., Sofia, H.J. and Zumft, W.G. (2003) FEMS Microbiol. Rev. **27**, 559–592
2 McKay, D.B. and Steitz, T.A. (1981) Nature (London) **290**, 744–749
3 Vollack, K.U., Hartig, E., Korner, H. and Zumft, W.G. (1999) Mol. Microbiol. **31**, 1681–1694
4 Arai, H., Igarashi, Y. and Kodama, T. (1995) FEBS Lett. **371**, 73–76
5 Van Spanning, R.J.M., De Boer, A.P.N., Reijenders, W.N.M., Spiro, S., Westerhoff, H.V., Stouthamer, A.H. and Van der Host, J. (1995) FEBS Lett. **360**, 151–154
6 Van Spanning, R.J.M., Houben, E., Reijenders, W.N.M., Spiro, S., Westerhoff, H.V. and Saunders, N. (1999) J. Bacteriol. **181**, 4129–4132
7 Hasegawa, N., Arai, H. and Igarashi, Y. (1998) FEMS Microbiol. Lett. **166**, 213–217
8 Arai, H., Kodama, T. and Igarashi, Y. (1997) Mol. Microbiol. **25**, 1141–1148
9 Arai, H., Mizutani, M. and Igarashi, Y. (2003) Microbiology **149**, 29–36
10 Green, J., Scott, C. and Guest, J.R. (2001) Adv. Microbiol. Physiol. **44**, 1–34
11 Heyduk, T. and Lee, J.C. (1989) Biochemistry **28**, 6914–6924
12 Horowitz, P.M. and Criscimagna, N.L. (1985) Biochemistry **24**, 2587–2593
13 Strangelo, I., Bismuto, E., Tavassi, S. and Irace, G. (1998) Biochim. Biophys. Acta **1385**, 69–77

Received 5 September 2004

The 11th Nitrogen Cycle Meeting 2005

N oxides sensing and denitrification: the DNR transcription factors

S. Rinaldo,[1] G. Giardina, M. Brunori and F. Cutruzzolà

Department of Biochemical Sciences 'A. Rossi Fanelli' and Istituto di Biologia e Patologia Molecolari – CNR, University of Rome La Sapienza, P. le A. Moro 5, 00185 Rome, Italy

Abstract

All denitrifiers can keep the steady-state concentrations of nitrite and nitric oxide (NO) below cytotoxic levels controlling the expression of denitrification gene clusters by redox signalling through transcriptional regulators belonging to the CRP (cAMP receptor protein)/FNR (fumarate and nitrate reductase regulator) superfamily.

Nitric oxide (NO)-responsive regulators belong to three different subgroups of the CRP (cAMP receptor protein)/FNR (fumarate and nitrate reductase regulator) superfamily [FNR, DNR (dissimilative nitrate respiration regulator) and NnrR] and can control N oxide homoeostasis both under anaerobic and aerobic conditions. The FNR-type share a cysteine-rich motif involved in the formation of an iron–sulphur cluster as a redox centre, which is not present in the other two subgroups.

Most of the regulators involved in the regulation of denitrification, belonging either to the DNR and NnnR subgroups, regulate nitrite reductase (*nir*), NO reductase (*nor*) and nitrous oxide reductase (*nos*) gene expression. The NO dependence of the transcriptional activity of promoters regulated by these transcription factors has suggested that these factors may act as NO sensors *in vivo*. To date, no structural information and little biochemical data are available on this class of regulators.

In order to gain insights into the molecular and structural basis of the NO-dependent regulation, we have recently expressed in *Escherichia coli* and partially characterized the DNR protein from *Pseudomonas aeruginosa*.

NO-responsive elements belonging to the CRP/FNR superfamily of transcription factors

The expression of the denitrification gene clusters is tightly controlled by redox signalling through a cascade of oxygen-responsive regulators activating the N oxides-responsive ones. These regulators control the NO homoeostasis maintaining the steady-state concentration of nitrite and NO below cytotoxic levels; as a consequence, free NO concentration is in the nanomolar range.

Key words: dissimilative nitrate respiration regulator (DNR), denitrification, cAMP receptor protein/fumarate and nitrate reductase regulator superfamily (CRP/FNR superfamily), nitric oxide, *Pseudomonas aeruginosa*, transcriptional regulation.

Abbreviations used: ANR, anaerobic regulation of arginine deaminase and nitrate reduction; CRP, cAMP receptor protein; DNR, dissimilative nitrate respiration regulator; FNR, fumarate and nitrate reductase regulator.

*To whom correspondence should be addressed (email serena.rinaldo@uniroma1.it).

The denitrification pathway is transcriptionally regulated by redox-linked transcription factors mostly belonging to the CRP/FNR superfamily [1], structurally related to the CRP protein from *E. coli* [2]. The CRP/FNR proteins are constant in size with approx. 230–250 amino acid residues, the first 150–170 residues corresponding to the effector domain [1]. These regulators respond to both extracellular and intracellular signals by binding the allosteric effector either directly (as for cAMP in CRP from *E. coli*) or through a prosthetic group (as for the iron–sulphur cluster of FNR from *E. coli*) [3]. All members of this superfamily bind DNA with a C-terminal helix–turn–helix domain which interacts with the major groove of target DNA sequence, the FNR box (TTGATN$_4$ATCAA) [1].

Multiple members of these regulators, belonging to different subgroups, can either coexist in the same host or regulate the same metabolic pathway in different organisms [1]. This is the case for the regulators of denitrification and in general for NO-responsive components which belong to three different subgroups of the CRP/FNR superfamily (FNR, DNR and NnrR) and can control N oxide homoeostasis both under anaerobic and aerobic conditions [1]. To date, no structural information and limited biochemical data are available on the last two subgroups involved in the regulation of denitrification, while the first one is well characterized. In *E. coli*, as an example, nitrosative stress induces expression of the flavohaemoglobin protein, encoded by the *hmp* gene, which acts as a NO scavenger. The *hmp* gene expression requires the FNR protein which is a repressor under normal conditions; in the presence of NO, the $[4Fe\text{-}4S]^{2+}$ cluster is converted into the $[2Fe\text{-}2S]^{2+}$ state inducing monomer formation in the FNR protein [4]. The FNR form modified by NO binds the *hmp* promoter with lower affinity, inducing flavohaemoglobin expression.

The DNR-type of transcription regulators

All members of the DNR subgroup share the same motif (E-SR amino acid residues) involved in recognition of the binding site on DNA, while most members of the NnrR

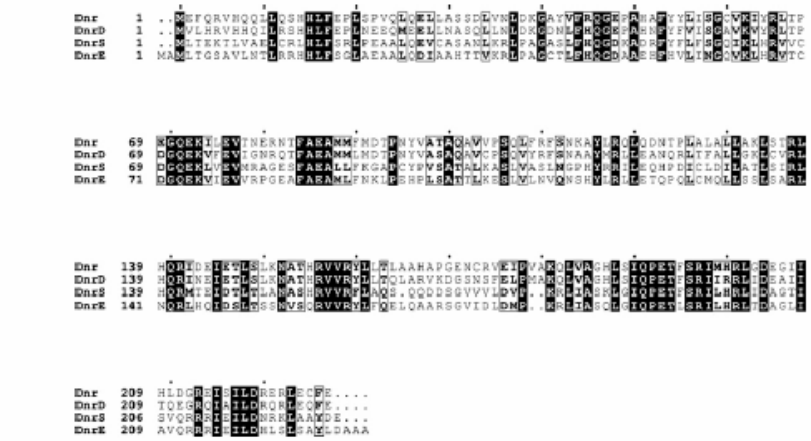

Figure 1 | Multiple alignment of DNR protein sequences from *Ps. aeruginosa* (DNR) and *Ps. stutzeri* (DnrD, DnrS and DnrE)
Amino acid one-letter codes are used. Dashes represent insertions and deletions; numbers at the beginning of each sequence indicate absolute sequence numbering. Invariant positions are boxed in black; alignment columns displaying amino acid with the same physicochemical properties are boxed in white with the conserved residues shown in boldface.

subgroup contain a histidine instead of a glutamate residue. Both groups of regulators (DNR and NnrR) do not contain enough cysteine residues for iron–sulphur clusters formation contrary to FNR, suggesting a different mechanism of N oxide(s) sensing.

Members of both NnrR and DNR subgroups are found in facultatively anaerobic bacteria; the transcriptional regulation is exerted in the presence of N oxide(s) and under low oxygen tension. In *Rhodobacter sphaeroides* and in *Paracoccus denitrificans* for example, it was shown, by genetic approach, that the transcriptional regulators designated respectively as NnrR (belonging to the NnrR-type) and Nnr (belonging to the DNR subgroup) can both activate the expression of the nitrite and NO reductase genes in response to NO [5,6].

The members of DNR-type class of regulators found in the *Pseudomonas* spp. [7,8] share a high sequence identity (Figure 1) but may not fulfil an identical physiological role. This is not surprising given that Pseudomonads are well known for their metabolic flexibility which reflects the capability of the different species to survive as free living organisms in soil, water and animals, where they are often responsible for diseases.

In *Pseudomonas stutzeri*, there are at least three regulators (DnrD, DnrS and DnrE) involved in the NO sensing (DnrD), activation of the nitrate pathway (DnrE) and possibly in redox sensing (DnrS) under anaerobic conditions [1].

The DnrD transcription factor induces the expression of *nirSTB*, *norCB* and *nosZ* operons (encoding nitrite, NO and nitrous oxide reductases respectively) in the presence of NO but not nitrite (the *nos* gene is activated also in presence of high concentration of nitrous oxide). The NO concentration required for the *nir-nor* operons activation is in the range of 5–50 n*M* [8]. DnrD overexpression itself is not sufficient for the transcription of the *nir-nor* operons, indicating that additional factors may be required [8].

NO sensing in *Ps. aeruginosa*

Ps. aeruginosa is one of the most important pathogens in lung chronic infections associated for example with cystic fibrosis, where it uses denitrification as the anaerobic energy producing pathway [9]. Low oxygen tensions and the presence of N oxides produced by the host defence mechanism induce high levels of expression of *nir-nor* operons [9]. Under anaerobic conditions, the denitrification pathway works both as a source of electrons and as NO scavenger given that the classical flavohaemoglobin-mediated detoxification pathway is not active [10].

The induction of denitrification by oxygen depletion requires ANR (anaerobic regulation of arginine deaminase and nitrate reduction), an FNR-like global regulator for anaerobic gene expression in *Ps. aeruginosa* [11]. ANR induces the expression of the DNR protein (dissimilative nitrate respiration regulator, belonging to DNR subtype), which activates, in the presence of N oxide(s), the *nirS*, *norCB* and *nosR* promoters [7,12,13]. Mutants without the *anr* or *dnr* genes are not able to induce *nirS* and *norCB* promoters under growth conditions where denitrification should be active [12]. *anr* defective strains are not able to activate the transcription

of the *dnr* gene but denitrification can be induced after transformation with a plasmid carrying the *dnr* gene [7]. DNR-mediated transcriptional activation of denitrification depends on endogenous NO concentration [13,14].

The sequence alignment shown in Figure 1 clearly indicates a higher degree of similarity of DNR from *Ps. aeruginosa* to DnrD, in agreement with the involvement of DNR in NO sensing. Given that only one DNR-type regulator is found in the *Ps. aeruginosa* genome, in this pathogen the role of DnrE and DnrS might be played by different factors.

In order to study the biochemical basis of the NO-dependent regulation of the DNR protein, after cloning the *dnr* gene from *Ps. aeruginosa*, we have purified to homogeneity the protein expressed in *E. coli* using the pET system [15]. The recombinant protein, produced in high yield (15 mg/l), is soluble and stable as a dimer [15].

To obtain some insight of the DNR structural organization, ANS (8-anilinonaphthalene-1-sulphonic acid) titrations were performed [15]. DNR has a hydrophobic pocket which is more accessible as compared with *E. coli* CRP ($K_{d\,DNR} = 7\ \mu M$ and $K_{d\,CRP} = 600\ \mu M$), suggesting that DNR may present a different structural organization of the effector domain. This hydrophobic cleft is a likely candidate for the binding of the cofactor(s) required for NO-mediated activation of the DNR protein.

DNA binding assays, crystallization and structure determination of DNR, now in progress, will shed more light on the structural determinants of the NO-dependent activation process.

Funds from the Ministero Istruzione, Università e Ricerca of Italy (COFIN 2003 – Structural dynamics of metalloproteins) and from the European Union COST Action 856 are gratefully acknowledged.

References

1 Korner, H., Sofia, H.J. and Zumft, W.G. (2003) FEMS Microbiol. Rev. **27**, 559–592
2 McKay, D.B. and Steitz, T.A. (1981) Nature (London) **290**, 744–749
3 Unden, G. and Schirawski, J. (1997) Mol. Microbiol. **25**, 205–210
4 Cruz-Ramos, H., Crack, J., Wu, G., Hughes, M.N., Scott, C., Thomson, A.J., Green, J. and Poole, R.K. (2002) EMBO J. **21**, 3235–3244
5 Kwiatkowski, A.V. and Shapleigh, J.P. (1996) J. Biol. Chem. **271**, 24382–24388
6 Van Spanning, R.J., Houben, E., Reijnders, W.N., Spiro, S., Westerhoff, H.V. and Saunders, N. (1999) J. Bacteriol. **181**, 4129–4132
7 Arai, H., Kodama, T. and Igarashi, Y. (1997) Mol. Microbiol. **25**, 1141–1148
8 Vollack, K.U. and Zumft, W.G. (2001) J. Bacteriol. **183**, 2516–2526
9 Hassett, D.J., Cuppoletti, J., Trapnell, B., Lymar, S.V., Rowe, J.J., Yoon, S.S., Hilliard, G.M., Parvatiyar, K., Kamani, M.C., Wozniak, D.J. et al. (2002) Adv. Drug Deliv. Rev. **54**, 1425–1443
10 Arai, H., Hayashi, M., Kuroi, A., Ishii, M. and Igarashi, Y. (2005) J. Bacteriol. **187**, 3960–3968
11 Gallmand, M., Gamper, M., Zimmermann, A. and Haas, D. (1991) J. Bacteriol. **173**, 1598–1606
12 Arai, H., Igarashi, Y. and Kodama, T. (1995) FEBS Lett. **371**, 73–76
13 Arai, H., Mizutani, M. and Igarashi, Y. (2003) Microbiology **149**, 29–36
14 Arai, H., Kodama, T. and Igarashi, Y. (1999) FEMS Microbiol. Lett. **170**, 19–24
15 Rinaldo, S., Giardina, G., Brunori, M. and Cutruzzolà, F. (2005) Biochem. Soc. Trans. **33**, 184–186

Received 23 September 2005

NITROGEN CYCLE BOOK

CHAPTER

NITRITE REDUCTASES IN DENITRIFICATION

Serena Rinaldo and Francesca Cutruzzolà*

Department of Biochemical Sciences “A.Rossi Fanelli”
University of Rome La Sapienza, Rome (Italy)

*corresponding author at:

Department of Biochemical Sciences “A.Rossi Fanelli”
University of Rome La Sapienza
P.le A. Moro,5
00185 Rome (Italy)
Tel. 39-0649910713
FAX 39-064440062

E-mail: francesca.cutruzzola@uniroma1.it

INTRODUCTION

The nitrogen cycle is a biogeochemical cycle consisting of several interconnected processes by which atmospheric dinitrogen is first fixed into NH_3, which is then converted into biochemical amines (proteins, nucleic acids, glycosamines); most of the NH_3 which then arises from organism's decay is oxidised to nitrites and nitrates during nitrification. In dissimilatory denitrification, to be distinguished from assimilatory processes producing NH_3 and amines, nitrate is used instead of oxygen as an electron acceptor for energy production, and reduced to gaseous nitrogen oxides (NO, N_2O, N_2) [1]. Dissimilatory denitrification is common to many facultative anaerobic bacteria and plays a key role in the nitrogen cycle being the only biological source of N_2. Moreover, substrates and products of this metabolic pathway are intensively monitored in the environment because of their involvement as soil, water and atmosphere pollutants. The denitrification trait is usually active under low oxygen tension or when nitrogen oxides are available as electron acceptors.

Several redox proteins are involved in the denitrification chain, namely the reductases for nitrate, nitrite, NO and nitrous oxide, and multiple electron donors specific for these enzymes. Some of these components are bound to the cytoplasmic membrane, while the soluble ones are found in the periplasmic space of the gram-negative bacteria.

Nitrite reductase (NIR) is a key enzyme in the dissimilative denitrification chain, catalyzing the reduction of nitrite (the toxic product of nitrate reductase activity) to NO. Although a matter of debate for a long time, it is now accepted that NO is produced from nitrite reduction as an obligatory intermediate in most denitrifiers, and that it is further reduced to N_2O by the NO reductase. Dissimilative nitrite reductase is therefore considered the major known source of NO in bacteria.

Purification and characterization of NIR from several bacterial sources has shown that there are two distinct classes of dissimilatory nitrite reductases which yield NO as the main reaction product, containing either copper (CuNIR) or heme (cd_1NIR) as cofactor, the heme containing enzyme being more frequent. The genes coding for the CuNIR and cd_1NIR are called *nirK* and *nirS*, respectively. Besides the species from which the enzyme has been purified, several others were shown to contain either type of NIR on the basis of DNA hybridization and/or inhibition of denitrification by the Cu chelator diethildithiocarbamate (DDC). The enzymes containing copper and heme never coexist within the same bacterial species; the biological relevance of this redundancy has not yet been clearly established, although some speculation can be made about availability of Cu and iron in different microenvironments. Functional complementation of a cd_1NIR deficient strain of *Psedomonas stutzeri* with the Cu NIR from *Pseudomonas aureofaciens* indicates that the two enzymes fulfill the same role *in vivo*.

This chapter mainly focuses on the structure-function relationships in the two classes of dissimilatory nitrite reductases and special attention is paid to recent structural informations on enzymes from different sources, which have different structures and catalyse the reduction of nitrite to NO *via* different mechanisms. For a more extensive bibliography the chapter refers mainly, if not indicated, to the recent reviews (and references therein) on cd_1NIR [2, 3, 4] and CuNIR [2, 5, 6].

CD_1 NITRITE REDUCTASE

General properties and structure

Heme nitrite reductases are generally dimers of two identical subunits, each containing one heme c and one unique heme d_1 (Figure 1). Up to now, cd_1 enzymes have been purified from *Alcaligenes faecalis, Azospirillum brasilense SP7, Magnetospirillum magnetotacticum, Pseudomonas aeruginosa*, *Pseudomonas nautica, Pseudomonas stutzeri*, *Paracoccus denitrificans*, *Paracoccus halodenitrificans*, *Paracoccus pantotrophus, Ralstonia eutropha, Roseobacter denitrificans*, and *Thiobacillus denitrificans*.

The cd_1 enzymes are periplasmic soluble proteins and involved in respiratory nitrite reduction, apart from those from *Roseobacter denitrificans* and *Magnetospirillum magnetotacticum*, which have been assigned an oxygen reductase and a Fe(II):nitrite oxidoreductase activity, respectively.

The first enzyme that has been characterized is that from *P. aeruginosa* (E.C. 1.9.3.2) discovered by Horio and coworkers and initially studied for its oxygen reductase activity, which is inhibited by both CO and CN^- and produces water. Later, the work of Yamanaka showed that the enzyme is also capable of catalyzing the reduction of nitrite, an activity which is now accepted to be the only physiological role of this enzyme. This assignement is based both on kinetic and equilibrium results with the two substrates (Table I) and on genetic evidence showing that strains of *P.stutzeri* and *P.aeruginosa* in which *nirS*, the gene coding for cd_1NIR, has been selectively inactivated cannot grow on nitrogen-oxides. The nitrite reductase activity is inhibited by CN^- but insensitive to CO and its reaction product is NO. The nitrite reductase activity is also pH dependent *in vitro* with an optimum of pH between 5.8 and 7. Interestingly, a pH dependence of cd_1NIR activity with accumulation of nitrite has been observed *in vivo* in cultures of *P. denitrificans* grown at suboptimal pH (6.8), indicating that an inactivation may occur in this species at low pH.

The peculiarity of cd_1NiR to catalyze both the monoelectronic reduction of nitrite to NO and the tetraelectronic reduction of oxygen to water, which are mechanistically very different, is a very intriguing feature of this enzyme. Other, less relevant activities have been attributed to cd_1NiR such as the reduction of NO to N_2O, the oxidation of CO to CO_2 and the reduction of NH_2OH to NH_3 .

A summary of the spectroscopic, redox and catalytic properties of the cd_1NIRs from *P. aeruginosa*, *P. stutzeri*, *P. nautica*, *T. denitrificans* and *P. pantotrophus* is given in Table I. In the optical visible spectrum of the oxidized protein from most species the c heme is characterized by absorption maxima at 520 and 411 nm, while the d_1 heme shows a broad shoulder around 470 nm and a band centred at 640 nm. Two bands are however seen in the region between 640 and 710 for the *P. pantotrophus* and *R. denitrificans* cd_1 NIRs. The reduced enzyme absorption maxima for the c heme are at 548, 520 and 417 nm, and for the d_1 heme at 650 and 456 nm. The midpoint redox potentials of the two hemes under various conditions, known for the *P. aeruginosa* and *P.nautica* enzymes, are reported in Table I: they range between +200 and +300 mV. It is noteworthy that the midpoint redox potential of the c heme is very sensitive to the ligation state of the d_1 heme, being more negative when CO is bound, and more

positive when NO is bound (Table I). Moreover, in the semiapoprotein containing only the c-heme, the midpoint redox potential of the c heme is at least 100 mV more positive than that of the holoprotein. These findings, together with data on specific ligands, suggest the existence of redox interactions among the different hemes.

Electron donors to cd_1NiRs have been identified *in vitro* with a survey of soluble electron carriers, either c-type cytochromes (cyt c_{550} , cyt c_{551} , cyt c_{554}) or copper proteins, like azurin or pseudoazurin. In a few cases the physiological electron donor could be identified *in vivo*, for example for the *P. aeruginosa* and *P. denitrificans* enzymes. However, the results do not give a unifying picture, since in the former case only cyt c_{551} is involved whereas in the latter both cyt c_{550} and pseudoazurin are implicated [7].

Structure

The primary structure of the enzyme from several species reveals that NiR is synthesized as a pre-protein, with a leader peptide responsible for the periplasmic export. The mature subunit is over 500 aminoacids long; it contains only two Cys at the amino terminal region covalently bound to the vinyl groups of the c heme (Figure 1A). The degree of homology between cd_1NIRs is much higher for the carboxy-terminal d_1 heme domain than for the amino-terminal c heme domain, and is particularly low at the N-terminus. Altogether a 52.7% identity and 70% homology can be calculated.

The total number of aminoacid sequences available for cd_1NIR (and also for CuNiR) in public databases is rapidly growing since oligonucleotide primers amplifying the d_1-heme domain of *nirS* (or the whole gene of *nirK*) are often used to monitor the presence of denitrifiers in the environment.

Cd_1NIR is a homodimer (MW= 120 kDa) and each subunit contains one c heme and one d_1 heme; thus the native dimeric protein carries four metal centres. The high-resolution structure has been determined for several derivatives of the enzyme from *Paracoccus pantotrophus* (hereinafter Pp-cd_1NIR) and *Pseudomonas aeruginosa* (hereinafter Pa-cd_1NIR). It shows a conserved overall architecture: each monomer is organized into two structurally distinct domains, one carrying the c heme and the other the d_1 heme (Figure 2). The former, which is the electron acceptor pole of the molecule, contains mainly α-helices whereas the latter has an eight-bladed β-propeller structure common to other proteins. The distances between the hemes within a subunit are about 11 Å edge-to-edge and 20 Å iron-to-iron; those between subunits are much larger (>35 Å). As discussed below, the d_1 heme is the site where substrate binds and catalysis occur. With regard to quaternary structure, non-covalent interactions between monomers in the dimer are very strong, since dissociation is not observed even in 3 M NaCl or 6 M urea, but only at extreme pH (>11), or after extensive succinylation.

A closer look at the structure reveals significant differences in the c and d_1 domains between the two species; some of these can be related to different primary sequences and are worthy of discussion since they may be relevant to the interpretation of the reaction mechanism.

In Pa-cd_1NIR the α-helical c heme domain has a topology similar to that of class I cytochromes c (Figure 2), whereas a different connectivity of the helices is observed in Pp-cd_1NIR. In both proteins a N-terminal segment from the c-

domain extends towards the d_1-domain and is inserted in the active site pocket. In the Pp-cd_1NIR this exchange occurs within the same monomer, but in the *P. aeruginosa* enzyme a "domain swapping" occurs, since the tail of one monomer contacts the d_1 site of the neighbouring monomer (Figure 2). The ligands of the c heme in the oxidized form of the two enzymes are strikingly different: His^{51}-Met^{88} in Pa-cd_1NIR (Figure 3A) and His^{17}-His^{69} for Pp-cd_1NIR. Spectroscopic studies (MCD, NMR, EPR) available on the oxidized form of both enzymes confirm that this pattern of c heme ligation is the same also in solution; the His-Met type ligation is also expected for the cd_1NIR of *P.stutzeri* on the basis of EPR and MCD studies. In Pp-cd_1NIR the axial ligands change to His^{69}-Met^{106} upon reduction, triggering a large conformational change which involves also the d_1 domain (see below). In the *P. aeruginosa* enzyme the c heme ligands are unchanged upon reduction.

The c heme is thus hexacoordinated and low spin in both reduction states; nevertheless it may form a complex in Pa-cd_1NIR with several heme ligands (NO, CN^-) under conditions in which eukaryotic cytochrome c does not.

The c-domain is the electron accepting pole of the molecule and the interaction with the electron donors is mainly electrostatic in nature. Several negatively charged residues (mainly glutamates) that could be involved in electron transfer complex formation were identified by analysis of the c-domain structure in both Pa-cd_1NIR and Pp-cd_1NIR. As for other systems, the formation of the electron transfer complex is mainly driven by the anisotropic distribution of surface charges which leads to strong dipolar moments in the redox partners. However, some cross-reactivity between electron donors and reductases from different species was observed and can be related to the relatively "loose" specificity of recognition of the interacting surfaces in the complex.

The d_1 heme is unique to denitrifiers containing the cd_1NIR, where it is synthesized starting from δ-aminolevulinic acid *via* uroporphyrinogen III, a precursor common to other heme biosynthetic pathways. The genes responsible for the d_1 heme-specific reactions of the pathway are mostly found in the same operon downstream to the *nirS* gene in *P. aeruginosa*, *P. stutzeri* and *P. denitrificans* and thus are also induced by low oxygen tension and presence of N-oxides.

Heme d_1 has been unequivocally identified as a 3,8-dioxo-17-acrylate-porphyrindione and its structure is reported in Figure 1B; since it is so unique, it was suggested that it could be responsible for some catalytic features of the enzyme. The presence of the electronegative oxo groups confers to the macrocycle distinct redox properties, rendering it harder to oxidise than the corresponding isobacteriochlorines, and thus shifting the redox potential of the iron to more positive values. The chemical nature of heme d_1 has been confirmed by inspection of the crystal structures of all cd_1NIRs: in the oxidized and reduced/NO bound Pp-cd_1NIR, heme d_1 adopts a planar conformation, whereas in the others a more distorted, saddle-like conformation is preferred.

The d_1 heme binds the physiological oxidants (O_2, nitrite) as well as other heme ligands. A semiapoprotein containing only the c heme can be obtained either by acidic aceton treatment or by recombinant DNA techniques. Reconstitution of both apoproteins with purified or chemically synthetized d_1 heme is possible, with good recovery of the spectroscopic properties of the

holoenzyme and of the oxygen and nitrite reductase activities.

On the basis of EPR, NMR and MCD measurements, the d_1 heme in Pa-cd_1NIR has been assigned as a low spin, hexacoordinated species in the ferric state, and high spin pentacoordinated in the ferrous state. One axial ligand is always provided by a histidine. The sixth ligand in the low spin ferric form, is a hydroxide ion in the oxidized Pa-cd_1NIR structure (Figure 3B). The ligation is different in the oxidized Pp-cd_1NIR structure where the sixth ligand is provided by the phenolate of Tyr^{25}, a residue belonging to the N-terminal segment and thus to the c-domain. The Tyr^{25}-coordinated enzyme is catalytically inert and needs to be activated by reduction (either with sodium dithionite or with the protein NapC [8]). Substitution of Tyr^{25} with Ser has no effect on the catalytic properties of the enzyme [8, 9]; it is possible that the Tyr^{25}-coordinated structure may represent a resting form of the enzyme, also considering that this residue is poorly conserved among the cd_1NIRs from different species. It has been suggested that Tyr^{25}-coordination could be protective towards unwanted reaction of the d_1-heme with harmful reactive oxygen species (ROS) that could be present in a partially aerobic environment; this hypothesis is still to be confirmed experimentally. In Pa-cd_1NIR a Tyr is found in the d_1 heme pocket, but is located further away from the iron: its mutation to Phe does not alter the catalytic and optical properties of the enzyme. Spectroscopic studies in solution have either directly confirmed, or are consistent with, these different ligation patterns of the two enzymes, in either oxidation state. A low spin ferric d_1 heme-associated α-band in the 636-644 nm region is common to all NIRs and may indicate a common His/OH or His/Tyr ligation: however, whether the latter form is *on* or *off* the catalytic pathway still remains unclear (see below).

Among the other residues found in close proximity of the d_1 heme, an important role in catalysis is played by two His residues which are hydrogen bonded to a water molecule in the Pp-cd_1NIR oxidized structure or directly to the ligand hydroxide in the Pa-cd_1NIR oxidized structure (Figure 3B). These residues are good candidates to be involved in the protonation and dehydration of nitrite (see below).

Catalytic mechanism

The monoelectronic reduction of nitrite to yield NO is the main activity of cd_1NIR *in vivo*. The mechanism of nitrite reduction to yield NO involves chemically complex steps such as transfer of a reducing equivalent into an electron-rich species, e.g. the nitrite anion, possibly followed by protonation and dehydration. Product inhibition may occur, since the NO produced at the catalytic site forms stable complexes with the ferrous d_1 heme and, at acidic pH, also with the c heme. A possible reaction scheme for cd_1NIRs as shown in Figure 4, panel A.

Catalysis occurs at the d_1 heme with the substrate (nitrite) and product (NO) bound to the iron via the nitrogen atom, as seen in the crystal structure of the nitrite bound transient species of Pp-cd_1NIR and NO bound reduced derivative of both Pa-cd_1NIR and Pp-cd_1NIR. A recent proposal from a theoretical study suggests an alternative O-nitrite ligation [10], but still awaits experimental support. A nitrosyl intermediate (d_1-$Fe^{2+}NO^{+}$) is formed during catalysis, as shown in $^{18}O/^{15}N$ exchange experiments. Spectroscopic evidence of this species, which is EPR silent, has also been obtained by FTIR on the oxidized, NO reacted *P.stutzeri* enzyme and by stopped-flow FTIR on Pp-cd_1NIR [11]. The nitrosyl intermediate (d_1-$Fe^{2+}NO^{+}$), which

is formally equivalent to (d_1-$Fe^{3+}NO$), is chemically unstable and rapidly decays to d_1-Fe^{3+} plus NO (Figure 4A). Complete reduction of the transient species leads to the formation *in vitro* of a paramagnetic (d_1-$Fe^{2+}NO$) stable adduct with slow NO dissociation rates, which has been observed by EPR. Data on the NO complexes of d_1 heme synthetic models show that the formation of a ferrous π-cation radical with a bent Fe-NO bond is also possible. Formation of this species is facilitated by the oxo groups of the macrocycle which increase the positive charge on the iron; under these conditions, a weakening of the Fe-NO bond is observed and NO dissociation occurs readily in the presence of a nucleophile. Whereas formation of NO can be monitored at steady state (for example using an NO-sensitive electrode), rapid reaction studies have failed to detect kinetically competent NO release from cd_1NIRs.

An important feature of the reduction of nitrite by cd_1NIR is that for the enzyme to accomplish a productive turnover, a balance between product release and re-reduction of the d_1 heme is critical to avoid product inhibitory effects (Figure 4A). Product release in the periplasmic space might be enhanced by the efficient scavenging activity of NO reductase. The internal electron transfer rate, relevant for the catalytic mechanism, might be under allosteric control in cd_1NIRs as suggested by Pecht and coworkers [12] who have shown that in *P. stutzeri* cd_1NIR and Pa-cd_1NIR a marked decline in the intramolecular electron transfer rate is seen with increasing enzyme reduction. Whether a tertiary or a quaternary conformational change is involved in this allosteric control is still under investigation; it is known that in a crystal form of Pa-cd_1NIR, reduction of the c heme alone does not trigger a conformational change in the d_1 heme environment. Noteworthy, large conformational changes (of unknown meaning) have been seen after mutagenesis of Pa-cd_1NIR [13] and in a crystal form of reduced Pp-cd_1NIR [14].

Although there is agreement on the chemical species populated along the reaction pathway (Figure 4A), the relative rates of the single steps are different in the enzymes characterized so far, in agreement with the different turnover numbers observed at steady state (Table I, [3]). For Pa-cd_1NIR at pH 8.0 the binding and dehydration step is very fast, almost diffusion-limited ($k \geq 10^8\ M^{-1}\ s^{-1}$), while the internal electron transfer is slow ($1\ s^{-1}$) and the final species is the d_1-$Fe^{2+}NO$ complex. In the reaction with nitrite of Pp-cd_1NIR at pH 7.0 the internal electron transfer rate is much faster (in agreement with pulse radiolysis experiments on the same enzyme) but no release of NO could be detected [11]. Although the origin of these differences is unclear, they may arise from variations in sequence and structure between the *Paracoccus* and *Pseudomonas* enzymes that result in substantially different electron transfer kinetics.

Insight into the molecular mechanism of catalysis comes from the results on the mutants of the two conserved histidines (His327 and His369 in Pa-cd_1NIR) located near the active centre. Substitution of either of the two His with Ala has a dramatic effect on nitrite reduction [13]. The two His are not equally important in controlling the affinity for the anionic substrate nitrite: His369 was shown to be essential. A common feature of the two His mutants in the reaction with nitrite is that they are both trapped in the reduced-NO bound species faster than the wild type Pa-cd_1NIR. Given that the intramolecular electron transfer rate was found to be unchanged in these mutants, the increased probability of trapping may originate in a decreased rate of NO dissociation from the ferric d_1 heme. Reduction of the positive potential in the d_1 heme pocket by substitution of either one of the two invariant

active site His with Ala may lead to the loss of the hydroxyl coordinated to the ferric d_1 heme iron in the wt enzyme which should assist NO dissociation (Figure 4A). This hypothesis is fully consistent with the unusually high affinity of the reduced protein for anions, both nitrite (the physiological substrate) and other anionic ligands as cyanide or hydroxide, which is controlled by the His side-chains.

Several key points of the reaction mechanism of cd_1NIRs have been clarified with the contribution of functional and structural information, and can be summarized as follows:

- the oxidized enzyme has both hemes in the low spin, hexacoordinate state;
- the c-heme is the electron entry site whereas the d_1-heme is the catalytic site;
- large conformational changes are seen upon reduction, leading to a pentacoordinated d_1 heme iron and a catalytic site open for the binding of ligands.
- catalysis occurs at the d_1 heme with the substrate (nitrite) and product (NO) bound to the iron *via* the nitrogen atom;
- the His residues in the distal pocket of the d_1 heme are involved in substrate binding and protonation;
- binding of anions to the reduced enzyme is facilitated by the positive potential of the distal pocket and by the presence of the specialized d_1 heme;
- a nitrosyl intermediate is formed during catalysis;
- in Pa-cd_1NIR dissociation of the product (NO) is assisted by the active site His residues which stabilize the OH^- bound to the oxidized enzyme.

There are still open questions, among which the most relevant during catalysis are the role of the d_1 heme and the role of the redox state of the c heme. The latter may be involved in triggering the conformational changes seen upon reduction and related to the low rate of c-to-d_1 electron transfer measured for the Pa-cd_1NIR and *P. stutzeri* cd_1NIR. Biochemical and structural chararacterization of cd_1NIRs from other species will be needed to shed more light on the reaction mechanism of this puzzling enzyme.

COPPER NITRITE REDUCTASE

General properties and structure

Copper-containing nitrite reductase (CuNIR) (E.C. 1.7.99.3) is present in about one-fourth of the denitrifiers isolated up to now. CuNIR has been described in both Gram-negative and Gram-positive (*Bacillus* sp.) eubacteria and in Archea (*Haloarcula* sp.). The better studied Gram negative group comprises the enzymes from *Achromobacter cycloclastes*, *Alcaligenes faecalis* S-6 and *Alcaligenes xylosoxidans*, *Rhodobacter sphaeroides* and *Pseudomonas aureofaciens*.

The CuNIR class is more heterogeneous than the cd_1NIR one in terms of molecular properties (see Table II for a summary) although the primary structure is well conserved within each subclass, ranging from 60 to 80 % identity in different species. The proteins are synthetised as longer precursors, with a leader peptide responsible for the periplasmic export. Common features are the trimeric quaternary structure in which a monomer (~ 40 kDa) contains two distinct Cu centres, one belonging to the type I Cu subclass and the other being a type II Cu. To date the only known exception was found in *Hyphomicrobium denitrificans* A3151 (HdNIR) [15], where the CuNIR is composed of six identical subunits (see below).

Spectroscopic and site-directed mutagenesis studies on the two Cu centres have shown that the type I site is the redox active site from which the electrons necessary for catalysis are transferred to the type II site, where

substrate binding occurs. The primary product of CuNIR is NO; however the enzyme can also yield a small amount (3-6%) of nitrous oxide (N_2O) if NO is allowed to accumulate. Other reactions such as the conversion of nitrite to ammonia or reduction of oxygen have also been described.

The total number of Cu atoms found in enzymes from different sources may differ considerably from the ideal six, depending on purification and storage, but six Cu atoms have been found in all crystal structures determined to date. The three-dimensional structure of different forms of the enzyme from *A. cycloclastes* [16], *Alc. faecalis* S-6 [2], *Alc. xylosoxidans* [17], *Rhodobacter sphaeroides* [18].

Structure

The overall architecture of the enzyme is organized as a homotrimer where the three identical subunits are tightly associated around a central channel of 5-6 Å in a 3-fold axis simmetry. Each monomer is composed of two distinct domains (Figure 5A), each consisting of a Greek key β-barrel fold similar to that of cupredoxins. An extensive network of hydrogen bonds, both within and between the subunits of the trimer, confers considerable rigidity to the molecule. The protein conformation does not experience large shifts in atom positions neither at different pH values nor in the different redox or ligand-bound states.

As outlined above, CuNIRs contain both type I and type II Cu centers; in the three-dimensional structure of CuNIR purified from *A. cycloclastes* it was shown for the first time that the type I Cu sites (two His, one Cys and one Met ligands) are located within each monomer, while the type II sites are at the interface between monomers in the trimer, with ligands (three His and one solvent molecule) provided by two different subunits. The two Cu sites are linked *via* a His-Cys bridge (Figure 5B) with a Cu-Cu distance of 12.5 -13 Å. The type II Cu is not essential for subunit stability; consistently, only minor structural changes are observed in the type II Cu-depleted enzyme from *A. cycloclastes*.

According to the spectroscopic properties of the type I Cu these proteins can be classified as blue and green CuNIRs [Table II]. The blue CuNIRs from *Alcaligens xylosoxidans* (NCIB 11015 and GIFU 1051 strains) share a 593 nm absorption band caused by the charge-transfer transition of type I Cu ($S_{(Cys)}$-->Cu^{2+}), which confers an EPR signal of this metal centre with axial simmetry. The green CuNIRs (*Achromobacter cycloclastes* and *Alcaligens faecalis*) show two bands at 460 nm and 584 nm also due to a $S_{(Cys)}$-->Cu^{2+} transfer transition of type I Cu but with a rhombic EPR signal.

The midpoint potential of the type I Cu is between +240 and +260 mV in enzymes from different species [Table II]; small copper proteins, like azurins and pseudoazurins, and bacterial cytochromes can donate electrons to CuNIR, the hemeproteins being less frequently involved. The interaction involves electrostatically complementary surfaces on both redox partners, as shown by site directed mutagenesis on CuNIR and by NMR on a pseudoazurin-CuNIR complex [19]. In this model the intermolecular electron transfer involves formation of a complex between the pseudoazurin as electron donor and the type I Cu-containing domain on CuNIR in a well-defined mode [19]. These experimental and theoretical data are supported by the recent studies on the HdNIR where each subunit is composed of one plastocyanin-like domain and one green CuNIR-like domain connected to each other, resembling the complex of green CuNIR and pseudoazurin [15].

Type II Cu, bound at the interface of two subunits lies at the bottom of a

12-13 Å deep solvent channel, is the substrate-binding and reduction site. Looking at the primary and 3-D structure, one of the three histidines involved in the type II Cu binding is located immediately upstream to the cysteine residue involved in the type I Cu binding (Figure 5B), suggesting that this stretch of amino acids can act as electron carrier during the catalysis. A redox potential of +260 mV was measured for type II Cu in *A. cycloclastes* nitrite reductase, but this value may vary in the presence of nitrite and can be as low as 200 mV, as is the case for *R. sphaeroides* enzyme. The nitrite-dependent modulation of the active site redox potential suggests that the intramolecular electron transfer is not energetically favoured in the absence of the substrate; the first order electron transfer rate measured by pulse radiolysis was found to be 1.4 10^3 s^{-1}, slower than reduction of type I Cu by external electron donors.

Catalytic mechanism

A mechanism for the monoelectronic reduction of nitrite from CuNIR was initially proposed which resembled that already described for cd_1NIR, involving a Cu nitrosyl intermediate (Cu^+-NO^+) formed at the type II Cu site. The presence of this species was inferred from isotope exchange experiments in which CuNIR was shown to produce N_2O in the presence of azide and hydroxylamine. The active site in the absence of substrate shows a type II Cu with nearly perfect tetrahedral geometry, with three out of four coordination bonds occupied by the Nε of three His, and the fourth by an oxygen atom from a water molecule (Figure 5B). The water ligand forms an hydrogen bond with the carboxylate group of the Asp^{98}, close to the active site; furthermore this residue together with the His^{255} residue bridge a second water molecule to form a hydrogen-bonding network.

Spectroscopic evidence from electron nuclear double resonance (ENDOR) studies on *Alc. xylosoxidans* CuNIR show that nitrite displaces a bound water ligand; no relevant coupling was however seen when $^{15}NO_2^-$ instead of $^{14}NO_2^-$ was used, raising the possibility that nitrite binds to the catalytic Cu *via* an oxygen atom. The structure of the type II Cu site in the absence and in the presence of nitrite has been elucidated for both oxidized (from *A. cycloclastes*, *Alc. faecalis* and *Alc. xylosoxidans*) and reduced CuNIR (from *Alc. faecalis* and *R. sphaeroides 2.4.3.* at high pH).

Analysis of nitrite-soaked crystals show that nitrite is coordinated to oxidized type II Cu in an asymmetric bidentate fashion through two oxygen atoms instead of the solvent molecule (Figure 4B). The nitrite's nitrogen atom is more bent away from the Cu in the *Alc. faecalis* structure than in the *A. cycloclastes* one. A lower occupancy (ie a weaker bond) of the nitrite molecule is found in the reduced form, with a less ordered hydrogen-bonding network. This evidence, together with the absence of a fourth ligand in the fully reduced *Alc. faecalis* CuNIR structure, has been used to support the hypothesis that *O*-coordinated binding of nitrite to oxidized Cu is the first event in catalysis, followed by reduction of the type II Cu. This mechanistic view is also supported by evidences on the *R. sphaeroides* CuNIR which show that upon nitrite binding a decreased covalency of the Cu-Nε(His) bond is observed. This may explain the nitrite-induced increase in type II Cu redox potential, and the increased probability of electron transfer from type I Cu.

The active site residues are more hydrophilic on one side and more hydrophobic on the other, suggesting a possible route for NO escape. The Asp^{98}

and the His^{255} residues are both involved in the catalysis as proton donors and in the control of internal electron transfer. Leu^{106} has also been shown to be important in the control of the Asp^{98} position in the active site pocket [16].

Mutants of Asp^{98} or His^{255} with Ala show, respectively, an increased and reduced intramolecular electron-transfer rate constant (k_{ET}), indicating that both residues around the type II Cu control the internal electron-transfer by the hydrogen-bonding network. The pH dependence of the catalytic activity, similarly to that of k_{ET}, shows an optimum around pH 5.5; the only ionizable and conserved residues around the type II Cu are the Asp^{98} and the His^{255}. All the Asp^{98} mutants show a decrease in the apparent rate constant, as in the case of the His^{255} mutants, and an increased K_M value, a parameter which is unchanged in the His mutants. Therefore His^{255} is not directly involved in the substrate binding but could control the rate of the catalysis either by positioning the Asp^{98} residue through the network of hydrogen bonds and/or by acting as a proton donor.

A possible reaction mechanism is summarized in Figure 4B, according with structure analysis of native and nitrite-soaked CuNIRs and kinetic analysis of mutants. In the first step, the water molecule bound to type II Cu is displaced by the substrate and presumably is released as OH^-; upon nitrite binding, type II Cu reduction occurs *via* intramolecular electron transfer; this step was proposed to be irreversible [16]. Nitrite protonation and electron transfer from type II Cu allow the N-O bond cleavage and release of a water molecule. Both Asp98 and His255 act as acid-base catalysts giving the two protons required for the nitrite reductase activity.

As previously shown for cd_1NIR, knowledge of structural data on different forms of CuNIR has helped considerably to unravel the mechanism of reduction of nitrite to NO. Also in the CuNIR system, some details still are unclear: among these, the apparent paradox between the implicit N-coordinated binding of the productive nitrosyl intermediate during catalysis and the observed O-coordinated substrate binding. The recent crystal structure determination of type II Cu-nitrosyl complex [20] may shed light on this apparent paradox. The crystals obtained using reduced-CuNIR in nitric oxide-saturated solution reveal a surprising “side-on” type II Cu-nitrosyl complex, suggesting a revised catalytic mechanism. Nitrite binds as O-coordinated the oxidised Cu site, displacing the water ligand, in the protonated form due presumably to the Asp^{98} residue; the internal electron transfer from type I Cu site reduces the active site triggering a rearrangement of nitrite to release water and form a Cu(I)-NO^+ intermediate (Figure 4B). The model leads to the hypothesis that the Cu(I)-NO^+ intermediate could be “side-on” bound according with the crystallographic data on the Cu-nitrosyl derivative. Furthermore the proposed intermediate may be stabilized by the negative charge of Asp^{98} residue. Finally, NO is displaced by water to form the resting state of the enzyme [20].

The resemblance of the CuNIR active site to that of carbonic anhydrase and other Zn-containing enzymes has been noted previously, suggesting that a common catalytic strategy might be operative in metalloenzymes-driven dehydration reactions. In both classes of enzymes, binding of the substrate occurs asymetrically with one oxygen bound to the catalytic metal (Cu or Zn) and a hydrogen bond formed to a proton-abstracting group (carboxylate or hydroxide). Release of the product leaves an hydroxide or a water molecule bound to the metal and hydrogen bonded to the same ionizable group.

References.

[1] W.G. Zumft, Cell biology and molecular basis of denitrification, Microbiol. Mol. Biol. Rev. 61 (1997) 533-616.

[2] F Cutruzzolà, Bacterial nitric oxide synthesis, Biochim. Biophys. Acta 1411 (1999) 231-49.

[3] J.W.A. Allen, S.J. Ferguson, V. Fulop, Cytochrome cd_1 nitrite reductase, Handbook of metalloproteins, Albrecht Messerschmidt, Robert Huber, Thomas Poulos, Karl Wieghardt Editors, Wiley, New York, 2001, pp. 424-39.

[4] F. Cutruzzola, S. Rinaldo, F. Centola, M. Brunori, NO production by *Pseudomonas aeruginosa* cd_1 nitrite reductase, IUBMB Life. 55 (2003) 617-21.

[5] S. Suzuki, K. Kataoka, K. Yamaguchi, Metal coordination and mechanism of multicopper nitrite reductase, Acc. Chem. Res. 33 (2000) 728-35.

[6] E.T. Adman and M.E.P. Murphy, Copper nitrite reductase, Handbook of metalloproteins, Albrecht Messerschmidt, Robert Huber, Thomas Poulos, Karl Wieghardt Editors, Wiley, New York, 2001, pp. 1381-89.

[7] B. I. V. Pearson, M. D. Page, R. J. M. van Spanning, S. J. Ferguson, A mutant of *Paracoccus denitrificans* with disrupted genes coding for cytochrome c_{550} and pseudoazurin establishes these two proteins as the in vivo electron donors to cytochrome cd_1 nitrite reductase, J. Biol. Chem. 185 (2003) 6308–15.

[8] R.S. Zajicek and S.J. Ferguson, The enigma of *Paracoccus pantotrophus* cytochrome cd_1 activation, Biochem. Soc. Trans. 33 (2005) 147-48.

[9] R. S. Zajicek, M. R. Cheesman, E. H. J. Gordon, Stuart J. Ferguson, Y25S variant of *Paracoccus pantotrophus* cytochrome cd_1 provides insight into anion binding by d_1 heme and a rare example of a critical difference between solution and crystal structures, J. Biol. Chem. 280 (2005) 26073–79.

[10] R. Silaghi-Dumitrescu, Linkage isomerism in nitrite reduction by cytochrome cd_1 nitrite reductase, Inorg. Chem. 43 (2004) 3715-18.

[11] S.J. George, J.W. Allen, S.J. Ferguson, R.N. Thorneley, Time-resolved infrared spectroscopy reveals a stable ferric heme-NO intermediate in the reaction of *Paracoccus pantotrophus* cytochrome cd_1 nitrite reductase with nitrite, J. Biol. Chem. 275 (2000) 33231-37.

[12] S. Wherland, O. Farver, I. Pecht, Intramolecular electron transfer in nitrite

reductases. hemphyschem. 6 (2005) 805-12.

[13] F. Cutruzzolà, K. Brown, E.K. Wilson, A. Bellelli, M. Arese, M. Tegoni, C. Cambillau, M..Brunori, The nitrite reductase from *Pseudomonas aeruginosa*: essential role of two active-site histidines in the catalytic and structural properties, Proc. Natl. Acad. Sci. U S A. 98 (2001) 2232-7.

[14] T. Sjogren and J. Hajdu, The Structure of an alternative form of *Paracoccus pantotrophus* cytochrome cd_1 nitrite reductase, J. Biol. Chem. 276 (2001) 29450-5.

[15] K. Yamaguchi, K. Kataoka, M. Kobayashi, K. Itoh, A. Fukui, S. Suzuki, Characterization of two type 1 Cu sites of *Hyphomicrobium denitrificans* nitrite reductase: a new class of copper-containing nitrite reductases, Biochemistry 43 (2004) 14180-8.

[16] S.V. Antonyuk, R.W. Strange, G. Sawers, R.R. Eady, S.S. Hasnain, Atomic resolution structures of resting-state, substrate- and product-complexed Cu-nitrite reductase provide insight into catalytic mechanism, Proc. Natl. Acad. Sci. U S A., 102 (2005) 12041-6.

[17] F.E. Dodd, J. Van Beeumen, R.R. Eady, S.S. Hasnain, X-ray structure of a blue-copper nitrite reductase in two crystal forms. The nature of the copper sites, mode of substrate binding and recognition by redox partner, J. Mol. Biol. 282 (1998) 369-82.

[18] F. Jacobson, H. Guo, K. Olesen, M. Okvist, R. Neutze, L. Sjolin, Structures of the oxidized and reduced forms of nitrite reductase from *Rhodobacter sphaeroides* 2.4.3 at high pH: changes in the interactions of the type 2 copper, Acta Crystallogr. D. Biol. Crystallogr. 61 (2005) 1190-8.

[19] A. Impagliazzo, L. Krippahl, M. Ubbink, Pseudoazurin-nitrite reductase interactions, Chembiochem. 6 (2005) 1648-53.

[20] E.I. Tocheva, F.I. Rosell, A.G. Mauk, M.E. Murphy, Side-on copper-nitrosyl coordination by nitrite reductase, Science 304 (2004) 867-70.

LEGENDS TO FIGURES

Figure 1. Chemical structure of the hemes of cd_1NIR. (A) Structure of c heme showing the covalent attachment to the protein. (B) Chemical structure of d_1 heme: notice that this cofactor is more oxidized than a classical b-type heme.

Figure 2. *P. aeruginosa* cd_1NIR. 3-D structure of the dimer in the oxidised form (PDB code 1NIR). Notice the swapping of the N-terminal arm between neighbouring monomers. The α-helical c heme domain is the electron acceptor pole, whereas the β-propeller domain contains the d_1 heme active site.

Figure 3. Structure of the c heme (A) and the d_1 heme (B) sites in the oxidised *P. aeruginosa* cd_1NIR (PDB code 1NIR). In panel B, the residues are labeled with the sequence number and a letter which refers to the different subunits (A and B).

Figure 4. Reaction mechanism of NIRs with nitrite. (A) Proposed mechanism of cd_1NIR, modified from [13]; (#) the histidine residues in the active site are involved in the product (NO) release by stabilizing the hydroxide (OH^-) ligand of the oxidised d_1 heme iron. Lack of this stabilization favours the formation of the dead-end state (reduced NO-bound adduct). (B) Proposed mechanism of CuNIR, modified from [5, 16]; in this model the “side-on” product (NO) binding is also included.

Figure 5. Structure of the *A. faecalis* CuNIR in the oxidised form (PDB code 1AS7). (A) Overall view of the homotrimer; the copper atoms are represented as filled circles. (B) Type I and type II Cu sites in the oxidized protein. Residues His^{255} and His^{306} come from the adjacent subunit.

Table I. Properties of cd$_1$NIR.

Property	*Pseudomonas aeruginosa*	*Pseudomonas stutzeri*	*Paracoccus pantotrophus*	*Pseudomonas nautica*	*Thiobacillus denitrificans*
Molecular mass (KDa)(homodimer)	119-121	119-134	120	131	118
VIS absorbance (oxidised form)	411,520 640	411,525 641	406,525, 644,702	409,521, 636	407,525,642
(nm) (reduced form)	418, 460, 521, 549, 554, 625-655	417, 460, 522, 548, 554, 625-655	418, 460, 521, 547, 553, 625-655	416,460,521, 548,552,625-655	418, 460, 523, 549, 553, 625-650
EPR parameters (g values)					
Heme d_1	2.51, 2.43, 1.71	2.56, 2.42, 1.84	2.52,2.19,1.84	2.51,2.33,1.67	2.50, 2.43, 1.70
Heme c	3.01, 2.29, 1.40	2.97, 2.24, 1.58	3.05	2.92,2.35	3.6
$E_{m,7}$ (mV)					
Heme c	+288[a] (>290[b]) (<214[c])		Hysteretic redox behaviour[d]	+234 (pH7.6)	
Heme d_1	+287			+199 (pH7.6)	
Electron donor(s)	Cyt c_{552} / azurin	Cyt c_{551}	Cyt c_{550} /pseudoazurin	Cyt c_{552}	
Km for NO_2^- (mM) (electron donor)	53 (hydroxyquinone) 6 (azurin)	1.8 (horse heart Cyt c)	6.7 – 12[e] (Cyt c_{550})		
Km for O_2 (mM) (oxygen electrode)	28		80		
k_{cat} (s^{-1})					
With NO_2^-	8	8	2.1 – 74[e]		
With O_2	0.6 – 6.4		3 - 6		

(a) When d1 heme is unbound.

(b) When d1 heme is NO bound.

(c) When d1 heme is CO bound.

(d) See ref. [3].

(e) These two values refer to "as isolated " and "pre-activated" states of the enzyme respectively.

Table II. Properties of CuNIR

Property	*Alcaligenes xylosoxidans*	*Achromobacter cycloclastes*	*Alcaligenes faecalis S-6*	*Rhodobacter sphaeroides*
Molecular mass (kDa) homotrimer	103	108	100.4-119	140
VIS absorbance (nm)	593, 770	400, 458, 585, 700	400, 457, 587, 700	390,457, 589, 700,810
No. of Cu atoms/holoenzyme	3.5 ± 0.8	4.6	4.5	
EPR parameters				
Type I Cu, g	2.212	2.195	2.19	2.19
Type I Cu A(mT)	6.3	7.3		7.8
Type II Cu, g	2.29	2.262	2.30	2.34
Type II Cu, A (mT)	14.2	17.5		16.3
Electron donor(s)	Cyt c_{553}	Pseudoazurin/ cyt c	Pseudoazurin	Cytochrome c_2
E_m (mV)				
Type I Cu	+260	+240		+247
Type II Cu		+260		< +200
Activity (μmol min^{-1} mg^{-1})				
$NO_2^- \rightarrow NO$	240	280	360	40
(Electron donor)[a]	(MV)	(PMS-Asc)	(MV)	(Yeast Cyt c)
Km for NO_2^- (μM)[b]	230	500	74	14 (Yeast Cyt c)
				35 (BV)

a) MV, methyl viologen; PMS-Asc, phenazine metosulphate plus ascorbate; BV, benzyl viologen.

b) Values obtained with the same electron donors as for the nitrite reductase activity, unless otherwise stated.

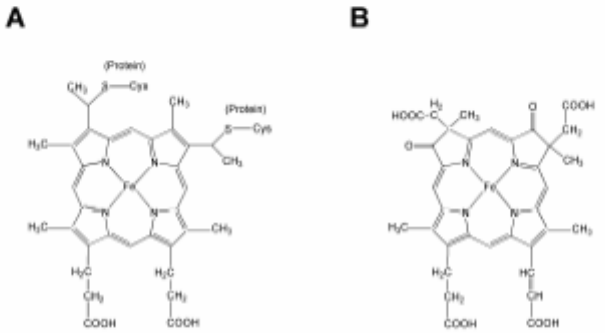

FIGURE 1

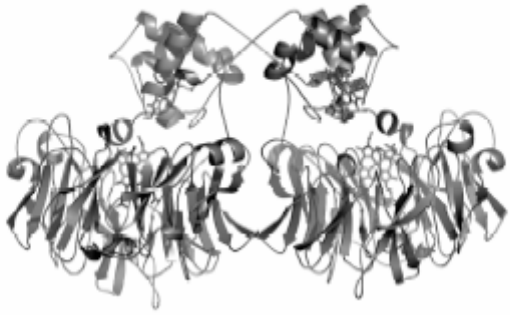

FIGURE 2

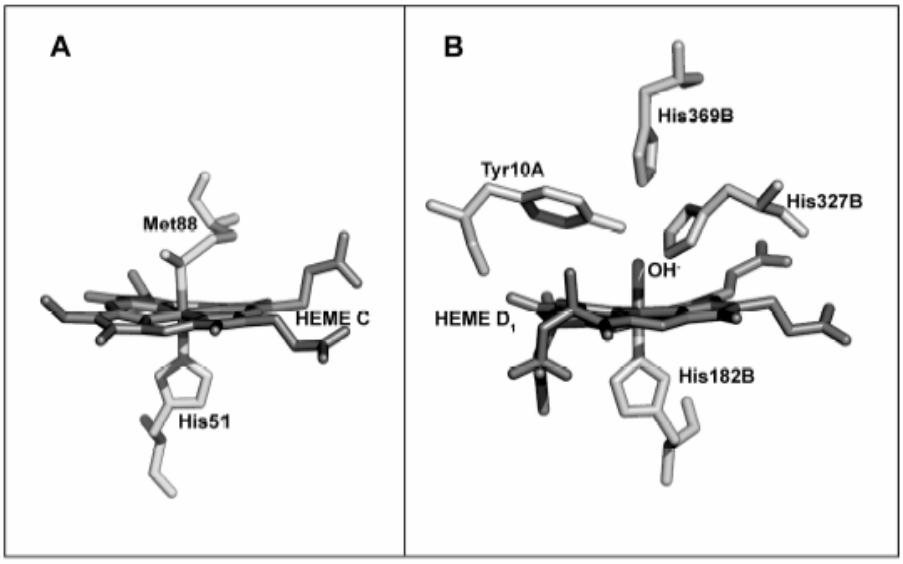
A
Met88
HEME C
His51
B
His369B
Tyr10A
His327B
OH-
HEME D1
His182B

FIGURE 3

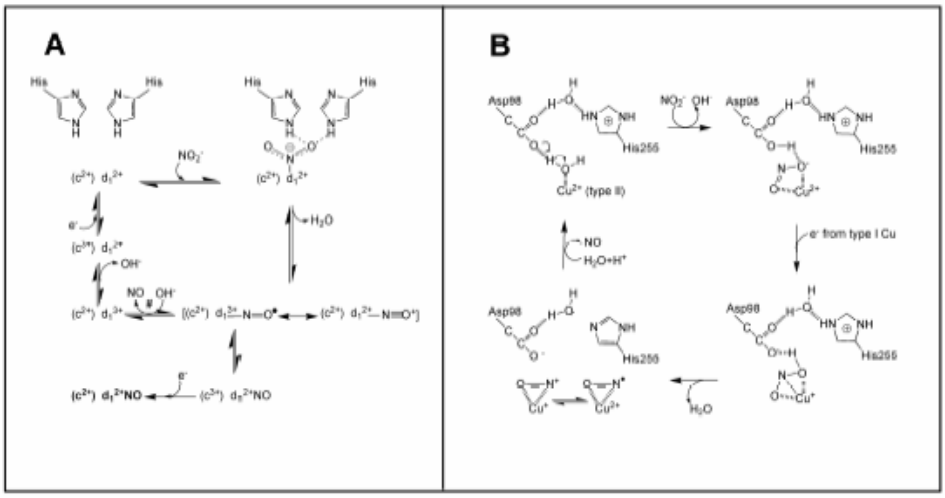
A
B
His
His
His
His
Asp98
His255
Cu2+ (type II)
NO
H2O+H+
e- from type I Cu
H2O

FIGURE 4

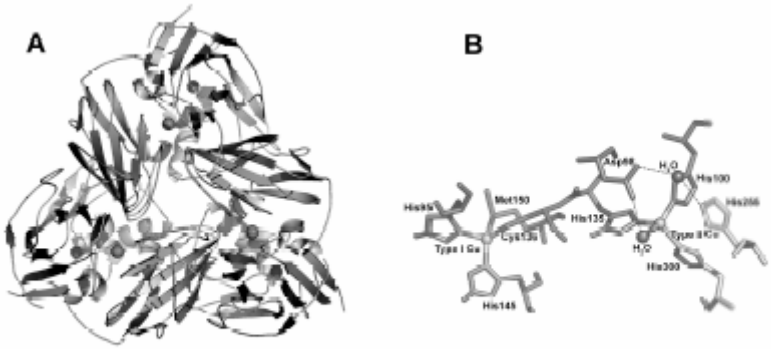
A
B
Asp98
H2O
His100
His255
His95
Met150
His135
Type I Cu
Cys138
Type II Cu
H2O
His300
His145

FIGURE 5

HISTIDINE 369 CONTROLS THE REACTIVITY OF *PSEUDOMONAS AERUGINOSA* CD1 NITRITE REDUCTASE WITH OXYGEN

Fabio Centola, Serena Rinaldo, Maurizio Brunori[#] and Francesca Cutruzzolà

Department of Biochemical Sciences 'A.Rossi Fanelli' and Istituto di Biologia e Patologia Molecolari – CNR, University of Rome La Sapienza, P.le A. Moro 5,00185 Rome, Italy

[#] Corresponding author at:

Dipartimento di Scienze Biochimiche "A.Rossi Fanelli"

Università di Roma La Sapienza

P.le A. Moro, 5 –00185 Rome (Italy)

Tel 39-06-4450291

FAX 39-06-4440062

E-mail: maurizio.brunori@uniroma1.it

Abbreviations: cd_1NIR, cd_1 nitrite reductase; cyt c_{551}, cytochrome c_{551}; H369A, Histidine 369 to Alanine mutant of cd_1 nitrite reductase; dHis, Histidine 369 to Alanine and Histidine 327 to Alanine double mutant of cd_1 nitrite reductase; eT, electron transfer.

ABSTRACT

In the denitrification pathway, *Pseudomonas aeruginosa* cytochrome cd_1 nitrite reductase catalyzes the reduction of nitrite to nitric oxide; *in vitro*, this enzyme is also competent in the reduction of O_2 to $2H_2O$. In this paper we compare the steady-state and transient kinetics of the O_2 reaction in the wild type cd_1 nitrite reductase with that of two site-directed mutants in which only one (His369) or both conserved histidines (His369 and His327) in the distal site of the d_1 heme have been mutated into alanines. These mutations, previously shown to affect the reduction of nitrite, also impair the reaction with O_2, the properties and lifetime of the intermediate species being affected by the mutation His --> Ala. The role of His369 is dominant, since the behaviour of the double mutant closely resembles that of the single one. Our findings allow to present an overall picture for the reactivity of cd_1NIR and extend our previous conclusion that the conserved distal histidines are essential for the binding to reduced d_1-heme of different anions (whether a substrate like nitrite, a ligand as cyanide or an O_2 intermediate) and play a key role in catalysis of cd_1 nitrite resuctase.

Keywords: cd_1 nitrite reductase, oxygen, intermediate, electron transfer.

INTRODUCTION

Cytochrome cd_1 nitrite reductase (cd_1NIR) catalyzes the reduction of nitrite (the toxic product of the nitrate reductase activity) to NO in the denitrification pathway of several bacteria, including *Pseudomonas aeruginosa*. Cd1NIR is also capable of catalyzing the reduction of O_2 to $2H_2O$ *in vitro*, a function which was actually identified earlier than the physiologically relevant nitrite reductase activity.

Cd_1NIR is a homodimer (M_r = 120000), each subunit containing one c-heme and one d_1-heme; thus the native dimeric protein carries four metal centres. Early evidence indicating that the product of O_2 reduction is water [1], was later confirmed by measuring the stoichiometry of O_2 reduction catalyzed by both *Paracoccus denitrificans* [2] and *P. aeruginosa* cd_1NIR [3]. A minimum kinetic scheme for the reaction of reduced cd_1NIR with O_2 was proposed by Greenwood and coworkers [4]:

$$NIR + O_2 \quad \Leftrightarrow \quad NIR{\cdot}O_2 \quad \rightarrow \quad A \quad \rightarrow \quad B \qquad \text{(Scheme 1)}$$

A bimolecular, O_2 dependent reaction ($k=3.3\times10^4\ M^{-1}\ s^{-1}$), yielding an apparent affinity constant for O_2 of $10^4\ M^{-1}$, was coupled to formation and decay of an intermediate state. Interestingly, oxidation of the c-heme was found to be synchronous with the binding of O_2 to the reduced d_1-heme, implying a fast internal electron transfer (eT) rate ($k \geq 100\ s^{-1}$) in the O_2 complex of the enzyme. This fast

rate constant has to be compared with the values of ~ 0.2-1 s^{-1} reported for the reduction of the d_1-heme measured under anaerobic conditions [5,6]; moreover also the reduction of nitrite proceeds at an equally slow rate [7]. The obvious conclusion is that the heme-to-heme internal eT rate is very variable and generally slow, except in some intermediate (as in the O_2 reaction). The general features of the reaction with O_2 observed for the *P. aeruginosa* enzyme [4], were more recently confirmed by Koppenhofer et al. [8] for *Paracoccus pantotrophus* cd_1NIR.

We have previously shown that mutation of the two conserved histidines (His327Ala and His369Ala) facing the d_1-heme on the distal site abolishes the nitrite reductase activity of *P. aeruginosa* cd_1NIR, while O_2 reduction is still possible [9]. This may indicate different underlying mechanisms when the reduced enzyme reacts with an anionic substrate (such as nitrite) or with the neutral dioxygen.

In the present work we report a detailed comparison of the kinetics of the O_2 reaction in the wild type NIR with two site-directed mutants in which either one (H369A) or both conserved histidines (H369A-H327A, hereinafter dHis) have been mutated to alanines. The main goal of this study was to understand the role of the distal histidine(s) in the binding and reduction of O_2 by *P. aeruginosa* cd_1NIR.

MATERIALS AND METHODS

Mutagenesis and protein purification

Wild-type cd_1NIR was purified following Parr et al. [10]. Mutagenesis of His 369 to Ala was carried out as described in [9]. The double mutant was obtained from the H327A template with the Chameleon® double-stranded site-directed mutagenesis kit (Stratagene, USA). Subcloning, expression in *Pseudomonas putida* and purification were obtained as reported previously [11]. In the *P. putida* expression system, the protein is synthetized with the c-heme, but no d_1-heme; this semiapo-NIR is then reconstituted *in vitro* with the d_1-heme extracted from wt cd_1NIR. Reconstitution was carried out by incubating the proteins at 15°C in 50 mM Bis-Tris buffer at pH 7.0 with a 1.5 stoichiometric excess of d_1-heme, followed by gel filtration.

Steady state experiments

Oxidase activity at steady state was measured for the wt protein and the H369A mutant following the oxidation of *P. aeruginosa* cytochrome c_{551} (cyt c_{551}) at 551 nm using a JASCO V550 spectrophotometer. Cyt c_{551} was reduced by addition of solid sodium dithionite and the excess of reductant was removed by gel filtration chromatography on a Sephadex G25 column. The measurements were carried out in 100 mM sodium phosphate buffer pH 7.0 at 20°C, with 20 μM of cyt c_{551} and 15 nM of cd_1NIR, varying O_2 concentration from 10 μM to 1.3 mM.

Stopped flow experiments

Reduced NIR (4-8 μM) was prepared in degassed 100mM sodium phosphate buffer pH 7.0 incubating with 30μM sodium ascorbate for 30 min. Ascorbate concentration was kept low in order to keep to a minimum the reaction cycles. The oxidase reaction was initiated by mixing the reduced enzyme with buffer at different O_2 concentrations (67-650 μM after mixing). In the double mixing experiments this initial mixture was sequentially mixed (at delay times 0.1-1 sec) with a buffered solution containing 1 mM carbon monoxide (CO).

All experiments were carried out anaerobically at 20°C in the presence of catalase (390 U/ml), glucose oxidase (6 U/ml) and 10 mM glucose. Kinetic measurements were carried out with an Applied Photophysics stopped-flow apparatus equipped with a multidiode array spectrophotometer (DX.17MV, Applied Photophysics, Leatherhead, UK), collecting 100 spectra in 10 sec. The time courses were followed in the wavelength range from 380 to 700 nm and analysis was carried out with the IgorPro program (Wavemetrics). In the double mixing experiment with CO the time course of the reaction was monitored at single wavelength (460 nm) using a monochromator.

RESULTS

Oxygen affinity.

The affinity for O_2 of the wild type (wt) and H369A cd_1NIRs was estimated by steady state measurements carried out using reduced *P.aeruginosa* cyt c_{551} as the electron donor. All experiments were carried out at a cyt c_{551} concentration (i.e. 20 μM) higher than the K_M for this substrate, previously determined to be 2.0 and 7.5 μM for wt and H369A, respectively [9]. Under these experimental conditions it was possible to measure a dependence on O_2 concentration of the observed rate of oxidation of cyt c_{551} (Figure 1). While the $K_M(O_2)$ = 36 μM measured for the wt enzyme is consistent with previous estimates (28 μM) [12], the $K_M(O_2)$ of H369A was found to be much greater, namely K_M = 990 μM.

The reaction with oxygen.

The time course of the reaction seen after mixing the reduced wt and mutant cd_1NIRs (H369A and dHIS) with a saturated solution of O_2 (650 μM a.m.) is shown in Figure 2 (left panels). The results for the wt protein are consistent with those published by Greenwood et al. [4] and can be described by a sum of two exponentials (Figure 2A). In the wt cd_1NIR the reduced protein (the only species present at 4 msec after mixing) disappears with a decay process (k_1 = 15.5 s^{-1}) involving synchronous changes at both the c-heme (followed at 551 nm) and the d_1-heme (followed at 640 nm). At the end of this faster phase (t~200 msec) the c-heme is >80% oxidized and large spectroscopic changes have occurred at the d_1-heme (Figure 2B), yielding the intermediate species A (see Scheme 1). Thus within 200 msec both O_2 binding and eT from the c-heme to the d_1-heme-O_2 complex have occurred.

For the two mutants the time course of the reaction with O_2 also shows two kinetic processes within the first 3 seconds (Figure 2C and E), with a transient species maximally populated around 150-200 msec. Examination of the spectrum of this intermediate in the mutants clearly shows that the degree of c-heme oxidation is much smaller (~25 ± 5%, Figure 2D and F) than that seen in intermediate A populated by wt cd_1NIR (~80 ± 5%, Figure 2A).

The second kinetic phase, corresponding to the decay of the first intermediate, is complete within 2 sec and occurs approximately at the same rate in all proteins (k_2=~2 sec^{-1}). In the wt NIR the second process involves only minor changes in the c-heme spectrum, whereas the d1-heme spectrum evolves to that of an oxidized form (Figure 2B). In the mutant proteins, at the end of this phase the

spectrum of the d_1-heme (above 600 nm) closely resembles that of the oxidized form, whereas the c-heme is still largely reduced (>50%) (Figure 2D and F).

A peculiarity with the two mutants is an additional slower phase observed to occur in the time range 3-10 seconds (Figure 2C and E). This very slow process involves a large decrease in the absorbance of the d_1-heme, but very limited changes in the c-heme spectrum. It is possible that in the mutants the d_1-heme is more exposed to side-reactions (as for example degradation by partially reduced O_2 species) which are not occurring in the wt enzyme (see Discussion for further details). Indeed a species with spectral properties similar to that seen in the stopped flow at ~ 10 sec is also observed in the spectrophotometer when the mutants cd_1NIRs are exposed to air in the presence of glucose oxidase but without catalase (data not shown). We attribute this side-reaction, seen only with the mutants, to d_1-heme bleaching, a process which has already been described for other hemeproteins [13].

Dependence on O_2 concentration.

The rate of the two kinetic phases observed in the oxidation of wt and mutant cd_1NIRs was determined as a function of O_2 concentration (between 65-650 μM). A plot of k_1 and k_2 (Figure 3) clearly indicates that only the first rate constant (k_1) depends on O_2 concentration, as for the wt protein, although the slope of the linear plot is less steep in the case of the H369A and dHis.

Therefore also in the mutants the first kinetic phase represents a bimolecular O_2 dependent process, as for the wt cd_1NIR; since a smaller fraction of the c-heme becomes oxidized during this phase (Figure 2D and F), limited eT between the c-heme and the d1-heme has occurred at this stage.

Properties of the intermediates.

In order to further characterize the properties of the intermediates populated during the reaction with O_2 additional experiments have been carried out. Since the overall behaviour of the single H369A mutant and of the double mutant (dHis) are very similar, showing that His369 plays a dominant role in catalysis, we have characterized only this single mutant in more detail.

Since the $K_D(O_2)$ in mutant H369A is much greater then that of the wt enzyme, it may be presumed that the incomplete oxidation of the c-heme seen in the stopped-flow experiments (Figure 2C and D) was due to incomplete saturation of the mutant protein with O_2. If this was the case, in the H369A mutant both the first transient species (maximally populated at 150-200 msec) and the species seen at 3 seconds should contain a significant fraction of reduced d1-heme available to bind other ligands.

CO, a ligand of the reduced heme iron, is known to form a stable derivative and therefore has been often employed to “trap” the reduced state of hemeproteins. The binding of CO to the H369A mutant has been characterized by mixing in the stopped flow the fully reduced enzyme with CO at different concentrations (not shown). The bimolecular rate constant (k_{on}= 5 x 10^5 M^{-1} s^{-1}) is more rapid than that of the wild type enzyme (k_{on}= 2 x 10^4 M^{-1} s^{-1}), but similar to that previously reported for the other single His327 to Ala mutant [14]. The faster binding of CO to both histidine mutants can easily be understood in terms of increased accessibility to ligands of the d1-heme iron in the absence of the imidazole side-chain(s).

To probe the active site of the H369A mutant for the presence of reduced d1-heme along the reaction pathway with O_2, we have sequentially mixed in the stopped-flow the reaction mixture (reduced NIR + O_2) at different ageing times (50 and 200 msec, 2.5 sec) with a solution containing millimolar CO. The data reported in Figure 4B for H369A show that, at the shortest delay time (50 msec), where the protein is still largely in the unbound reduced form (Figure 4B,inset), CO binding is obviously observed and it occurs with a rate constant of about 100 sec^{-1}, in agreement with that measured for the fully reduced H369A NIR. However at longer delay times (200 msec and 2.5 sec) no reaction with CO was detectable excluding the presence of significant fraction of unbound reduced d_1-heme. As a negative control, the same reaction was run on the intermediate A of wt cd1NIR (Figure 4A), where binding and reduction of O_2 has already taken place [4, this paper] and, as expected, no reaction with CO was observed.

DISCUSSION

Although the reactivity of *Pseudomonas aeruginosa* cd_1NIR has been studied for quite a while, the reaction mechanism and the role of the structure of the distal site are still elusive, both in terms of intermediates and kinetic scheme. Essential information on the reaction mechanism with the physiological substrate nitrite was obtained by site-directed mutagenesis studies in which the two conserved histidine residues (His327 and His369) in the active site d_1-heme pocket were substituted with alanines [9]. Together with binding experiments carried out using the anionic ligand cyanide [15], we concluded that these two conserved His are essential to stabilize the adduct of reduced d_1-heme with anions. Here we report new data on the kinetics of the reaction with O_2 of the wt enzyme and two site-directed mutants (a single mutant H369A and a double mutant H369A and H327A), in order to unveil the O_2-reduction mechanism of *P. aeruginosa* cd_1NIR and thereby of the other enzymes of the same family.

A clear-cut feature of the reactivity of these mutants is that, whereas the nitrite reductase activity is completely abolished by substitution of even only one histidine with alanine, O_2 reduction can still take place [9]. However, steady-state experiments at different O_2 concentrations show that the $K_M(O_2)$ of H369A is increased 25-fold with respect to the wt enzyme. This large drop in overall O_2 "affinity" obtained by a single His to Ala mutation may in principle depend on the binding of O_2 and/or other steps associated to catalysis at the reduced d_1-heme. Here we report the pre-steady state kinetics under experimental conditions where the reducing agent (ascorbate) is almost stoichiometric with protein; thus the electron flow into the enzyme is sufficient to accomplish a few (1-2) reaction cycles. This condition is the same employed by Greenwood and coworkers [4], but different from data reported by other groups on cd_1NIR from different sources [8], using high reductant concentrations.

The rate of population of the first observable intermediate A (see Scheme 1) is O_2 concentration dependent. In agreement with Greeenwood et al. [4], we confirmed that in the wt cd_1NIR (i) the second order rate constant is k_{app} = 2-3 x 10^4 $M^{-1}s^{-1}$ and (ii) intermediate A is a species in which the c-heme is largely (> 80%) oxidized and the d_1-heme spectrum is modified relative to reduced. This implies that a *bona fide* O_2 adduct to reduced d_1-heme ($NIR^{\cdot}O_2$) is never significantly populated

and therefore intermediate A was presumed to be a peroxi-intermediate. The slower decay of intermediate A to state B, which optically corresponds to the oxidized form of the enzyme, implies donation of two more electrons to achieve complete reduction of O_2 to $2H_2O$, the reaction product in *P. aeruginosa* [3]. Working with *P. pantotrophus* cd_1NIR, Koppenhofer et al. [8] confirmed that a bimolecular reaction with O_2 leads to an intermediate (populated at about 100 msec) in which ~ 100% of the c-heme is oxidized, and showed that this species displays an EPR radical signal decaying (in ~ 500 msec) to a Fe(III) state, probably with an OH^- ligand. These authors suggested that, early during the reaction, the peroxide-bound species is rapidly converted in a Fe(IV)-oxo derivative plus a radical, whose further reduction leads to the ferric derivative. Thus in the reaction with O_2 of the *P. pantotrophus* cd_1NIR the lifetime of the peroxide-intermediate is presumed to be very short, with early rupture of the oxygen-oxygen bond and electron supply from the protein. In summary, available results suggest that in wt cd1NIRs the first intermediate is either a Fe(III)-peroxi or Fe(IV)-oxo state.

The first two kinetic processes seen in the mutants are qualitatively reminiscent of those observed for the wt cd_1NIR (Figure 2). The first rate constant is O_2 concentration dependent (Figure 3), the apparent second order rate constant being about 7×10^3 $M^{-1}sec^{-1}$ for both mutants. This value, which is significantly lower than that of the wt protein ($k = 2\text{-}3 \times 10^4$ $M^{-1}sec^{-1}$) [6], is relevant to the interpretation of the much increased $K_M(O_2)$ measured at steady state for the H369A mutant. On the other hand, while in the wt enzyme oxidation of the c-heme occurring synchronously with O_2 binding [4, 8] and is almost complete (> 80%), in the two mutants a much smaller fraction (~25%) of the c-heme is oxidized in the first intermediate, although the d_1-heme spectrum has significantly changed (Figure 2). In both His mutants, the c-heme oxidation at the end of the reaction is always lower than 50%, indicating a large effect of the mutation, on the internal c-to-d_1 eT.

From the data presented above, it may be assumed that in the H369A mutant the first intermediate in the reaction pathway (see scheme 1) corresponds to a state partially O_2 bound, because the absence of the distal imidazole side-chain may enhance O_2 dissociation, as seen for other hemeproteins [16]. However, the double-mixing experiment with CO clearly shows that in the H369A mutant (at delay times longer than 50 msec) there is no unbound reduced d_1-heme available to be trapped by CO, in contrast with the possibility outlined above. Thus the first species populated in the reaction with O_2 of reduced H369A mutant, where very limited c -> d_1 heme eT has occurred, must be different form than intermediate A of wt cd1NIR; this state could be either Fe(II)O_2 or Fe(III) O_2^-, but no unbound reduced d_1-heme competent to bind CO is present.

A histidine residue on the distal side of the heme iron is a common feature in hemeproteins involved in O_2 binding and chemistry [17]; the imidazole side-chain is known to play an important role in the stabilization of O_2 and its partially reduced species. The partial population of a superoxide anion state in oxygenated complexes (Fe(II)O_2) of myoglobin (Mb) or hemoglobin (Hb) is generally accepted [16-19], and autoxidation to the ferric state occurs with liberation of superoxide. In these cases, the distal histidine (*via* its imidazole ring) increases the stability of the oxygenated complex by forming a H-bond to the bound O_2, thus decreasing the autoxidation rate of MbO_2 or HbO_2, as demonstrated by site-directed mutagenesis [16, 20].

Another role for the distal histidine is seen in heme peroxidases, where the

substrate is a peroxide molecule bound to the Fe(III) state of the heme; in these enzymes, the protonation state of the distal histidine is directly involved in facilitating O-O bond cleavage [21, 22].
Taking into account these observations, we may propose a possible scenario for the reaction of mutants of cd_1NIR and O_2:
- the absence of the histidine side-chain in the H369A mutant may destabilize the presumed peroxi-intermediate and possibly favour the superoxide-bound Fe(III) state;
-the Fe(III) O_2^- derivative (which is never significantly populated in wt cd_1NIR) might thus be the transient species seen in the H369A mutant, consistently with the results of the CO experiment;
-further eT to this species eventually leads to a Fe(III) O_2^{2-} adduct where no O-O bond cleavage can occur (due to the lack of the histidine) preventing further chemistry;
- dissociation of the reactive O_2 species (superoxide and/or peroxide) leads to the state seen at >3 sec in the H369A mutant, which has an oxidized d1-heme and a (partially) reduced c-heme;
- this event, due to the loss of stabilization in the absence of the imidazolium side-chain, causes d_1-heme degradation, an event clearly seen in the mutants (at reaction times > 3 sec) but not in the wt enzyme;
- further reduction and O_2 binding is therefore impossible in the H369A mutant because, with the low concentration of ascorbate used in the experiment, the internal (c-> d_1) eT rate is prevented and chemical degradation of the d1-heme occurs more rapidly.

In conclusion, substitution of the two invariant histidines with alanines in the d_1 heme pocket, previously shown to control the reduction of nitrite [9], imposes significant changes also in the reaction of reduced cd_1NIR with O_2. The effect of the His369 to Ala mutation appears dominant, since the behaviour of the dHis mutant closely resembles that of the single one. Moreover, we have evidence that His369 exerts a protective role towards degradation of the specialized d_1-heme, by preventing accumulation of the reactive O_2 species (normally populated along the reaction pathway) which rapidly destroy the d_1-heme. This finding has physiological implications given that denitrification can occur also under low O_2 tension and that strict anaerobiosis is not required for the biosynthesis of cd_1NIR in *P. aeruginosa* and other denitryfiers [23]. Our findings provide evidence for a unifying picture of the reactivity of cd_1NIR, and support the general conclusion that stabilization of anions and protonation steps, the key event of catalysis, are controlled by the conserved distal His. The negatively charged molecule which interacts with the reduced d_1-heme can either be a substrate (nitrite) [9], a ligand (cyanide) [15] or a reaction intermediate, like in the present study with O_2.

Acknowledgements

Funds from the Ministero della Istruzione, Università e Ricerca of Italy (to M. B.) and of European Union COST Action 856 (to F.C.) are gratefully acknowledged.

FIGURE LEGENDS

FIGURE 1

Dependence on O_2 concentration of the steady-state rate of oxidation of *P. aeruginosa* cyt c_{551} catalyzed by wt cd_1NIR and H369A mutant. Reduced cyt c_{551} concentration is 20 μM. Continuous lines are best fits of the experimental data with the Michaelis-Menten equation. Experimental conditions are 100 mM sodium phosphate buffer pH 7.0 and 20°C.

FIGURE 2

Time course of the reaction with O_2 (650 μM after mixing) of cd_1NIRs wt (panels A,B) and mutants H369A (panels C, D) and dHIS (panels E, F). The reaction was followed acquiring at the full spectrum (from 400 to 700 nm), but only the time course at the absorption peaks characteristic of the two chromophores, i.e. 551 nm for the c-heme (circles) and 640 nm for the d_1 heme (triangles), is shown (left panels). The difference spectra recorded at selected times are shown (right panels) by reference to the fully reduced enzyme; the negative peak at 551 nm is indicative of oxidation of the c-heme. The static difference spectrum between the oxidized and the reduced cd_1NIR (ox-red) is also reported.

Experimental conditions as in Figure 1.

FIGURE 3

Dependence on O_2 concentration of the observed rate constants of wt and mutant cd_1NIRs. Experimental conditions as in Figure 1.

FIGURE 4

Time course of the sequential mixing experiments with O_2 and CO, carried out with wt (panel A) and H369A (panel B) mutant cd_1NIRs. Experimental data indicate absorbance changes at 460 nm in the following experiments: (**closed circles**) reduced protein mixed with degassed buffer containing CO (1.0 mM); (**open triangles**) reduced protein first mixed with O_2 (1.3 mM) and then after with degassed buffer (delay time 100-200 msec); (**open squares**) reduced protein first mixed with O_2 (1.3 mM) and then after with CO (1.0 mM) (delay time 100-200 msec). Two additional delay times are shown in the H369A experiment (bottom panel): (**open circles**) at 50 msec and (**open diamonds**) 2.5 sec. The insets show the time course at 460 nm observed by mixing the reduced enzyme with O_2 (1.3 mM before mixing); the arrows indicate the time delay after the first mixing at which the second mixing with CO was performed.

Experimental conditions as in Figure 1.

REFERENCES

[1] T. Yamanaka, Studies on *Pseudomonas* cytochrome oxidase, Annu. Rep.Sci.Works Fac. Sci. Osaka Univ., 11 (1963) 77-115.

[2] R. Timkovich, M.K. Robinson, Evidence for water as the product for oxygen reduction by cytochrome cd, Biochem. Biophys. Res. Commun. 88 (1979) 649-655.

[3] M.G. Tordi, M.C. Silvestrini, A. Colosimo, L. Tuttobello, M. Brunori, Cytochrome c-551 and azurin oxidation catalysed by *Pseudomonas aeruginosa* cytochrome oxidase. A steady-state kinetic study, Biochem. J. 230 (1985) 797-805.

[4] C. Greenwood, D. Barber, S.R. Parr, E. Antonini, M. Brunori, A. Colosimo, The reaction of *Pseudomonas aeruginosa* cytochrome c-551 oxidase with oxygen, Biochem. J. 173 (1978) 11-17.

[5] S.R. Parr, D. Barber, C. Greenwood, M. Brunori, The electron transfer reaction between azurin and cytochrome oxidase from *Pseudomonas aeruginosa*, Biochem. J. 167 (1997) 447-455.

[6] K. Kobayashi, A. Koppenhofer, S.J. Ferguson, N.J. Watmough, S. Tagawa, Intramolecular electron transfer from c heme to d1 heme in bacterial cytochrome cd_1 nitrite reductase occurs over the same distances at very different rates depending on the source of the enzyme, Biochemistry 40 (2001) 8542-8547.

[7] M.C. Silvestrini, M.G. Tordi, G. Musci, M. Brunori, The reaction of *Pseudomonas* nitrite reductase and nitrite, J. Biol. Chem. 265 (1990) 11783-11787.

[8] Koppenhofer, R.H. Little, D.J. Lowe, S.J. Ferguson, N.J. Watmough, Oxidase reaction of cytochrome cd(1) from *Paracoccus pantotrophus*, Biochemistry 39 (2000) 4028-4036.

[9] F. Cutruzzolà, K. Brown, E.K. Wilson, A. Bellelli, M. Arese, M. Tegoni, C. Cambillau, M. Brunori, The nitrite reductase from *Pseudomonas aeruginosa*: essential role of two active-site histidines in the catalytic and structural properties, Proc. Natl. Acad. Sci. U S A 98 (2001) 2232-2237.

[10] S.R. Parr, D. Barber, C. Greenwood, B. W. Phillips, J. Melling, A purification procedure for the soluble cytochrome oxidase and some other respiratory proteins from *Pseudomonas aeruginosa*, Biochem. J. 157 (1976) 423-430.

[11] M.C. Silvestrini, F. Cutruzzolà, R. D'Alessandro, M. Brunori, N. Fochesato, E. Zennaro, Expression of *Pseudomonas aeruginosa* nitrite reductase in

Pseudomonas putida and characterization of the recombinant protein, Biochem. J. 285 (1992) 661-666.

[12] F. Cutruzzolà, Bacterial nitric oxide synthesis, Biochim. Biophys. Acta 1411 (1999) 231-249.

[13] E. Nagababu, J.M. Rifkind, Heme degradation by reactive oxygen species, Antioxid. Redox Signal 6 (2004) 967-978.

[14] E.K. Wilson, A. Bellelli, S. Liberti, M. Arese, S. Grasso, F. Cutruzzola, M. Brunori, P. Brzezinski, Internal electron transfer and structural dynamics of cd1 nitrite reductase revealed by laser CO photodissociation, Biochemistry 38 (1999) 7556-64.

[15] W. Sun, M. Arese, M. Brunori, D. Nurizzo, K. Brown, C. Cambillau, M. Tegoni, F. Cutruzzolà, Cyanide binding to cd(1) nitrite reductase from *Pseudomonas aeruginosa*: role of the active-site His369 in ligand stabilization, Biochem. Biophys. Res. Commun. 291 (2002) 1-7.

[16] B.A. Springer, K.D. Egeberg, S.G. Sligar, R.J. Rohlfs, A.J. Mathews, J.S. Olson, Discrimination between oxygen and carbon monoxide and inhibition of autooxidation by myoglobin. Site-directed mutagenesis of the distal histidine, J. Biol. Chem. 264 (1989) 3057-60.

[17] M.F. Perutz, Myoglobin and haemoglobin: role of distal residues in reactions with haem ligands, Trends. Biochem. Sci. 14 (1989) 42-4.

[18] H.P. Misra, I. Fridovich, The generation of superoxide radical during the autoxidation of hemoglobin, J. Biol. Chem. 247(1972) 6960-2.

[19] T. Gotoh, K. Shikama, Generation of the superoxide radical during autoxidation of oxymyoglobin, J. Biochem. (Tokyo) 80 (1976) 397–399.

[20] T. Suzuki, Y. Watanabe, M. Nagasawa, A. Matsuoka, K. Shikama, Dual nature of the distal histidine residue in the autoxidation reaction of myoglobin and hemoglobin. Comparison of the H64 mutants, Eur. J. Biochem. 267 (2000) 6166-6174.

[21] J.E. Erman, L.B. Vitello, M.A. Miller, J. Kraut, Active-site mutations in cytochrome c peroxidase: a critical role for histidine-52 in the rate of formation of compound I, J. Am. Chem. Soc. 114 (1992) 6592-6593.

[22] M. Tanaka, K. Ishimori, M. Mukai, T. Kitagawa, I. Morishima, Catalytic activities and structural properties of horseradish peroxidase distal His42 --> Glu or Gln mutant, Biochemistry 36(1997) 9889-9898.

[23] W.G. Zumft, Cell biology and molecular basis of denitrification, Microbiol. Mol. Biol. Rev. 61 (1997) 533-616.

figure 1
Click here to download high resolution image

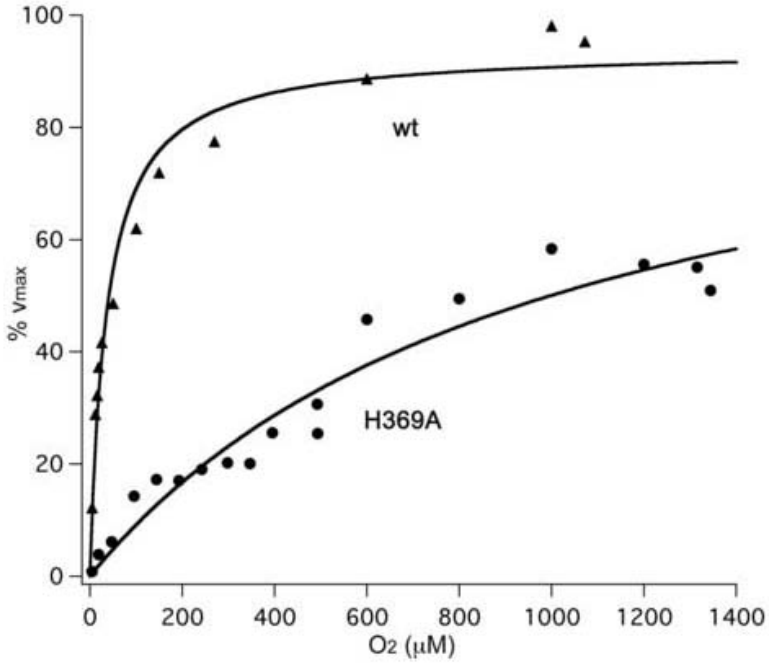

figure 2
Click here to download high resolution image

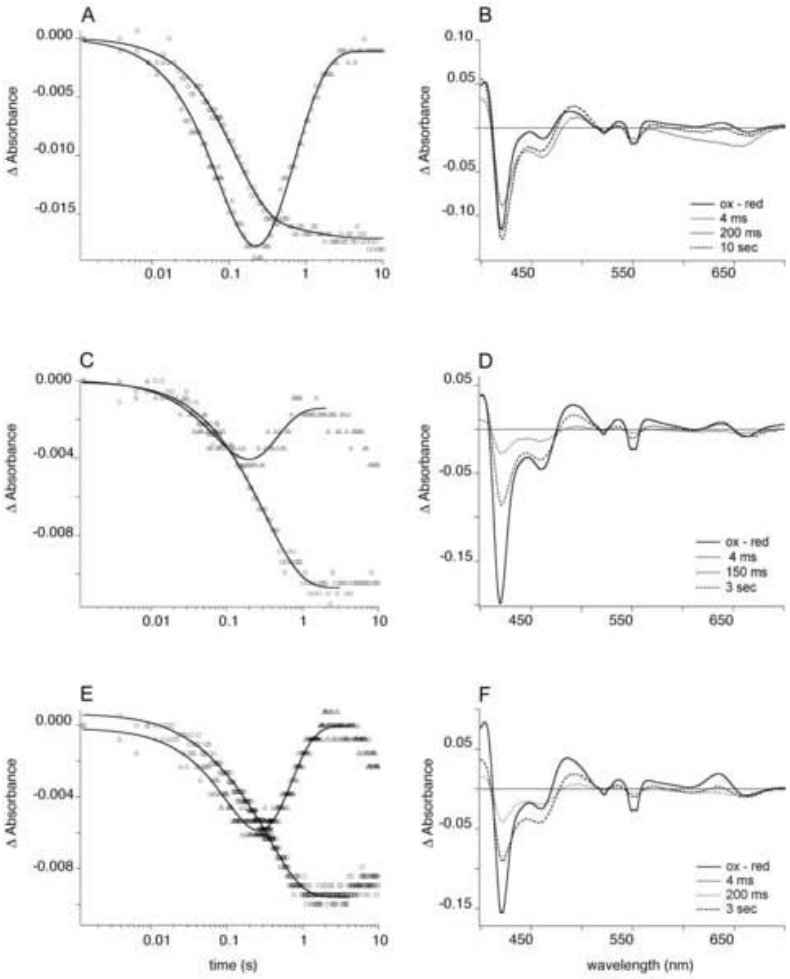

figure 3
Click here to download high resolution image

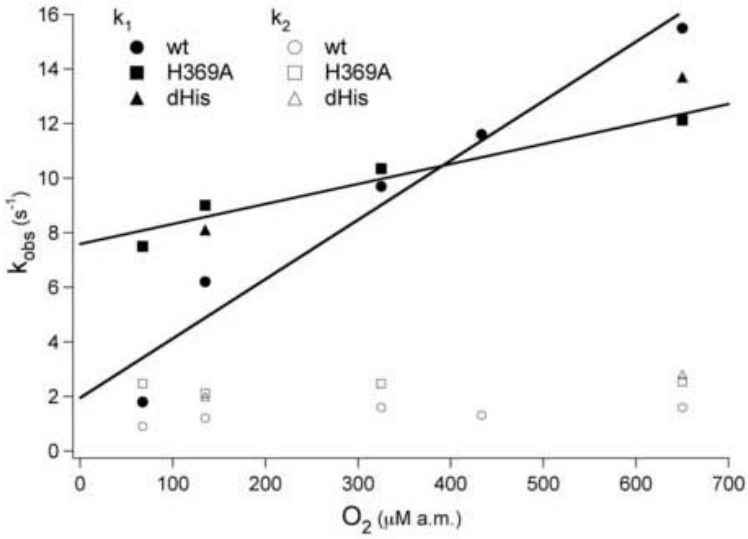

figure 4
Click here to download high resolution image